Beach Scarp Morphodynamics

Formation, Migration, and Destruction

C.W.T. van Bemmelen

Technische Universiteit Delft

NUS National University of Singapore
TU Delft
Witteveen Bos

Beach Scarp Morphodynamics

Formation, Migration, and Destruction

by

C.W.T. van Bemmelen

in partial fulfillment of the requirements for the degree of

Master of Science
in Civil Engineering

at the Delft University of Technology,
and the National University of Singapore,

to be presented publicly on Monday February 26, 2018 at 08:30 AM (GMT+1).

Supervisor:	Prof. dr. ir. S.G.J. (Stefan) Aarninkhof	TU Delft
Thesis committee:	Dr. ir. M.A. (Matthieu) de Schipper	TU Delft
	Ir. M.H.P. (Maarten) Jansen	Witteveen+Bos
	Prof. P.L.F. (Philip) Liu	NUS
	Dr. P. (Phil) Vardon	TU Delft

NUS National University of Singapore

TU Delft Delft University of Technology

Witteveen+Bos

Rijkswaterstaat
Ministerie van Infrastructuur en Milieu

I would like to thank the Dutch Directorate-General of Public Works and Water Management (Rijkswaterstaat, RWS) for the financial support of the field experiments performed in this study.

Preface

In this master thesis, my graduation work on the morphodynamics of beach scarps is presented. This thesis is the final product of my master Hydraulic Engineering and Water Resources Management at the Delft University of Technology and the National University of Singapore. I have carried out this thesis in cooperation with Witteveen+Bos.

First, I would like to thank my thesis committee for their time invested in me. Many thanks to Matthieu de Schipper, for your endless optimism and very constructive feedback during this thesis. I will always be grateful for the opportunities you provided me with to elevate this study to a next level. Many thanks to Stefan Aarninkhof and Maarten Jansen for the constructive meetings we had and for the different viewpoints you provided on this topic. Furthermore, thanks to Philip Li-Fan Liu and Phil Vardon for you valuable feedback.

Second, I would like to thank the students at Witteveen+Bos 2.73 (Guus, Laurens, Louwrens, Lucas, Tolga, Etienne, Niels, and Rik) for their involvement in the first field experiment of this thesis, helpful discussions and enjoyable moments outside of the office. Furthermore, I would like to thank the group of students involved in the second field experiment; Al, David, Esther, Giovanni, Greg, Lennard, Maria, Menno, Mohamed, and Remy. This group managed to make the measurement campaign one of the most memorable weeks of my academic career. Quirijn Lodder, thank you for arranging the financial support in order to perform the field experiments and our fruitful discussion on the topic of beach nourishments. Special thanks to Sander de Vos, for your help with the delicate laser measurements at the Sand Engine.

Third, thanks to Martine Rutten, for your guidance throughout my study and for the opportunity to study in Myanmar for almost half a year. For my time in Singapore I would like to thank Nico and Inge den Boer, who took me in whilst I was studying at NUS. I will always be grateful for the sense of 'home' whilst being more than 10000 km away from Delft.

Fourth, my friends throughout college, I would like to thank you for making the journey towards becoming a civil engineer very enjoyable. David Kroon, our philosophical conversations paired with your concept of 'meer benen' have kept me going at all times during this thesis and provided for some unforgettable experiences outside the TU Delft lecture halls. Menno de Ridder, thanks for your endless optimism, friendship, and help throughout the years. I will never forget the unique measurements the two of us performed on the 2nd of October 2017, when the experiment was hit with highly energetic conditions.

Last but not least, many thanks to my family. I owe much to my mom and dad, Claudia and Roland, and to my brother and sister, Jostijn and Leonie, on whom I could always count for moral and financial support throughout my study. I would like to express my gratitude and appreciation to my girlfriend, Dorien, for you love and support. Thank you for your patience to listen to my talks about beach scarp morphodynamics, field experiments, conceptual models and measurement techniques. Your unconditional love and support, paired with critical questions on what I was doing, resulted in the best discussions and motivated me throughout this thesis.

Cas van Bemmelen
Delft, February 2017

Abstract

Beach scarps are nearly vertical seaward facing walls within the cross-shore beach profile. These features are often associated with eroding (nourished) coastlines and can reach heights of $\mathcal{O}$(2-3 m), leading to serious hazards to beach users and negatively impacting local ecosystems. New insights into beach scarp morphodynamics related to geometrical, geotechnical and hydrodynamic parameters are presented in this thesis. Aimed at increasing our general understanding of these features, these insights are provided by means of analysing beach scarp presence at (large scale) nourishments and conducting field experiments.

An analysis of beach scarp presence at the Sand Engine between 2011 and 2017 has shown that the formation is linked to mildly erosive (summer storm) conditions, whereas destruction is related to both extremely erosive (winter storm) conditions (overwash or inundation, ∼50%) and non-hydrodynamic controls (drying collapse or burying by aeolian transport, ∼50%). Newly obtained measurements of beach scarps at this nourishment indicate that the toe elevation is 'fixed' around the maximum runup elevation, providing a direct relation between the final scarp height, nourishment platform height and hydrodynamic conditions. The associated beach scarp slope can be derived from a Culmann-type stability analysis, in which the matric suction provides the apparent cohesion necessary for the stability of scarps.

Field experiments were carried out, which consisted of monitoring the formation, migration, and destruction of scarps from artificially constructed linear slopes. Video observations show that the formation of beach scarps takes place between the 15% and 2% exceedance runup elevation ($R'_{15\%}$ and $R'_{2\%}$) and can be influenced by geometrical controls. High platform nourishments will lead to the formation of beach scarps, as overwash is required for a diffuse beach profile. The field experiments have furthermore shown that steep initial slopes are more susceptible to beach scarp formation. Beach scarp migration will take place when the maximum swash elevation exceeds the scarp toe, initiating the undercutting and slumping mechanism. Topographical measurements have shown that the migration rate is inversely related to the beach scarp height. The beach scarps reported in these experiments were found to be in accordance with the new definition proposed in this study; a non-vegetated, subaerial beach feature with a slope larger than the critical angle of repose of 32^o and a minimum height of 0.30 m.

Based on these findings, a conceptual model relating beach scarp morphodynamics to geometrical, geotechnical and hydrodynamic parameters is presented. In general, the formation of beach scarps is preceded by a continuous steepening of the beach slope (between $R'_{15\%}$ and $R'_{2\%}$) until a small vertical discontinuity of $\mathcal{O}$(10 cm) is present. Upon landward migration of this small scale feature, the scarp height changes depending on the backshore topography. The natural destruction of beach scarps can be initiated by four mechanisms; hydrodynamically controlled overwash (1), drying collapse (2), burying by aeolian transport (3) and swash deposition (4).

The findings presented in this study provide a better understanding of beach scarp morphodynamics and their relation to various geometrical, geotechnical and hydrodynamic parameters. Furthermore, it was found that the design of beach nourishments can be adjusted to limit the formation of beach scarps and to increase the natural destruction of these features.

Keywords: beach scarp; morphodynamics; formation; conceptual model; nourishment; runup

Contents

Nomenclature

Acronyms

GPS	Global Positioning System
LiDAR	Light Detection And Ranging
MHW	Mean High Water
MLW	Mean Low Water
MSL	Mean Sea Level
NAP	Normaal Amsterdams Peil, Dutch local datum ($\sim$ MSL)
SE	Sand Engine
SSCC	Soil Suction Characteristic Curve
SWCC	Soil Water Characteristic Curve
SWL	Still Water Level

Symbols

α	Air entry pressure for saturated soils	[kg/m/s^2]
β_f	Foreshore slope	[rad]
β_l	Lower foreshore slope	[rad]
β_u	Upper foreshore slope	[rad]
β_i	Initial beach slope	[rad]
$\beta_{seaward}$	Seaward slope of DUROS+	[rad]
χ	Bishop effective stress parameter	[-]
η	Water level	[m]
ϕ'	Internal friction angle	[rad]
σ	Total stress	[kg/m/s^2]
σ'	Effective stress	[kg/m/s^2]
θ	Moisture content	[-]
θ_0	Offshore wave direction	[rad]
θ_r	Residual moisture content	[-]
θ_s	Saturated moisture content	[-]
D_{50}	Median sediment particle size	[m]
D_{60}	60% passing particle size	[m]
D_{high}	Dune crest elevation	[m]

D_{low}	Dune toe elevation	[m]
g	Gravitational acceleration	[m/s^2]
H_0	Offshore wave height	[m]
H_b	Breaking wave height	[m]
$h_{n,p}$	Beach nourishment platform elevation	[m]
$H_{s,0}$	Offshore significant wave height	[m]
i	Beach scarp slope	[rad]
L_0	Offshore wave length	[m]
n	Pore size distribution parameter	[-]
$R'_{x\%}$	Total runup elevation ($R_{x\%} + \eta$)	[m]
R_{high}	Wave runup	[m]
R_{low}	Wave rundown	[m]
$R_{x\%}$	x% exceedence value of the runup	[m]
S	Total swash	[m]
S_c	Scarp crest elevation	[m]
S_e	Grain skeleton saturation	[-]
S_h	Scarp height	[m]
S_t	Scarp toe elevation	[m]
S_{ig}	Infragravity swash	[m]
S_{inc}	Incident swash	[m]
T	Wave period	[s]
t	Swash uprush duration	[s]
T_p	Peak wave period	[s]
u_a	Pore air pressure	[kg/m/s^2]
u_w	Pore water pressure	[kg/m/s^2]
w_s	Sediment settling velocity	[m/s]
x, y, z	Cross-shore, alongshore and vertical axis coordinate	[m]
z_a	Zapata et al. (2000) fitting parameter	[m]
z_m	Zapata et al. (2000) fitting parameter	[-]
z_n	Zapata et al. (2000) fitting parameter	[-]

1

Introduction

1.1. Background

Coastal erosion, one of the key processes impacting the heavily populated coastal zones, may increase due to sea level rise (Leatherman et al., 2000). During recent decades coastal protection strategies and methods have therefore gained significant attention. The applied measures can be roughly separated into 'hard' and 'soft' methods. 'Soft' methods are based on compensating for the eroded sand by replenishing the coastal system with nourished sand. These so called sandy mitigation methods have become increasingly popular due to the adverse side effects of 'hard' measures (Bosboom and Stive, 2013). With this trend, the desire to understand morphological processes on nourished beaches has also increased. One of the features often associated with coastal erosion are nearly vertical seaward facing cliffs. In coastal sciences these cliffs are referred to as scarps, of which two types can be distinguished; beach scarps and dune scarps. Dune scarps are vegetated features located on the backshore, whereas beach scarps are located close to the waterline and are non-vegetated.

Beach scarps can be found on naturally eroding coastlines, but have often been observed after large scale nourishment projects were completed (e.g. Anfuso et al., 2001; Jackson et al., 2010; Ruiz de Alegria-Arzaburu et al., 2013; de Schipper et al., 2017). These interventions in the coastal system add a surplus of material to structurally eroding coastlines. Erosion of these nourishments is therefore to be expected, but the formation of beach scarps can come as a surprise to coastal engineers (Bonte and Levoy, 2015). Figures 1.1 and 1.2 show beach scarps of $\mathcal{O}(1\text{ m})$ after erosion occurred at different nourished beaches in the United States and Mexico.

Figure 1.1: Beach scarp at Ft Pierce Beach, US. Source: Gammons (2011).

Figure 1.2: Beach scarp at Cancun Beach, MX. Source: Uluapa (2011).

Societal and ecological relevance

After their formation, beach scarps can remain rather small ($\mathcal{O}$(5 cm)), but are at times capable of reaching heights of up to 2-3 meters (Sherman and Nordstrom, 1985; Ruiz de Alegria-Arzaburu et al., 2013). High beach scarps can pose serious hazards to beach users (de Zeeuw et al., 2012). The collapse of these high vertical walls can result in injuries of beach visitors as they may fall off. Visitors tend to rest at the toe of these rather unstable walls, which can provide a shelter from (strong) winds and direct sunlight. Lifeguards in the Netherlands furthermore reported that their view on the waterline from their observation stations was blocked by beach scarps (de Zeeuw et al., 2012). If beaches become unusable due to the formation of large beach scarps, the economic implications can be significant according to Ruiz de Alegria-Arzaburu et al. (2013).

These vertical features do not solely have an impact on humans; local ecosystems are impacted by the restricted faunal interactions between the foreshore and the backshore (Jackson et al., 2010). One striking example is the reproduction of sea turtles, which are not able to crawl over large vertical cliffs. It has been reported that a significant part (up to 10%) of abandoned crawls can be related to the presence of beach scarps (Herren, 2010). Beach scarps can furthermore act as interceptors of aeolian transport, leading to a reduction in wind transported sand reaching the backshore and eventually the dunes. The trapped sediment will collect in front of the scarp, leading to an eventual decrease of its height.

Scientific relevance

Beach scarp have been observed widely, but only little is known about the conditions under which they form. The studies reporting beach scarps have shown that they occur all around the world and are not only limited to sandy beaches (e.g. Nicholls and Webber, 1989). Furthermore, these features have not only been reported in field studies, but also during laboratory experiments (e.g. Payo et al., 2008; Roberts et al., 2010; Masselink et al., 2014).

The formation of beach scarps is a poorly understood process and was first theorized by Sherman and Nordstrom in 1985. They separated the formation of these features into two groups; initiation by *process controls* and initiation by *structural controls*. *Process controls* contain the influence of waves and currents (e.g. swash runup) whereas *structural controls* are based around natural and human impact on beach characteristics (e.g. beach freezing).

The migration and destruction of beach scarps has been studied before, and has been related to wave characteristics and tidal elevations (Erikson et al., 2007; Ruiz de Alegria-Arzaburu et al., 2013; Bonte and Levoy, 2015; Schubert et al., 2015). The presence of beach scarps at a Dutch mega-nourishment has been described in de Schipper et al. (2017). Their study showed that beach scarps tend to form during relatively mild conditions and are destroyed during storms at this nourishment. Spatial patterns in beach scarp existence along the Sand Engine were also reported, but no clear explanation for these patterns could be given.

A consensus on the conditions required for their formation is thus lacking (de Schipper et al., 2017). Furthermore, a better understanding of the migration and destruction of these features is desired. The subject of this thesis will therefore be the morphodynamics of beach scarps with a focus on their formation. Morphodynamics is described as the mutual adjustment of morphology and hydrodynamics involving sediment transport (Bosboom and Stive, 2013). This terminology will be used throughout this study to summarize beach scarp formation, migration and destruction.

1.2. Problem definition

The negative impact that beach scarps can have on swimmer safety and local ecosystems calls for a better understanding into the formation of these features. As previously introduced, the current knowledge on beach scarp formation is rather limited. Yet, these features have been observed at many (nourished) coastlines around the world. A better understanding the of conditions impacting formation, migration and destruction is therefore desired. In addition, our current understanding of the relationship between beach nourishments and the formation of beach scarps is rather limited. This study could provide additional guidelines that will aid in reducing the probability of beach scarp formation in the future. Furthermore, current models are not capable of predicting beach scarp behaviour, which could be improved upon based on the findings presented in this study.

Within the design space for engineers, several choices have to be made regarding the design of nourishments. First of all, the required nourishment volume per meter alongshore has to be determined. For the Dutch coast this is around 10-30 m^3/m per year, resulting in beach nourishments with a volume of $\mathcal{O}(200\ m^3/m)$ (Stronkhorst et al., 2016). Next, the origin of the sand to be used for the nourishment has to be chosen. This information has to be kept in mind when choosing the cross-shore location of the nourishment; directly on the beach, on the shoreface or on the dunes. Finally, the coastal engineer has to determine the appropriate design in terms of geometry (e.g. platform height and initial beach slope). If certain parameters influence the probability of beach scarp presence, adjustments to the design could be made to limit the formation and persistence of these unwanted features at nourished beaches in the future.

In sum, the current knowledge about beach scarp morphodynamics is too limited, resulting in a poor understanding of these features and their relationship to eroding (nourished) coastlines.

1.3. Research questions and objectives

In this thesis, the formation, migration and destruction of beach scarps will be studied. Especially the conditions under which they form are of interest, as they often form following man-made adaptations to the beach profile. The overarching research question of this thesis is therefore formulated as follows:

> **Which combinations of hydrodynamic conditions and geotechnical/geometrical parameters will result in beach scarp formation, migration, and destruction?**

To answer this main research question, the following additional research questions are defined:

1. What environmental conditions cause the formation, migration and destruction of beach scarps at the Sand Engine?
2. What causes the alongshore variability of beach scarps at the Sand Engine?
3. Is there a geotechnical limit to beach scarp heights (at the Sand Engine)?
4. How does the design (initial slope and platform height) of nourishments influence the formation and shape of beach scarps?
5. To what extent and how can we predict the formation of beach scarps?

The main objective of this thesis is to gain a better understanding of beach scarp morphodynamics, focussing on the prediction of beach scarp formation. Ultimately, we would like to predict the formation of a beach scarp for different combinations of hydrodynamic conditions and profiles. The following secondary thesis deliverables will help in achieving the main objective:

- An overview of the current literature available on beach scarps.
- A set of hypotheses regarding beach scarp morphodynamics.
- An analysis of long term data of beach scarp existence at the Sand Engine.
- The design and execution of field experiments in which the hypotheses can be evaluated.
- A conceptual model in which beach scarp morphodynamics can be predicted.

1.4. Approach and thesis outline

In order to answer the research questions and to fulfil the objectives presented above, three research phases are distinguished in this thesis:

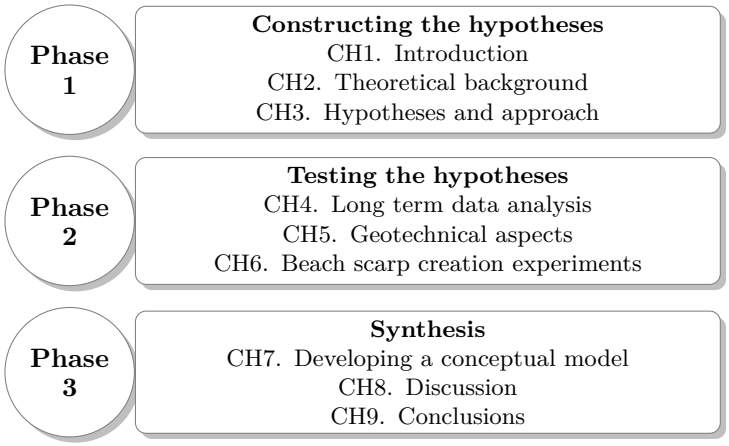

This thesis is separated into nine chapters; **chapter 1** contained background information about the topic of this study into beach scarp morphodynamics. The problem definition was furthermore described, along with the research questions and objectives for this thesis. **Chapter 2**, the theoretical background, provides a more in-depth description of the definitions used throughout this thesis and a summary of the currently available literature on the topic of beach scarp morphodynamics. Based on this literature study and new field observations, the hypotheses are presented in **chapter 3** along with the approach used to answer the research questions of this study. **Chapter 4** contains an analysis of the existing beach scarps at the Sand Engine and builds upon findings by de Schipper et al. (2017). The geotechnical aspects of beach scarps are discussed in **chapter 5**. In **chapter 6**, the design and results of the field experiments performed for this study are presented. In **chapter 7**, a conceptual model is presented that allows for an assessment of beach scarp morphodynamics. Lastly, **chapters 8 and 9** contain the discussion and conclusion of this thesis.

The complete literature study is presented in the first supporting document **Appendix A**. This part contains a chronological overview of the currently available studies reporting beach scarps. **Appendix B** contains background information about the field visits performed at the Sand Engine. **Appendix C** contains additional information about the measurement equipment and processing methods used during the field experiments. Furthermore, this appendix provides additional results concerning the topographical developments during the experiments. Lastly, **Appendix D** contains the formulae used for the statistical analyses presented in this thesis.

2

Theoretical background

The formation of scarps remains a rather unknown subject amongst coastal scientists. This chapter will therefore present the various concepts and definitions used throughout this study alongside a summary of the performed literature study. First, this chapter will start with the definitions used throughout this study. Second, an overview of the processes inside the swash zone is presented, which is an important part of the beach profile when studying beach scarp morphodynamics. Third, a summary of the available literature on beach scarps is presented. Fourth, a description of beach scarp life cycles and the comparison to regime theory is presented. Fifth and last, information on the geotechnical stability of these vertical features is presented.

2.1. Definitions

2.1.1. The coastal region

Various beach models can be found throughout literature that describe the zones within a coastal region (Longhitano, 2015). The major difference between the various models can be found in the defined boundaries of the back-and foreshore. A graphical representation of the cross-shore beach model used in this study is based on Sorensen (2005) and the Coastal Engineering Manual (Figure 2.1). The shoreface is bounded by the depth of closure (at which sediment transport is very small or even non-existent) and the shore. The shore is separated into back-and foreshore, which contains the instantaneous swash zone. The foreshore is bounded by the Mean High Water (MHW) and Mean Low Water (MLW) line intersections with the beach profile. Attention should be given to the location of the beach scarp, which is positioned on the foreshore, i.e. the intertidal zone, in this beach model.

2.1.2. Beach scarps

Throughout literature, several coastal scientists have struggled with distinguishing dune scarps from beach scarps (e.g. Alves and El-Robrini, 2006; Fernandez et al., 2011; Addad and Martins-Neto, 2012). In order to prevent confusion, this thesis follows a slightly modified version of the definition according to Ruiz de Alegria-Arzaburu et al. (2013) which is stated below.

A **beach scarp** is defined as a non-vegetated, subaerial beach feature with a slope larger than the critical angle of repose of 32^o and a minimum height of 0.30 m.

This definition encompasses an important factor differentiating beach scarps from dune scarps which was touched upon in the introduction; the presence of vegetation. The importance of vegetation on scarping dunes has been shown to increase the shear strength by an order of magnitude (Carter and Stone, 1989). The definition presented above can be used to detect beach scarps based on topographical measurements (Ruiz de Alegria-Arzaburu et al., 2013; Darnall, 2016). During their studies automated procedures were developed, which use the second derivative of the cross-shore beach profile to detect the scarp crest and scarp toe locations.

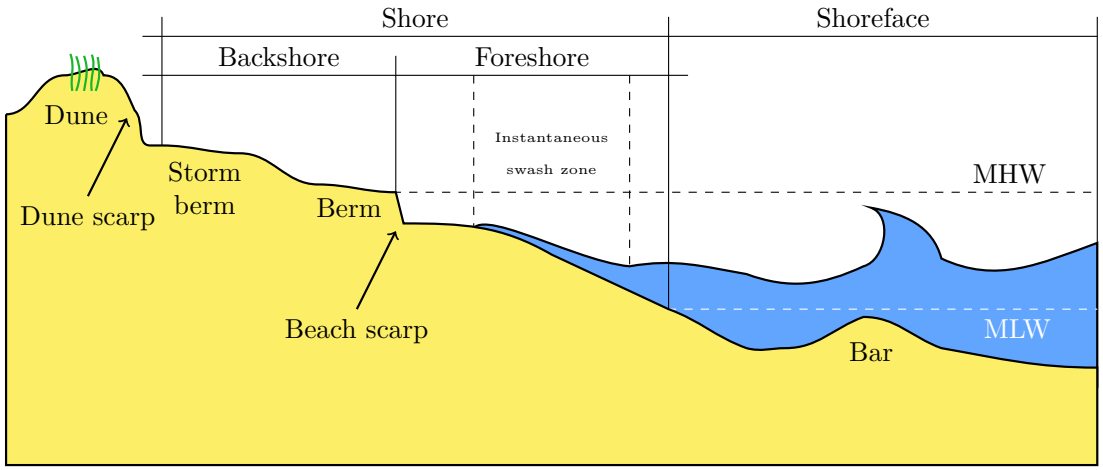

Figure 2.1: Graphical representation of the coastal region, adapted from the Coastal Engineering Manual (2002) and Sorensen (2005)

2.1.3. The foreshore slope

In the beach model presented above, the foreshore is located between MHW and MLW (Figure 2.1). From this figure it can already be observed that finding a representative slope for this region can be challenging. Wave runup depends on the foreshore slope and is often found to interact with beach scarps located on this part of the cross-shore profile. A clear definition of the foreshore slope is thus necessary in this study. This definition is however often omitted in coastal studies and the interpretation varies amongst researchers (Roberts et al., 2010). Three definitions for the foreshore slope are:

1. The average slope over a region of two times the standard deviation of a continuous water-level record (Stockdon et al., 2006).
2. The slope of the section approximately 1 m landward and 1 m seaward of the shoreline (Roberts et al., 2010).
3. The slope of the profile between MLW and MHW.

From just these three examples it can already be concluded that these definitions will lead to a different value of the foreshore beach slope. The definition used throughout this study will be the one proposed by Stockdon et al. (2006), which is also used for their empirical runup formulation.

The **foreshore slope** is defined as the average slope over a region of two times the standard deviation of a continuous water-level record of $\mathcal{O}(20\text{ min})$.

2.2. Swash zone

The swash zone is the transitional area between land and water for most coastal regions. Beach scarps are present just above this zone and can have a significant impact on swash statistics (Erikson et al., 2007; Bonte and Levoy, 2015). Understanding the processes within this zone is therefore important when discussing beach scarp morphodynamics. Finding a clear definition of the seaward edge of the swash zone can be a challenge however. Puleo (2004) suggested that the swash zone starts where bore turbulence starts to 'significantly' impact the bed. This definition is however less practical than the two used by most researchers (Puleo, 2004).

1. The region of the beach profile where there is intermittent (i.e. periodic) fluid coverage.
2. The time varying region extending from the point of bore collapse on the beach face to the maximum uprush limit.

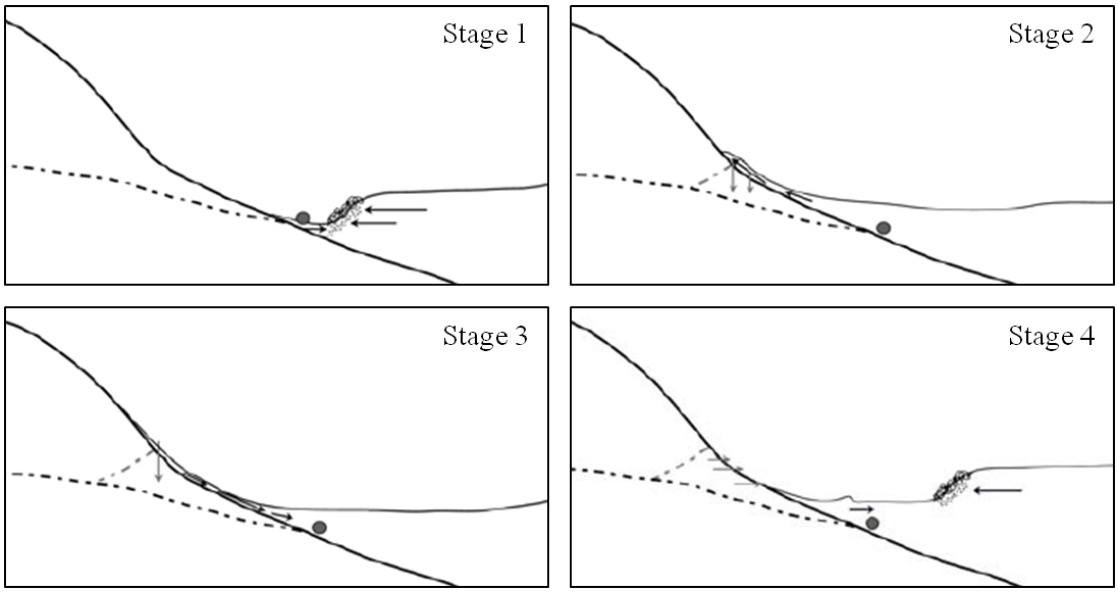

Figure 2.2: Schematic overview of a swash cycle. Thick solid lines represent the foreshore, thin solid represents the water surface, dashed line represents the water table level in the beach due to runup. Source: Puleo (2004).

By applying the second formulation of the swash zone, a clear (idealised) history of swash motions can be described (Puleo, 2004). The top left panel represents the initial stage of the swash cycle (Figure 2.2, Stage 1). During the initial stage, a bore approaches the fluid intersection with the foreshore. This is paired with a strong onshore directed flow at the bore and strong offshore directed flow near the bed. The second stage can be described as the uprush of the collapsing bore. During this stage, the majority of flow is directed onshore and infiltration of the foreshore surface can occur (grey arrows). During the third stage, the swash has reached is maximum uprush and is starting to travel into the offshore direction. The fourth stage is characterised by the interaction of the next bore transitioning into the swash zone. The type of interactions are discussed in the upcoming section.

2.2.1. Swash interactions

Swash interactions, which were described in Bauer and Allen (1995), have shown to be important in *beach step* formation. These steep seaward facing features show some resemblance to submerged beach scarps. Clear differences have to be noted however: *beach steps* can be formed through 'carving', 'excavation' or 'building'. These three initiations of *beach steps* occur during eroding, neutral or accreting events respectively. A link between the transition from surging to plunging waves ($t/T \approx 0.5$) and *beach step* formation was found to exist (Bauer and Allen, 1995). The notation t/T has been introduced by Kemp in 1975 as a means of indicating the 'phase difference' between uprush duration ($t = 3H_b^{0.5}/(g^{0.5} \tan \beta_f)$) and wave period ($T$). The question remains whether the interactions between up-rush and down-wash can also be related to beach scarp formation. Erikson et al. (2005) provide some insight into the mechanisms of swash-swash interactions; erosion and foreshore flattening is expected when swash duration (up-rush and down-wash) is shorter than the period of incoming waves. Steepening of the foreshore on the other hand is expected when swash duration is longer than the period of incoming waves.

Two types of interactions between consecutive waves in up-rush and down-wash stages can be identified; 'catch-up and absorption' and 'up-rush and back-wash collision' (Figure A.2). It was found that swash interactions play an important role in cases with gentle foreshore slopes ($\tan \beta_f = 0.07$). For steep slopes ($\tan \beta_f = 0.20$) however, swash interactions were found to be of less importance.

2.2.2. Wave runup

By superimposing the swash runup onto the wave setup (induced by wave breaking), the maximum landward extent of the waterfront can be determined. Several formulations have been developed to predict the wave runup (e.g. Hunt, 1959; Bowen et al., 1968; Hedges and Mase, 2004). One of the most used formulations is dependent on the aforementioned superposition of swash and wave setup (Stockdon et al., 2006). The following general formulations were derived after reverse shoaling[1] of nearshore measurements from 10 field experiments;

$$R_{2\%} = 1.1 * [\bar{\eta} + S/2] \tag{2.1}$$

$$\bar{\eta} = 0.35 * \beta_f * \sqrt{H_0 * L_0} \tag{2.2}$$

$$S = \sqrt{(S_{inc})^2 + (S_{ig})^2} \tag{2.3}$$

$$S_{inc} = 0.75 * \beta_f * \sqrt{H_0 * L_0} \tag{2.4}$$

$$S_{ig} = 0.06 * \sqrt{H_0 * L_0} \tag{2.5}$$

In which the 2% exceedence wave runup is dependent upon the wave setup and total swash. The wave setup ($\bar{\eta}$) is based on a combination of the foreshore slope β_f, offshore wave height H_0 and offshore wave length L_0. The total swash is represented by S and is based on the the incident swash S_{inc} and the infragravity swash S_{ig}. By means of substitution, these equations can be combined into a single equation for the (2% exceedence) wave runup,

$$R_{2\%} = 1.1 \left(0.35\beta_f (H_0 L_0)^{1/2} + \frac{[H_0 L_0 (0.563\beta_f^2 + 0.004)]^{1/2}}{2} \right) \tag{2.6}$$

By applying this equation to combinations of typical wave conditions and foreshore slopes, an indication of runup values can be presented (Figure 2.3). In this figure, typical foreshore slopes measured at a Dutch mega-nourishment were combined with a range of wave conditions obtained at an offshore measurement station.

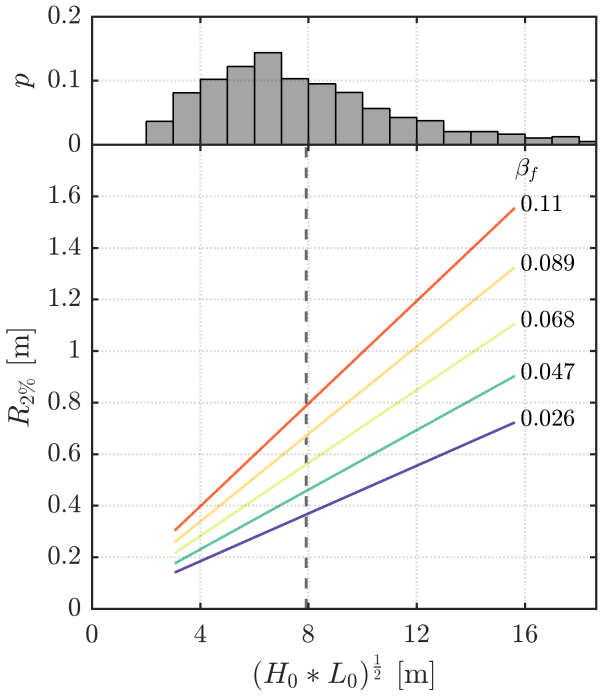

Figure 2.3: Wave runup ($R_{2\%}$) for typical Sand Engine foreshore slopes including the offshore distribution of daily averaged values for $(H_0 * L_0)^{\frac{1}{2}}$ at the Europlatform between 06-2010 and 02-2017 (mean is dashed line).

[1]Based on linear wave theory and assuming shore-normal approach.

2.3. Literature review

In order to collect the available information on beach scarps and to determine the most important parameters governing their morphodynamics, a literature study was performed. The reader is referred to Appendix A for more detailed summaries of the literature used in this thesis. First, the most important studies of beach scarps observed in the field are treated. Second, the main laboratory experiments reporting (often unexpected) beach scarp formations are presented. By means of summarizing the literature on beach scarps, this section finishes with an overview of all studies (field and laboratory) reporting beach scarp presence (Table 2.1).

2.3.1. Field studies

One of the first studies describing the formation and migration of beach scarps was performed at Debidue Beach in the United States (Kana, 1977). It was noted that the location of beach scarps seemed to coincide with beach cusp horns, which was echoed to be the case at Ibeno Beach in Nigeria (Antia, 1989). Short and Wright discussed the various beach systems of the Sydney region of Australia and noted that beach scarping occurred at various dissipative and intermediate beaches. Their findings were summarized in Short and Wright (1981), which described beach scarps in the plan and profile configurations of intermediate-dissipative beach states.

Sherman and Nordstrom (1985) were the first to discuss the complete beach scarp morphodynamics. Their paper starts with an overview[2] of beach scarps reported in scientific literature found prior to 1985. Second, the factors affecting formation, migration and destruction are discussed. The various findings presented in their study are further treated in section 2.4.

The beach scarps that have been described until 1989 were observed at sandy beaches, but it was in this year that Nicholls and Webber described the formation of 2 m high beach scarps made of shingles (a mix of pebbles and cobbles) after a nourishment was completed at Hurst Beach, Great Britain. The difference between the nourished material properties (D_{50}) and the original beach material was pointed out to be one of the main causes for beach scarp formation.

Nishi et al. (1995) showed that storm conditions caused by typhoons are capable of producing massive dune and beach scarp formations. In 1991, when a rather large typhoon passed Japan, a large dune scarp formed at Kashiwabara Beach (maximum height of 7 meters). Shortly after a beach nourishment had been completed to restore the beach, another typhoon caused rather energetic hydrodynamics conditions. These conditions resulted in the formation of massive beach scarps of $\mathcal{O}$(3 m), which was attributed to the steep nearshore beach profile present after the nourishment. In their study a numerical model was developed to study the impact of beach geometry to beach scarp characteristics. Based on this model, it was claimed that beach scarp height increases with increasing initial beach steepness.

The beach scarps at Cancun Beach (Figure 1.2) were studied by Ruiz de Alegria-Arzaburu et al. (2013). In their study, profile measurements were carried out on foot using a two-wheeled GPS trolley. This allowed for measurements close to the scarps at the recently nourished Cancun Beach. The method used to detect beach scarps from these profiles was based on minimum and maximum values of the second derivatives of the cross-shore profile. Next, relations between the scarp morphology and hydrodynamic conditions were investigated. The authors claim that scarp behaviour was related to three parameters; wave runup, tidal elevation and longshore energy flux. No clear relation between the formation of beach scarps and wave conditions is given, the authors do however indicate the importance of the nourishment performed at Cancun Beach.

Bonte and Levoy (2015) studied the migration of an artificially created beach scarp at Luc-sur-Mer Beach, France. At this macrotidal sandy beach an artificial beach scarp was constructed and its morphological development and nearshore hydrodynamics during rising tides and oblique

[2]The scarp heights in their paper range from 0.2 to 3.0 m, with most of the reported sightings in the United States. Most of these differ from the observations in scientific literature presented in Table 2.1 with Melbourne Beach, US, being the exception. Interestingly, the beach scarp presented in both Sherman and Nordstrom (1985) and van Gaalen et al. (2011) sources describe a beach scarp with a height of 0.5 m at this site.

waves were monitored. During this study, the beach scarp migrated landward and an increase in toe elevation was found. This increase in toe elevation is most likely related to the increasing water levels during the experiment. Regime theory, as described by Sallenger Jr (2000), was compared to their observations and a similarity to the collision regime was suggested. This comparison to regime theory was further studied by Darnall (2016) and de Schipper et al. (2017). The existence of beach scarps at the Dutch mega-nourishment (The Sand Engine) was assessed in their studies. It was found that the existence (Darnall, 2016; de Schipper et al., 2017) and migration (Bonte and Levoy, 2015) of beach scarps was highly non-uniform along the shoreline.

Until recently, most papers describing beach scarps at coastal zones were based on observations with tidal variation (Table 2.1). Neshaei and Ghanbarpour (2017) however, reported the formation of beach scarps at the Caspian Sea, which has a relatively small tidal amplitude.

2.3.2. Laboratory studies

Beach scarps have also been observed during laboratory experiments, where they often form unexpectedly. Undoubtedly, more beach scarps have formed in laboratory experiments than reported and discussed in this section. This section illustrates however that the formation of beach scarps is not limited to field cases, where both cross-shore and longshore sediment transport influence the changes in beach profile. During wave flume experiments the longshore transport is often found to be negligible, leading to the hypothesis that the formation of beach scarps is mainly caused by cross-shore processes.

Erikson et al. (2007) studied the migration of artificially created beach scarps in a wave flume. Various geotechnical and geometrical aspects of beach scarp migration and stability are given in their paper. Furthermore, this paper presents an analytical model to calculate the notch development of scarps. This model is largely based on sediment transport equations, elementary engineering statics and soil mechanics. During experiments performed by Payo et al. (2008), the formation of beach scarps was monitored in a multi-directional wave basin. Starting with a smooth beach profile, the resulting profile after approximately 2.5 hours showed the formation of beach scarps ($S_h \approx 5$ cm).

Apart from these studies directly aimed at understanding beach scarp morphodynamics, several sources report the unexpected formation of beach scarp in laboratory experiments; the formation of beach scarps was reported for a variety of (hydrodynamic) conditions in Roberts et al. (2010) (H_0= 0.60 - 1.15 m, T_p= 3.0 - 4.5 s), whereas a single beach scarp was observed in Masselink et al. (2014) during the least energetic conditions.

The infiltration mechanism, which increases the overburden leading to the slumping of a scarp face, has been shown to increase the predictive capabilities of dune erosion forecasting models (Palmsten and Holman, 2011). Although this study has been done in order to assess dune erosion, beach scarp morphodynamics could should a very similar behaviour (especially since the experiments were performed without the inclusion of vegetation, Figure 2.4).

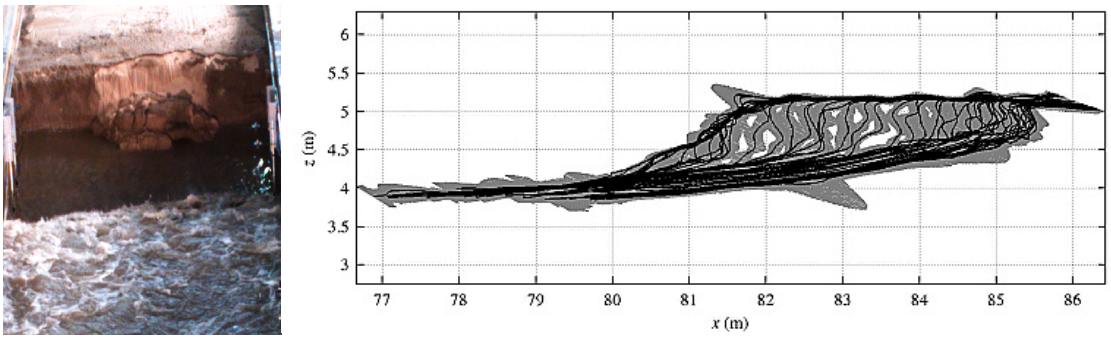

Figure 2.4: Image of a *dune* in laboratory conditions after a slumping event (left). Beach profiles with 95% confidence intervals (right). Source: Palmsten and Holman (2011).

Table 2.1: Studies reporting beach scarp formation (**F**), migration (**M**), destruction (**D**) ordered by publication year. Types of studies are categorized into: observation (O), experiment (E), modelling (M). Tidal ranges are of the neap-spring format and yearly averaged wave conditions offshore are given: significant wave height (H_s); peak wave period (T_p). The median grain size (D_{50}), (foreshore) slope ($\tan\beta$), maximum beach scarp height (S_h^m).

Field studies	Study	Stage	Tide [m]	H_s [m]	T_p [s]	D_{50} [mm]	$\tan\beta$	S_h^m [m]	Reference
Debidue Beach, US	O	**F,M**	0.6-1.6	1.0	6.30	0.25	∼0.056	1.0	Kana (1977)
Narrabeen Beach, AU	O	**F**	1.3-1.6	1.0-1.5	7.0-9.0	-	∼0.02	-	Short and Wright (1981)
Dewey Beach, US	O	**F**	1.05	-	-	0.33	∼0.01	0.6	Dubois (1988)
Ibeno Beach, NG	O	**F**	3.0-4.0	0.5-1.0	6.0-15.0	0.18-0.34	-	-	Antia (1989)
Hurst Beach, GB*	O	**F,M**	2.2	∼2	9.0	0.13-45	0.14	2	Nicholls and Webber (1989)
Fukiage Beach, JP*	O,M	**F,M**	-	-	-	-	-	3.0	Nishi et al. (1995)
Concheiros Beach, BR	O	**M**	0.47	1.5	9.0	0.23	0.087	0.7	Calliari et al. (1996)
Cádiz Province, ES*	O	**F**	1.1-3.2	2.00	7.0	0.22-0.47	0.02-0.06	1	Anfuso et al. (2001)
Torrey Pines Beach, US*	E	**M**	1.0-2.5	∼3	∼16	0.25	0.25	2.0	Seymour et al. (2005)
Slaugther Beach, US*	O	**F,M**	1.4-1.7	0.40	4.2	0.31-1.29	0.1	0.3	Jackson et al. (2010)
Rio de Janeiro, BR	O	**F,M**	-	4.0-5.0	-	-	-	1.6	Fernandez et al. (2011)
Melbourne Beach, US	O	**F,M**	1.0-1.2	0.50	10.0	0.17-0.35	0.05-0.14	0.5	van Gaalen et al. (2011)
Faro Beach, PT*	O	**F,M,D**	1.3-2.8	1.30	9.20	0.50	0.01	2.0	Vousdoukas (2012)
Alcobaca Beach, BR	O	**F,M**	2.0	0.4-1.0	-	-	-	-	Addad and Martins-Neto (2012)
Cancun Beach, MX*	O	**M,D**	0.07-0.32	2.0-3.0	6.0-8.0	0.60	0.15	2.0	Alegria-Arzaburu et al. (2013)
Luc-sur-Mer Beach, FR	E	**M,D**	8.0	0.5-1.0	4.0-6.0	0.22	0.03	1.0	Bonte and Levoy (2015)
Sand Engine, NL*	O	**M,D**	1.48-1.98	1.3	5.0-6.0	0.28	0.02-0.04	∼2.0	de Schipper et al. (2017)
Caspian Sea, IR	O	**F**	-	-	-	0.26-0.53	0.01	∼ 1.1	Neshaei and Ghanbarpour (2017)
Laboratory studies									
Vicksburg, US	E	**M**	-	0.06-0.18	2.20	0.13	0.067	0.21	Erikson et al. (2007)
Delaware, USA	E,M	**F,M,D**	-	0.07-0.08	1.08	0.19	0.2	∼0.05	Payo et al. (2008)
Delaware, USA	E,M	**F,M**	-	0.18-0.19	2.57	0.18	0.25	?	Kobayashi et al. (2009)
Delta Flume, NL	E	**M**	-	1.41-1.52	4.9-7.3	0.20	0.06	1.90	Kobayashi et al. (2009)
Oregon, US	O	**F**	-	0.60-1.15	3.0-8.0	0.22	0.08-0.12	∼1.20	Roberts et al. (2010)
Oregon, USA	E	**F,M**	-	1.0-1.2	4.0-5.0	0.23	0.125	0.60	Palmsten and Holman (2011)
Delta Flume, NL	O	**F**	-	0.80	4.00	0.43	0.07	-	Masselink et al. (2014)

*Nourishment projects.

2.3.3. Literature summary

Beach scarps are observed to occur under a wide range of conditions (Table 2.1). The tide could potentially influence the location of the beach scarp on the cross-shore profile, but neither high (8 m) nor low tidal ranges are a requirement for beach scarps to develop. The yearly averaged wave conditions offshore also indicate that there is no global relationship between beach scarp presence and wave conditions. Beach scarps can form on sites with rather large waves (4 - 5 m) and on sites with very small waves (0.5 - 1.0 m). They exist on both sheltered coasts (4 - 6 s) and ocean coasts with higher wave periods (6 - 15 s). Geometrical and geotechnical characteristics of the prototype locations also range from very coarse material (Hurst Beach) to 'normal' sand, and gently sloping (Faro Beach) to very steep beaches (Slaughter Beach). From this literature study it seems as if the highest beach scarps ($\geq$ 2 m) occurred after nourishment projects (Hurst Beach, Fukiage Beach, Torrey Pines Beach, Faro Beach, Cancun Beach, Sand Engine). Based on the fact that beach scarps have also been found to form during laboratory experiments, the formation of beach scarps is most likely initiated by cross-shore processes.

2.4. The life cycle of beach scarps

2.4.1. Formation

One of the first to describe the different stages in the life cycle of beach scarps were Sherman and Nordstrom in 1985. Their study started with a description of the formation of beach scarps, which can be separated into two groups; initiation by *process controls* (e.g. swash runup & tidal currents) and initiation by *structural controls* (e.g. beach freezing & beach steepening). *Process controls* contain the influence of waves and currents whereas *structural controls* are based on natural and human impact on beach characteristics. One could also state that *process controls* are the forces that influence beach scarp formation whereas *structural controls* (both horizontal as vertical) represent the resistance.

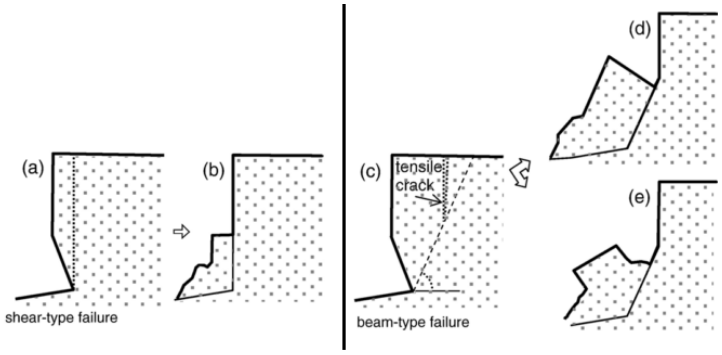

Figure 2.5: Types of failure as presented in Erikson et al. (2007). Shear-and beam-type failure are given in the left and right panes respectively.

In both of these groups, the vertical discontinuity was theorized to form due to the lowering of the foreshore slope whereas the backshore slope remains unaltered. Sherman and Nordstrom describe the initial increase of upper foreshore slope due to swash deposits under increased wave energy and steepness for an ideal case[3]. When failure (liquefaction or slumping) of the increased upper foreshore slope occurs, a beach scarp was hypothesised to form.

2.4.2. Migration

Migration of a beach scarp can be described as a process of undercutting and slumping by which the scarp face moves landward. Sherman and Nordstrom furthermore noted that the landward migration does not necessarily increase the height of the scarp. An extensive lab study was performed by Erikson et al. (2007), which describes two modes of mass failure that initiate the migration of scarps: shear-and beam-type failures (Figure 2.5). These modes of mass failure are both initiated by the impact of swash on the scarp foot causing undercutting of the beach scarp. Shear-type failures occur when the shear strength of the material is not capable of supporting the weight of the overhanging material, causing the overhang to slide down. Beam-type failure is initiated by crack formation landward of the beach scarp. When these tensile cracks intersect an internal failure plane, a block of material slides down.

The migration rate of beach scarps in the field have been studied by both Ruiz de Alegria-Arzaburu et al. in 2013 and Bonte and Levoy in 2015. Both studies related the migration of beach scarps to the governing hydrodynamic conditions. For the beach scarp at Cancun Beach, migration of the scarps was in 40% of the cases explained by a combination of tidal ranges, wave runup and longshore energy (Ruiz de Alegria-Arzaburu et al., 2013). Due to the low variability of wave conditions at Lac-sur Mer, the tide is mentioned to be an important parameter to explain scarp migration (Bonte and Levoy, 2015). Their study furthermore showed that the scarp did not retreat in an alongshore uniform manner, which was attributed to a variable beach evolution in front of the scarp. It should be noted that a groin was present close to the east side of the study area. This affects the longshore sediment transport and might have had an influence on the retreat rates, which was also mentioned by Nishi et al. (1995).

2.4.3. Destruction

Lastly, the destruction of beach scarps marks the last stage of their life cycle. Several causes for (natural) destruction of the beach scarp have been described by Sherman and Nordstrom (1985). Continued upward migration, until the beach scarp coalesces with its dune counterpart (1). Onshore migration of a swash bar, which can merge with the beach scarp (2). Retreating water levels, which causes the scarp to dry and returns the sediment to its natural angle of repose (3). Deposition of sediment in front of the scarp by either swash or aeolian transport (4). High amounts of overwash, which causes the near vertical cliff to collapse (5).

[3]This case is described as an equilibrium profile with a high berm and steep foreshore slope in Sherman and Nordstrom (1985).

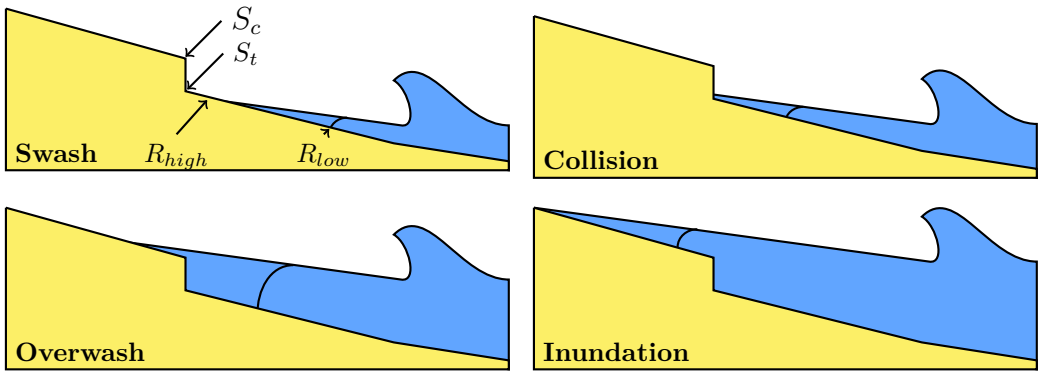

Figure 2.6: Regime theory applied to the combined wave and water level impact on beach scarps. Terminology adopted from Darnall (2016).

2.4.4. Regime theory

Storm regimes were first defined by Sallenger Jr (2000) in order to categorize impacts to natural barrier islands. The borders between these regimes are based on dune dimensions and extreme water levels. The dune dimensions used within this theory consist of two parameters: crest elevation (D_{high}) and base elevation (D_{low}). The extreme water levels also consist of two parameters: runup (R_{high}) and rundown (R_{low}). In this framework the following four regimes were defined: Swash Regime ($R_{high} < D_{low}$), Collision Regime ($D_{low} \leq R_{high} < D_{high}$), Overwash Regime ($R_{high} \geq D_{high}$ & $R_{low} < D_{high}$) and Inundation Regime ($R_{low} \geq D_{high}$).

This type of conceptual framework has also been suggested to be valuable in determining the impact on beach scarps (Darnall, 2016; de Schipper et al., 2017). These studies both follow a very similar terminology when compared to Sallenger Jr (2000), the only difference being the usage of scarp dimensions. The application of regime theory to the hydrodynamic impact on beach scarps consists of scarp dimensions and swash elevation[4]. Based on these parameters, the following regimes were distinguished in Darnall (2016):

1. **Swash Regime**: $R_{high} < S_t$
   The scarp remains unaffected as wave runup is limited to the lower foreshore.
2. **Collision Regime**: $S_c > R_{high} > S_t$
   During this regime the runup regularly impacts the area around the scarp toe. This can cause undercutting of the scarp, leading to notching and slumping of material. As a result of this process, the scarp will migrate landward.
3. **Overwash Regime**: $R_{high} > S_c > R_{low}$
   During this regime the runup is capable of overtopping the scarp, which can potentially lead to destruction of the near-vertical feature.
4. **Inundation Regime**: $R_{low} \geq S_c$
   If the rundown level exceeds the scarp crest, a complete inundation of the feature will occur. This will in (most cases) lead to a destruction of beach scarps, leaving a diffuse cross-shore beach profile.

A visualisation of the scarp impact regimes is presented in Figure 2.6. Due to the fact that wave properties and beach geometry can vary in the alongshore direction, a spatial variation of these regimes can potentially be observed. A developing storm or rising tide can also change the governing regime over time. We could therefore be faced with both spatial and temporal variations of these regimes along a beach scarp. It is important to note however, that regime theory is only applicable for migration and destruction of existing beach scarps (de Schipper et al., 2017). Additional conceptual models are therefore necessary to predict whether beach scarps will form in the first place.

[4]Including the tidal elevation, storm surge level and wave runup.

2.5. Beach scarp stability

The seaward facing slope of beach scarps can become near-vertical. The stability of these features is of great importance when determining scarp morphodynamics. Two important aspects are reported for non-vegetated slopes; soil suction and shell content.

Soil suction can be separated into two components; matric and osmotic suction. These two components are linked to the water content between the sand grains. The importance of soil suction can be observed when building sandcastles: without water, the natural angle of repose will be achieved; with a small amount of water, steep faces can be achieved; with too much water, the sand will become fluid-like (Pakpour et al., 2012). Matric suction is directly linked to the ratio between water and air inside the pores. A thin film of water around the sand grains will cause capillary bridges to form between the grains, increasing the stiffness of the material. In engineering applications, a fictitious cohesion is often added to take this affect into account (Erikson et al., 2007). Osmotic suction is related to the presence of chemicals (e.g. salt) and has been found to be less important in engineering applications. This component of the soil suction could still be valuable in understanding (the saline) beach scarp formations, but is often omitted in engineering applications as changes in osmotic suction are rather rare (Fredlund and Rahardjo, 1993). Interestingly, the effect of osmotic suction increases when drying of the sand occurs.

Another aspect which might be capable of influencing the stability of beach scarps is the presence of shells. Due to the interlocking of shell fragments, the sediment properties could be in favour to the formation and persistence of beach scarps. During drying of the beach scarps, the shells could act as a vertical armouring layer which appears to prevent local collapse of the scarp (Figure C.3). From literature, various beach scarp sightings were at locations which also contained a high amount of shell content: Narrabeen Beach (Short and Wright, 1981); Cádiz Province (Anfuso et al., 2001); Torrey Pines Beach (Seymour et al., 2005); Cancun Beach (Ruiz de Alegria-Arzaburu et al., 2013); the Sand Engine (Darnall, 2016).

2.6. Riverbank erosion

Large scarp-like features can be observed at sites faced with severe riverbank erosion. Although the flow of water is mainly parallel with respect to the riverbank, the formation of scarps in these systems could improve our understanding of beach scarps. During riverbank erosion the undercutting mechanism is governed by the local flow velocity and geotechnical properties. Due to the fact that the water level changes rather slowly, continuous undercutting occurs on the same elevation. The stability of riverbanks is different from that of beach scarps in two major ways; cohesion of the soil and the presence of vegetation increase the overall stability of riverbanks.

It is therefore not surprising that near-vertical riverbanks can reach heights of more than 4 meters (Rinaldi et al. (1999); Dapporto et al. (2003)). The types of mass-failure observed for riverbank erosion are very similar to the types described for beach scarp failure. In studies of streambank stability the most commonly observed types of failure are; slab-type failure, rotational failure, alcove-type failure, cantilever failure, shallow slide, soil fall, and pop-out failure. Of these failure types, the first two are very similar to the shear-type and beam-type failures described in subsection 2.4.2. The destruction of riverbank failure scarps can be related to a re-stabilization of the river bed and banks, also referred to river aggradation (Rinaldi et al., 1999). This type of destruction is similar to the mentioned swash deposition capable of reducing beach scarp heights. Destruction mechanisms such as drying of the material and water levels exceeding the *scarp* crest are not often observed for streambank erosion.

2.7. Beach scarp modelling

Predicting the morphological development of beach profiles remains one of the most challenging issues confronting coastal engineers and managers (de Vriend et al., 1993; Reeve et al., 2016). Various models are at the disposal of coastal engineers, but predicting the morphological developments at the transitional zone has been proven to be a challenge. Precisely these morphological

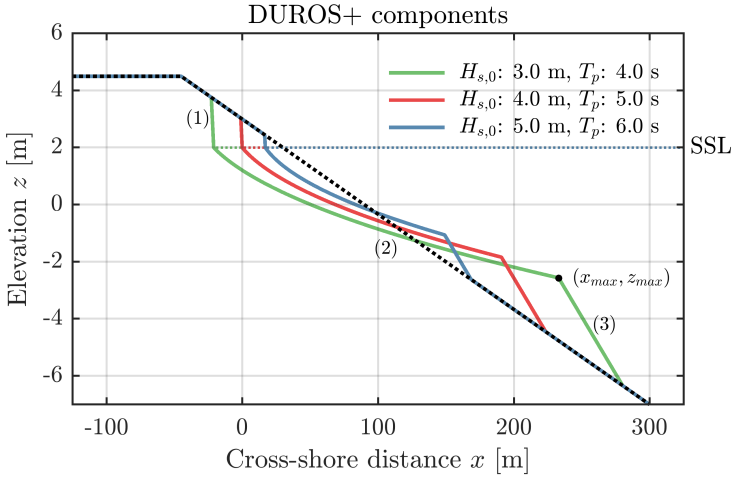

Figure 2.7: Beach profile predictions using the DUROS+ empirical model, composed of three elements: landward dune slope (1), parabolic 'equilibrium' slope (2), and seaward slope (3). Calculations have been performed from an initial slope of 1:30, SSL of 2.0 m NAP and w_s of 0.01 m/s.

changes initiate the formation of beach scarps on (nourished) beaches. The quantitative understanding about the processes in the intertidal zone is rather limited, which can be attributed to the lack of detailed measurements in shallow water (Payo et al., 2008). This information is required to understand the balance between onshore and offshore transport rates, which are of the same order of magnitude. It is therefore not surprising that accurate modelling of the morphological changes in this zone, resulting from gradients in sediment transport, has been proven rather difficult (van Rijn et al., 2007).

Despite the (generally) limited capabilities of these numerical models to predict morphological changes in the swash zone, it is nevertheless interesting to see how the development of the beach profile around this zone is included. Process-based models such as XBeach and CROSMOR have been extensively validated using laboratory *dune erosion* experiments, without the presence of vegetation. Both models contain a procedure in which the *dune face* slides down as a result of increasing profile steepness. Within XBeach, this procedure is referred to as 'avalanching' and is initiated if the slope exceeds the user-defined critical dry slope (default 45^o). A comparable procedure is applied in the CROSMOR model; 'sliding' of the dune face is initiated when a user-defined critical slope is exceeded. Empirical beach profile models generally define a fixed landward slope above the Storm Surge Level (SSL). For example, the DUROS+ model incorporates a landward slope of 45^o (Figure 2.7). Compared to observed dune and beach scarps in both laboratory and field studies, modelling the scarp dynamics based on a fixed (critical) slope value can lead to:

1. Under-prediction of scarp characteristics (height and slope) compared to those observed during laboratory experiments (e.g. van Rijn, 2009; Hoonhout and van Thiel de Vries, 2012; Palmsten and Splinter, 2016).

2. Scarp-like erosion of the upper beachface, whilst not observed from field observations (e.g. Vousdoukas et al., 2011; van Rijn et al., 2011; van Thiel de Vries et al., 2011).

The parametrization of the critical beach slope indicates an important shortcoming in these models; the inclusion of geotechnical aspects. More advanced models are capable of accounting for water infiltration into the scarp face (Erikson et al., 2007; Palmsten and Holman, 2011). The (horizontally) infiltrated water provides stabilizing and destabilizing forces. More stability is gained from including the apparent cohesion in the slope failure analysis. On the other hand, the infiltrated water also leads to destabilization caused by the increased overburden. Due to the added apparent cohesion, these models are capable of producing steeper scarp faces which are more in-line with the observed (beach) scarp characteristics.

3

Hypotheses and approach

In order to answer the research questions presented in the introduction, the hypotheses based on the literature review and new observations are formulation in this chapter. In addition, the approach used to answer the research questions are presented. First, the main research question is repeated:

> **Which combinations of hydrodynamic conditions and geotechnical/geometrical parameters will result in beach scarp formation, migration and destruction?**

3.1. Field observations

A large number of studies have reported the formation of beach scarps in the past (Table 2.1). These studies generally describe the presence or appearance of a beach scarp, without describing the formation process in detail. Capturing the formation of a beach scarp on a prototype scale requires some degree of timing, which has not been reported thus-far. Based on the seasonal trends of beach scarp existence at the Sand Engine it was expected that beach scarps would form during the summer (de Schipper et al., 2017). For this study, a series of basic field visits to the Sand Engine were therefore undertaken in the summer of 2017 (Appendix B). During one of these field visits, the formation and migration of a beach scarp was observed (Figure 3.1). This visit was performed during typical summer-storm conditions ($H_{s,0} \sim 3.5$ m). The formation occurred during high tide, when steep sections of the cross-shore profile were eroded without major changes in the swash elevation. This is in-line with the fact that high water levels have been associated with beach scarp formation (Bonte and Levoy, 2015). Prior to, and during the formation and migration of this beach scarp some overtopping took place (visually estimated at $R_{10\%}$). This can be observed from the wetted slope just above the scarp crest, the foam indication might be misleading as aeolian foam transport was noted during these storm conditions (Figure 3.1). The newly formed beach scarp rapidly grew to a height of approximately 0.7 m, which was paired with a landward migration of $\mathcal{O}(2$ m).

3.2. Hypotheses

The literature review and field observations provided valuable insight into the various stages of beach scarp development. These findings aided in postulating the hypotheses investigated in this study. Based on the stages in beach scarp development, the hypotheses were categorized into two main groups; formation (1) and migration-destruction (2). The main focus for this thesis will be on testing the hypotheses regarding the formation of beach scarps.

3.2.1. The formation of beach scarps

The hydrodynamic, geotechnical and geometrical conditions required for the formation of beach scarps are poorly understood. A set of four hypotheses were therefore constructed, which are based on the literature review and described field observations:

Figure 3.1: Field photographs showing the formation of a beach scarp during summer storm conditions at the Sand Engine (52°03′24.1″N, 4°11′14.6″E). Photo's facing south, taken on 07/06/2017 14:16-15:44 with a water bottle (0.20 m) for scale.

1. A combination between steep sections in the beach profile and eroding hydrodynamic conditions are required for beach scarp formation.
2. Beach scarps form during small variations in water level, which could otherwise result in inundation of the steep profile section before formation. (e.g. peak of the high tide, $\frac{\partial \eta}{\partial t} \approx 0$).
3. Two design parameters for nourishment projects influence the formation of beach scarps; the nourishment platform and the initial nourishment slope.
4. The alongshore variability in scarp existence (and height) can be explained from the topography in relation to the hydrodynamic conditions.

3.2.2. The migration and destruction of beach scarps

As presented in the literature review, regime theory was found to be applicable when assessing the next phases in beach scarp development. The following hypotheses have been constructed for beach scarp migration and destruction:

1. Growth of beach scarps during migration is related to the hydrodynamic conditions and backshore beach profile. Beach scarp migration is therefore not necessarily linked to a reduction or increase in scarp height.
2. Mild overtopping of the beach scarp ($\sim R_{<10\%}$) does not lead to destruction.
3. Beach scarps are destructed during large overwash events (or even inundation) caused by storm events.

3.3. Hypothetical model

Based on the literature study and the described observations, a first hypothetical model can be assimilated (Figure 3.2). In this model, the formation of a beach scarp is related to the flattening part of the cross-shore profile, referred to as 'lower slope'. Due to the fact that the cross-shore profile has to connect to the (unchanged) backshore, the 'upper slope' of the beach profile will steepen. This process will continue until a vertical discontinuity, a beach scarp, forms above the water line. If the processes are limited to the cross-shore, a balance between the eroded and deposited area is to be expected (e.g. in wave flume experiments, DUROS+). On a prototype

scale (and especially at protruding mega-nourishments) longshore processes will have a major influence on the balance between eroded and deposited material within a cross-shore transect. Various aspects of this hypothetical model (e.g. toe elevation, scarp slope, and scarp height) are unknown for now. The approach presented in the upcoming section will describe the methods used to further improve and validate this model.

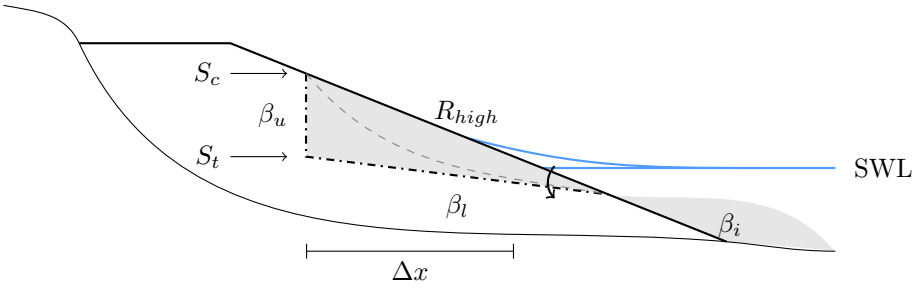

Figure 3.2: Hypothetical model of beach scarp formation from a linear nourishment slope during constant hydrodynamic conditions. The thin solid line represents the initial beach profile and the thick solid line represents the nourished profile with slope β_i. The dashed thin line indicates the first stages of erosion. The profile with a developed beach scarp, upper foreshore slope β_u and lower foreshore slope β_l is indicated with a thick dash-dotted line.

3.4. Approach

In order to test the presented hypotheses and hypothetical model, two approaches will be used. First, the existence of beach scarps at the Sand Engine from a long term dataset will be analysed. Second, beach scarp creation experiments will be conducted on a prototype scale. The next chapters will present the approaches in more detail, but a short introduction can be found in the subsections below.

3.4.1. Long term data analysis

Beach scarps have been reported to form at the Sand Engine, which has been extensively monitored over the past few years. This monitoring programme has resulted in a long term dataset stretching from 2011 to 2017, which contains topographical surveys of the SE every couple of months. Following the seasonal trend at the SE presented in de Schipper et al. (2017), beach scarps are expected to form along the perimeter of this nourishment during summer storms. For this study, additional detailed topographic measurements will therefore be carried out in July and August of 2017, aimed at mapping various beach scarp characteristics (e.g. scarp height and slope).

3.4.2. Beach scarp creation experiments

In this study, field experiments on a prototype scale will be performed in which beach scarp morphodynamics are analysed. The field experiment is based on monitoring the morphological evolution of a linearly sloping mounts under wave attack. Several artificial mounts will be constructed at the Sand Engine with varying slopes and platform heights over the course of two experiments in the summer of 2017, with a combined volume of $\mathcal{O}(700\ \mathrm{m}^3)$. The construction will be followed by two monitoring campaigns, which mainly focus on topographical measurements.

4

Long term data analysis

Based on the assessment of beach scarp presence along a (large scale) nourishment such as the Sand Engine, various beach scarp characteristics (e.g. average scarp toe elevation and spatial variability) can be related to hydrodynamic and geometrical conditions. The spatio-temporal patterns of beach scarp existence at the Sand Engine have been studied by de Schipper et al. (2017). Their findings report the formation of beach scarps during (mild) summer conditions and destruction during (storm) winter conditions. An explanation for the spatial variability along the Sand Engine perimeter is however lacking. This chapter contains a closer look at the available data on beach scarps for the Sand Engine and builds upon the findings presented in de Schipper et al. (2017). The performed data collection and analysis will provide additional insight into when and where beach scarps are formed at the Sand Engine. First, an introduction into the design and monitoring programme for this nourishment is given. Second, the long term dataset containing topographic measurements between 2011 and 2017 is presented and analysed. Third, the high resolution (spatial) measurements performed during this study are presented and analysed. Fourth, the applicability of video observations from the Argus tower is investigated. Fifth and last, the general conclusions of this chapter are presented.

4.1. Introduction

Sandy mitigation measures can be divided into two main types; beach and dune nourishments (1) and shoreface nourishments (2). Beach and dune nourishments usually focus on resupplying sediment directly on weak spots along the coastline. Shoreface nourishments are based on resupplying sediment in the active shoreface, which is theorized to reduce the impact of waves on the shoreline and resupply the coast through onshore sediment transport. The latter type of nourishment is often considered to be more economical despite the larger nourishment volumes required (Bosboom and Stive, 2013).

Nourishment works can be very effective, but strongly eroding coasts either require very large amounts of sediment to be supplied or a frequent re-nourishment. Especially the re-nourishment strategy can have a significant impact on local ecosystems (Jackson et al., 2010). Instead of repeatedly impacting the local ecosystem with 'small' nourishments one localised mega-nourishment can be performed, which is capable of feeding adjacent coasts. It was with this idea in mind that the Sand Engine was designed and constructed on the Dutch coast between Hoek van Holland and Scheveningen (Figure 4.1). This mega-nourishment was constructed between March and July in 2011 and contained approximately 21.5 million m^3 of dredged material. The majority of this volume (19 million m^3) was used to create the hook-shaped peninsula of the nourishment, the remaining 2.5 million m^3 was used for two shoreface nourishments (de Schipper et al., 2016).

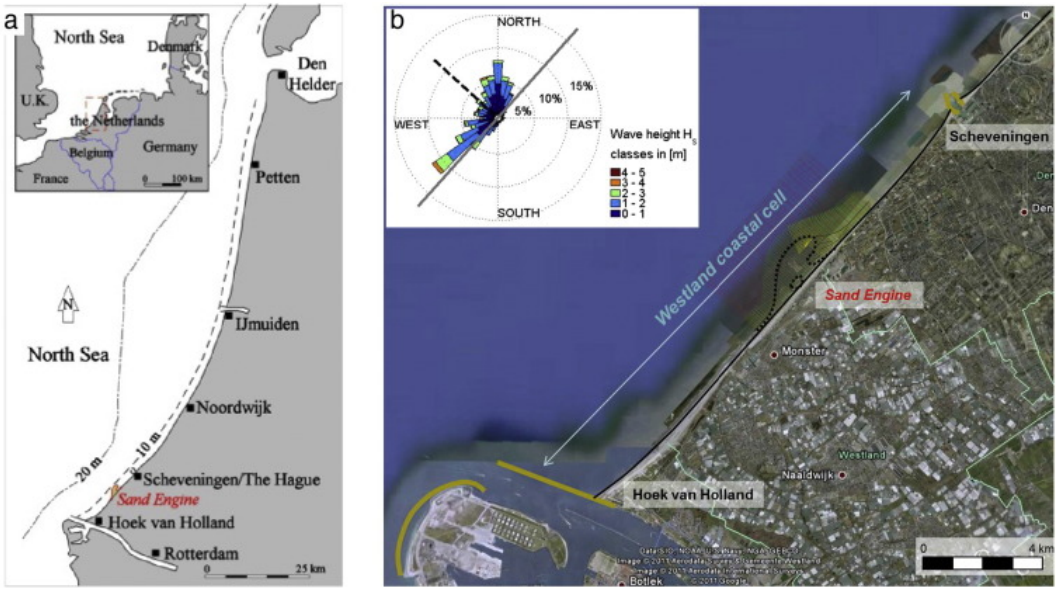

Figure 4.1: a) Location of the Sand Engine with respect to the Netherlands. b) Zoom into the *Westland coastal cell*, wave climate given in top left. Source: de Schipper et al. (2016).

Figure 4.2: The various measuring techniques applied at the Sand Engine; a) ATV next to a beach scarp of approximately 1.3 meter, b) jetski, c) GPS dolly for the lagune. Source: de Schipper et al. (2016).

4.2. Data collection

Extensive monitoring of the Sand Engine has been performed between August 2011 and January 2017, during which the topography of this nourishment was regularly measured. A total of 39 survey campaigns were performed, with a maximum interval of 3 months between two consecutive surveys. The field reports corresponding to these surveys reported beach scarps in 18 out of 39 cases. The scarps described ranged between 0.3 m to more than 1.3 m in height (Figure 4.2a). Various surveying methods have been applied to obtain the long term topographic data of the Sand Engine. All-terrain vehicles (ATV's) have been used to obtain the sub-aerial data, whereas a combination of jetski and GPS-dolly measurements were used to map the bathymetry. These GPS-dolly measurements were performed at locations unaccesible to the jetski, such as certain parts of the lagune (Figure 4.2c).

During this study, additional topographic measurements were performed of beach scarps at the Sand Engine. Two detailed surveys were performed between July and August 2017, when beach scarps with heights of $\mathcal{O}(1.5$ m) were present. Along the length of the beach scarp ($\sim$ 500 m) the crest and toe elevation were measured. Additionally, several cross-shore transects from the backshore to the waterline during low tide were taken. The topographic measurements presented in this chapter have been transformed to a local coordinate system (Figure 4.4).

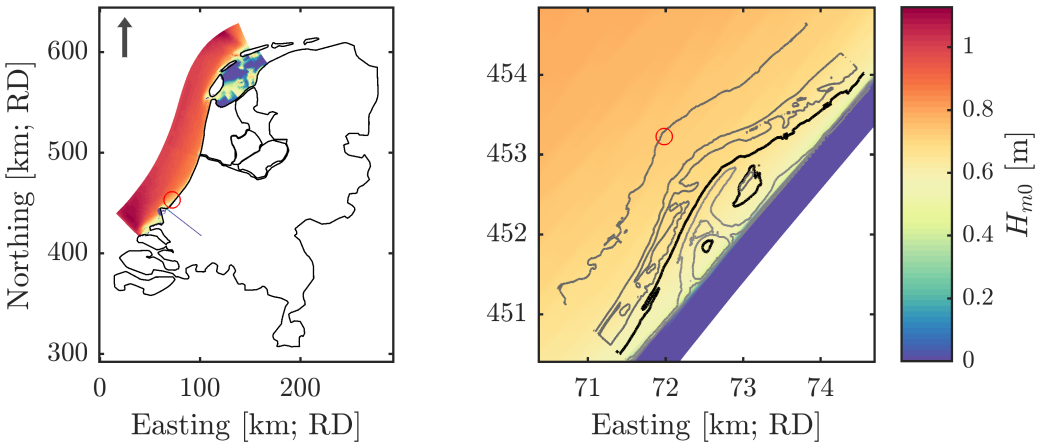

Figure 4.3: Wave height transformation of Europlatform wave data using the OET wave transformation table (left) indicated by the colours along with the depth contours of the Sand Engine (right). Location of offshore waves used in the presented analysis is indicated with a red circle (10 m depth contour).

4.3. Hydrodynamic conditions

Offshore wave conditions were taken from Europlatform 3, a measuring site located approximately 35 kilometres south west from the Sand Engine. These wave conditions contain the mean wave direction (θ_0), the significant wave height ($H_{s,0}$) and the peak wave period (T_p). Water levels (including storm surges) have been taken from Scheveningen Harbour, located approximately 7 kilometres north-east from the Sand Engine (Figure 4.1).

Wave transformation

The nearshore wave conditions (refracted, but not shoaled) are required for the assessment of wave runup according to equation 2.6. A transformation matrix based on stationary SWAN calculations was used to transform the obtained Europlatform data to nearshore conditions at the Sand Engine (Figure 4.3). This matrix, available from the Open Earth Tools (OET) was computed for 269 combinations of wave directions (θ_0 = 190 - 30^o) and wave conditions (H_{m0} = 0 - 7.5 m, T_{m0} = 0 - 14 s) (de Fockert and Luijendijk, 2010).

4.4. Beach scarp detection

Beach scarps can be detected by examining the 1st and 2nd order derivatives of the cross-shore beach profile (Ruiz de Alegria-Arzaburu et al., 2013). In order to detect the rapid slope changes around scarps, this method requires a high cross-shore resolution (< 2 m) which is not present in the Sand Engine data (Darnall, 2016). The scarp detection methods and parameters presented in Ruiz de Alegria-Arzaburu et al. (2013) had to be optimized for the long term Sand Engine dataset. Darnall (2016) found that a more 'relaxed' definition of the beach scarp slope of 15^o and height of 0.30 m produced the best results. One of the major issues with this automated procedure, is that beach scarps could be detected whilst only a steep slope is present. Compared to beach scarp detection by expert judgement of the measured cross-shore profiles, some discrepancies between the two methods can be observed. For this study, the manually detected beach scarps were chosen for the long term data analysis of the Sand Engine (Figure 4.4).

The existence of beach scarps at the Sand Engine is subject to an alongshore and temporal variability (Figure 4.4). Most beach scarps form at the 'sides' of the Sand Engine (y = 500 m to 1100 m) during summer periods. Large reset events occur during winter storms, which is underlined by the lack of beach scarps during this season.

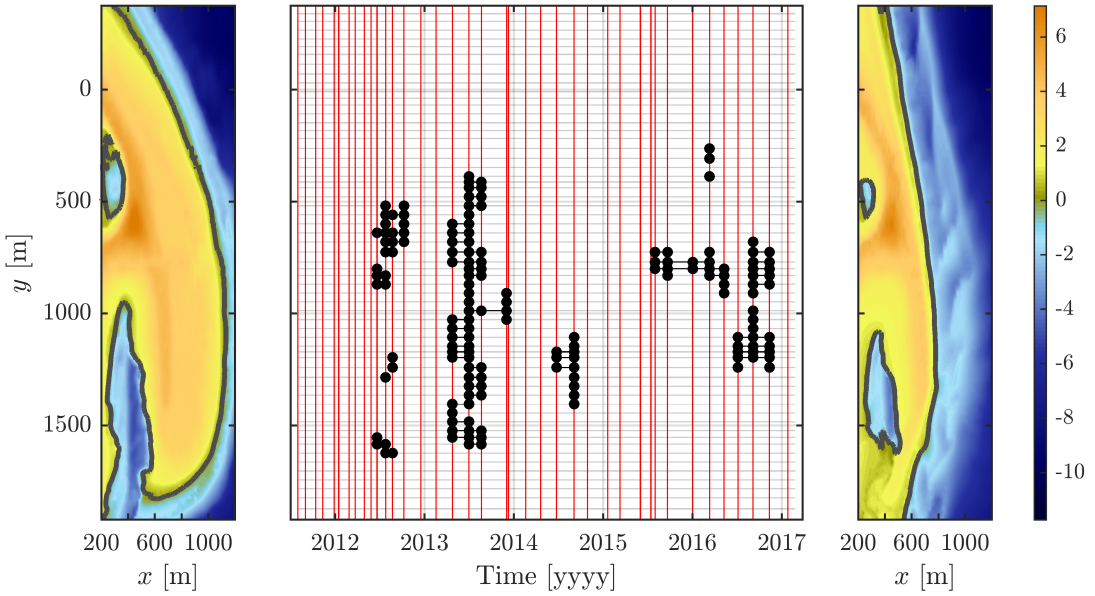

Figure 4.4: Beach scarp occurrence at the Sand Engine over time along with the topographies mid-2011 (left) and 2017 (right). Black dots represent the presence of a scarp at a transect (grey line) during a survey (red line). Adjusted from de Schipper et al. (2017).

4.5. Alongshore averaged behaviour

Beach scarps have been present at the Sand Engine during 18 out of the 39 topographical surveys. Scarps started to form mid-2012 at the Sand Engine, approximately one year after completion of the project. Since mid-2012, beach scarps have been reported every year and are found to be most often present in the months July to September (de Schipper et al., 2017). Between each consecutive survey, the location of these beach scarps along the nourishment perimeter changed. This is indicative for the spatial and temporal variability of scarps at the Sand Engine, which can be observed from Figure 4.4.

De Schipper et al. (2017) showed that high maximum water levels and high average wave conditions between two survey periods are required to completely remove the scarps from the Sand Engine[1]. Furthermore, relatively calm conditions are required to create beach scarps. The figure presented in this study is slightly modified with respect to their assessment (Figure 4.5). The main difference is the use of the maximum offshore significant wave height (daily averaged, transformed) instead of the mean offshore significant wave height (daily averaged). The conditions under which the beach scarps form (green barred) are relatively calm; during the periods with the lowest maximum water level elevations and relatively low wave heights. The conditions under which beach scarps are completely removed along the Sand Engine perimeter are of very energetic nature; the highest water levels and above average wave heights.

Based on this seasonal occurrence of beach scarps at the Sand Engine, the general life cycles of these features can be plotted with respect to the water level and offshore wave height. The general overview of created and destructed beach scarps is presented in Figure 4.6. Interestingly, 3/4 survey periods during which beach scarps were created are grouped between $H_{s,0}$ from 1.40 to 2.25 m and around η of 1.40 m NAP. Destruction of the beach scarps occurs during very energetic conditions ($\eta > 2.10$ m NAP and $H_{s,0} > 3.90$ m), which is most likely the result of large overwash events or even (local) inundation.

Based on this graphical representation of beach scarp presence related to hydrodynamic conditions, beach scarp life cycles (formation, migration, and destruction) can be assessed (Figure 4.7).

[1]For this assessment on the scale of the entire Sand Engine, creation and destruction is based on the presence or absence of scarps in all transects between survey periods.

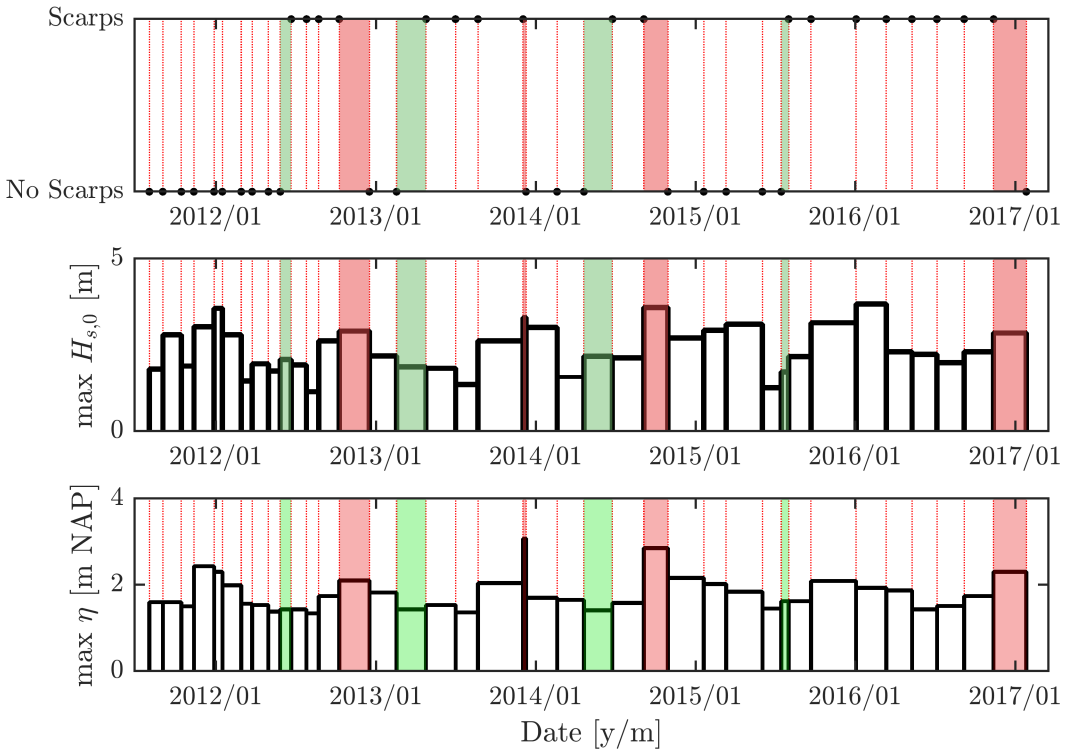

Figure 4.5: Seasonal occurrence of beach scarps compared to the maximum (daily averaged and transformed) significant offshore wave height ($H_{s,0}$) per survey period and maximum daily water level elevation (η) per survey period. Adjusted from de Schipper et al. (2017).

The individual beach scarp life cycles reveal that the destruction is most dependent on the maximum water level. This can be concluded from the conditions required to destroy the beach scarps at the Sand Engine between 08/2015 and 01/2017, during which very high water levels were required whereas large waves were not able to cause destruction (Figure 4.7, bottom right). During the first beach scarp life cycle at the Sand Engine, the conditions capable of destruction ($H_{s,0}$ ∼2.8, η ∼2.1 m NAP) were not capable of removing the scarps during later life cycles. This suggests either an increase of the scarp crest height (1) or a reduction in overwash amount during similar hydrodynamic conditions (2). The first explanation is in line with the hypothesis that the scarp crest elevation is limited to the nourishment platform level. The elevation of the scarp crest level shows a slight increase (∼ 10 cm) as a result of the retreating shoreline (Figure 4.9). The second explanation could be the result of a decreasing foreshore slope (according to Equation 2.6), whereas it has been shown that the profile slope between +1 and -4 m NAP has remained relatively stable after the first six months of development (de Schipper et al., 2016).

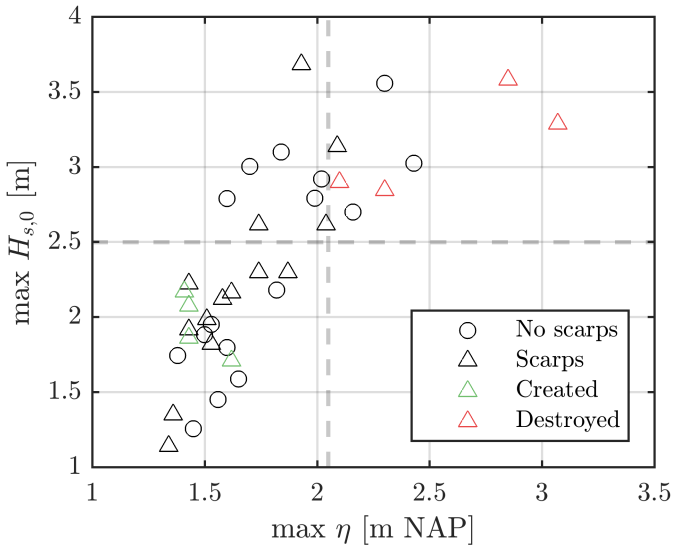

Figure 4.6: Maximum water levels (η) and offshore wave heights ($H_{s,0}$, daily averaged and transformed) for each survey period (38) at the Sand Engine. Round or triangular markers indicate the absence or presence of beach scarps, whereas the creation and destruction within a survey period is indicated by green and red colours.

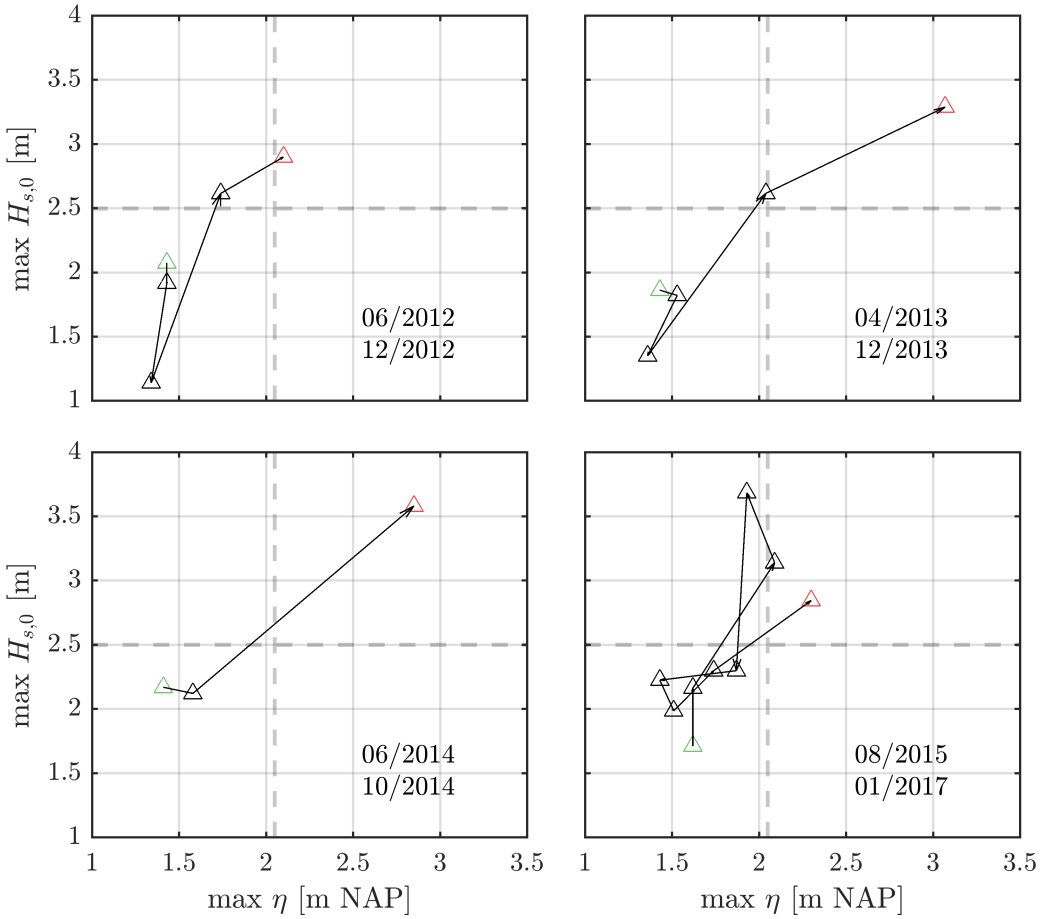

Figure 4.7: Beach scarp life cycles on the scale of the Sand Engine. The months corresponding to creation and destruction are given in the lower right corner. Parameters and markers are the same as Figure 4.6.

Table 4.1: Beach scarp destruction at the Sand Engine derived from the long term dataset, grouped by hydrodynamic (platform overwash or inundation) or non-hydrodynamic controls (scarp collapse as a result of drying or scarp burying by aeolian deposition).

Forcing	Requirement	Destruction type	Percentage
Hydrodynamic	$R_2' \geq h_{n,p}$	Inundation Overwash	52% (44/84)
Non-hydrodynamic	$R_2' < h_{n,p}$	Drying collapse Aeolian transport	48% (40/84)

4.6. Analysis per transect

Important information about the local (geometric) parameters can be overlooked by assessing beach scarp morphodynamics on the scale of the entire Sand Engine. Under the hypothesis that beach scarps form during wave attack on steep slopes, this relationship could very well be present in the long term dataset. The creation and destruction periods of individual beach scarps differ from the alongshore averaged behaviour, which could readily be observed from comparing Figure 4.4 to Figure 4.5. These differences in local beach scarp destruction can be explained in four ways:

1. Local differences in nourishment platform leading to quick beach scarp destruction positioned on lower parts of the Sand Engine.
2. Local differences in beach slope resulting in an alongshore varying wave runup, leading to localised destruction of the beach scarps at the Sand Engine.
3. Local collapse of beach scarps due to drying of the material.
4. Local burying of the beach scarp due to aeolian transport.

Beach scarps have often been observed around the 2 m NAP contour at the Sand Engine (Figure 4.9). It is therefore interesting to see what the value of the beach slope for each transect in this region is. Figure 4.8 shows scatter plots indicating the maximum water level with the corresponding beach slope for all survey periods (38) and all transects (y = 260 m to 1620 m); no scarp formed (A), scarp formed (B), scarp remained present (C), and scarp was destroyed (D). The beach slope used in this analysis has been calculated between 1.75 m NAP and 2.50 m NAP (grey indication Figure 4.9).

Detection of beach scarp presence at the Sand Engine based solely on this beach slope is impossible as we can see from Figure 4.8; the values for the beach slope do not vary significantly between panels A to D. One would expect the slopes in the survey periods with beach scarps (C, D) to be significantly higher compared to the panels without (A, B). Based on this per transect analysis, it can however be confirmed that the presence of beach scarps is paired with relatively low maximum water levels. The destruction of individual scarps shows a larger spread over the various water levels compared to the scatterplots presented in Figure 4.6. This implies that beach scarps can even get destroyed during periods with low maximum water levels ($\eta \sim 1.25$ m NAP). The exact causes for beach scarp destruction under low water levels remains unknown, but this could be an effect of drying collapse or burying by aeolian transport.

Based on the individual transects it is possible to calculate the wave runup, which is highly dependent on the (local) foreshore slope. Note that the assumption is made that the foreshore slope does not change during a survey period (between two measuring campaigns). In this part of the study a parameter combining the wave runup and water level is used,

$$R_{2\%}' = R_{2\%} + \eta \tag{4.1}$$

From Figure 4.9 it can be observed that some of the destruction periods are paired with $R_{2\%}'$ exceeding the scarp crest (red solid markers). This is in-line with regime theory, but in some

instances the scarps might have been destroyed by other causes. The formation of beach scarps seems to occur when large values of $R'_{2\%}$ ($\sim$ 2 m NAP) reach steep parts ($\sim$ 1:10) of the cross-shore beach profile. In one instance the beach scarp remains intact although high values of $R'_{2\%}$ indicate overtopping of the scarp crest (Figure 4.9 bottom panel). By analysing all Sand Engine transects it was found that $\sim$50% of the beach scarp destructions can be linked to wave overtopping or local inundation of the nourishment platform (Table 4.1). The remaining beach scarp destructions ($\sim$50%) can be attributed to non-hydrodynamic destruction in the form of scarp collapse resulting from drying, or scarp burying by aeolian transport.

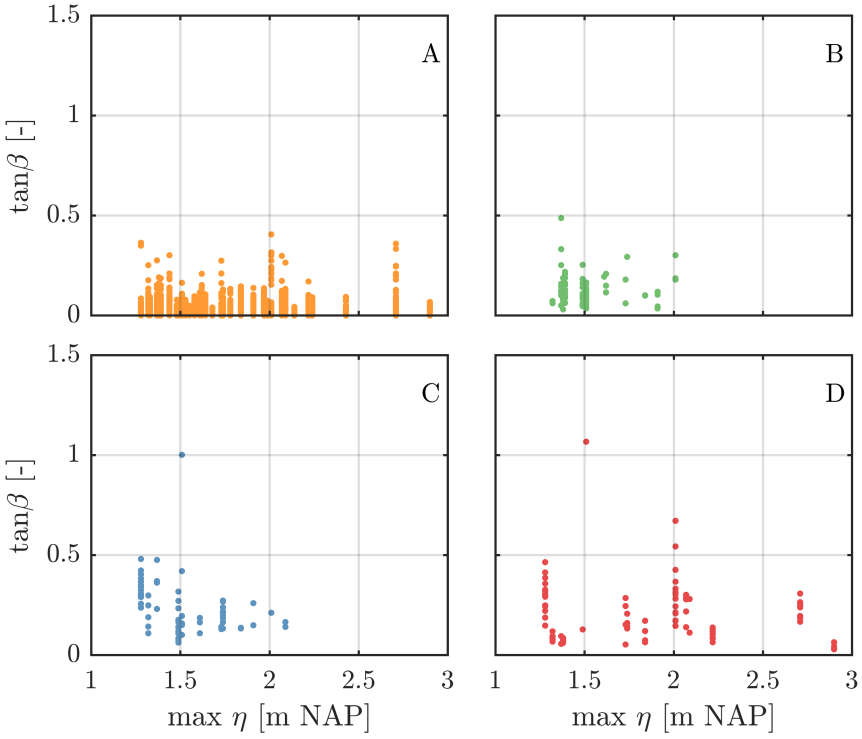

Figure 4.8: Maximum water level (η) versus the beach slope (β) between y = 1.75 m NAP and 2.5 m NAP. The four quadrants contain data of all the survey periods (38) and the transects between 260 m to 1620 m. No beach scarp during survey period (A), beach scarp created during survey period (B), beach scarp remained present (C), beach scarp was destroyed (D).

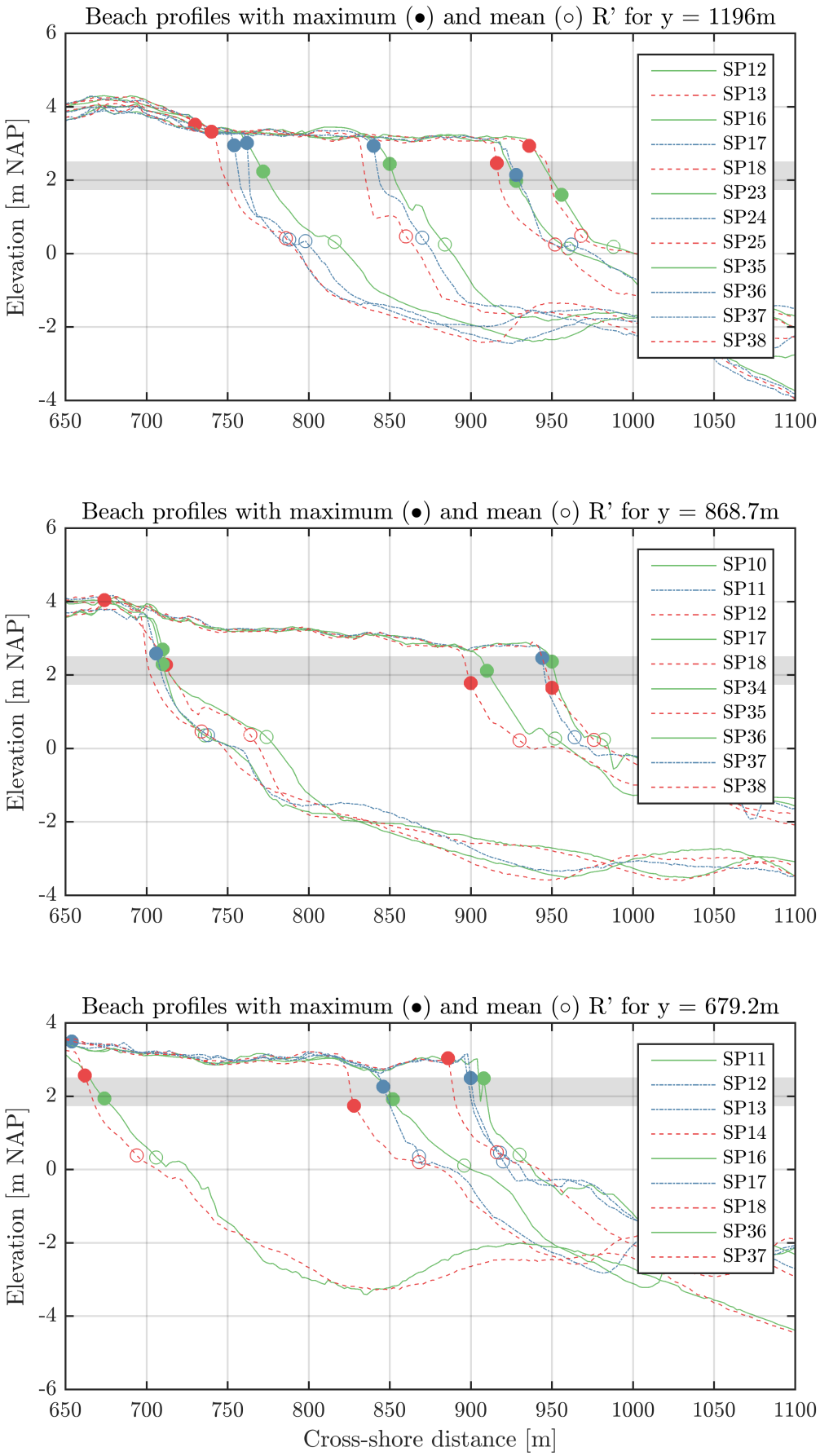

Figure 4.9: Beach scarp dynamics during survey periods (SP) at transects y = 1196 m, 868.7 m and 679.2 m (top to bottom). Formation (solid green line), existence (dashed-dotted blue line), destruction (dotted red line). The maximum and mean combined runup ($R'_{2\%}$) are given in solid and open circles and follow the profile colours.

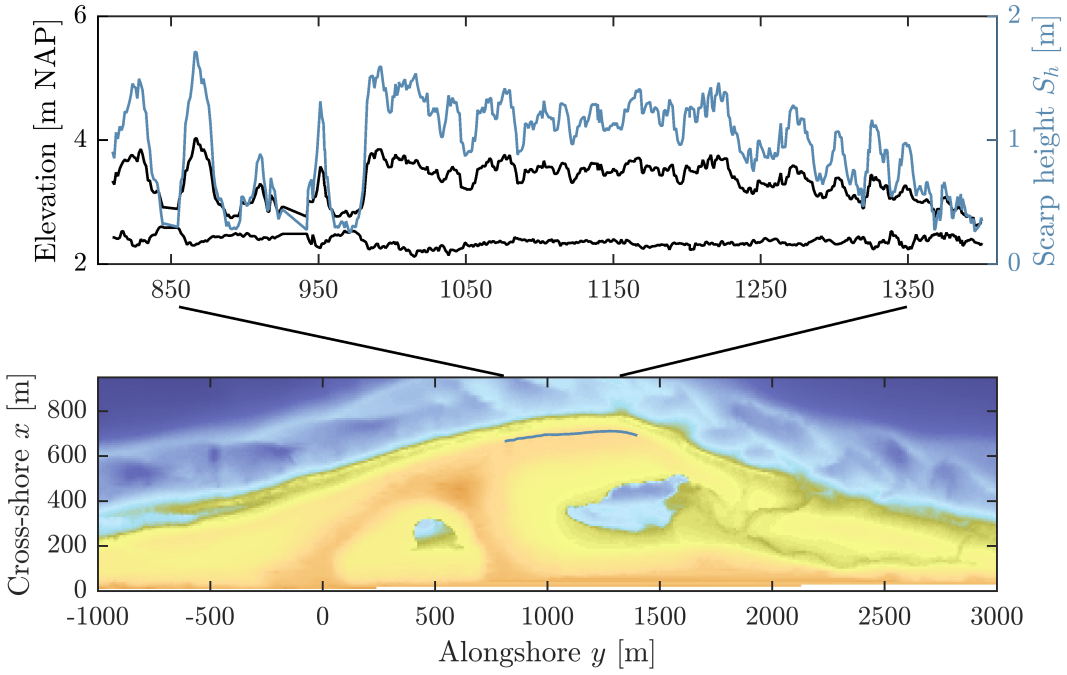

Figure 4.10: Scarp toe and crest elevation (black) and corresponding scarp height (blue) indicating the spatial variability of beach scarps at the Sand Engine measured on 04/10/2017 (upper panel). The location of the measurements with respect to the Sand Engine is indicated on the lower panel with blue markers.

4.7. Spatial variability

Based on the presence of beach scarps at the Sand Engine, it was shown that these features follow a spatial and temporal pattern along the nourishment perimeter (Figure 4.4). Whereas these temporal variations have been treated in the previous sections, still little is known about the spatial patterns of scarps at this site. During the field visits and experiments it was noticed that the scarp toe locations seemed to be at an almost constant elevation, whereas large differences in scarp height in the alongshore direction were present (Figure B.5). To better understand these patterns, detailed GPS-measurements were carried out along beach scarps at this nourishment in the summer of 2017.

To map the topographical variations in scarp crest and toe elevation, measurements were carried out along the scarp length at both elevations using a GPS-dolly (Figure C.1). Two surveys were carried out; 24/09/2017 (several days after formation) and 04/10/2017 (directly after formation). During the first measurements it was found that measuring the toe elevation was not straightforward. In fact, the scarp toe was buried by dry sand, which resulted in a so called 'fake upper toe' and 'fake lower toe'. The exact origin of this material remains unknown, but two different destruction mechanisms could have played a role; destruction by aeolian transport (1) or destruction by drying and collapse (2). In our case, the sediment deposition was most likely a result of drying and partial collapse of the beach scarp as wind conditions were rather mild during the days before the measurements took place. According to measured wind-speeds at Hoek van Holland the average wind speed was equal to 3.9 m/s, which can be considered too low with respect to the initiation of motion required for aeolian transport[2]. In order to approximate the effective beach scarp toe elevation S_t, these two 'fake toe' elevations were measured and the average level was taken.

[2]Critical shear velocity for the initiation of motion is of $\mathcal{O}$(6 m/s) and is amongst others dependent on the surface moisture content and grainsize, which might be relatively high on the Sand Engine (Bergsma, 2016; Davidson-Arnott and Law, 1990)

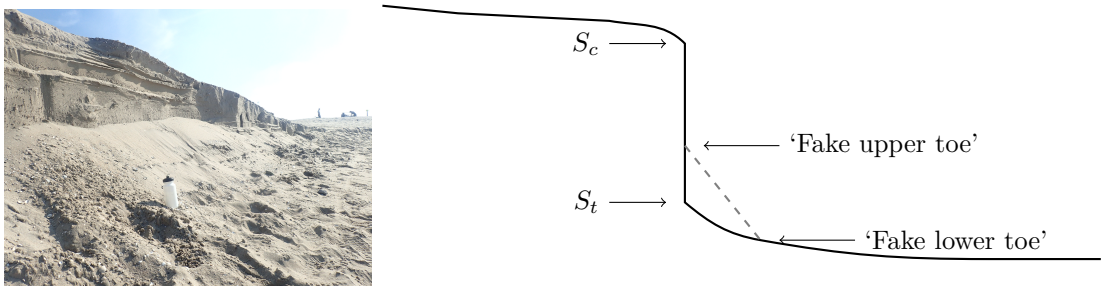

Figure 4.11: Schematization of beach scarps observed at the Sand Engine (right); photograph indicating sedimentation at the beach scarp toe on the 25th of September 2017 with a water bottle (0.20 m) for scale (left).

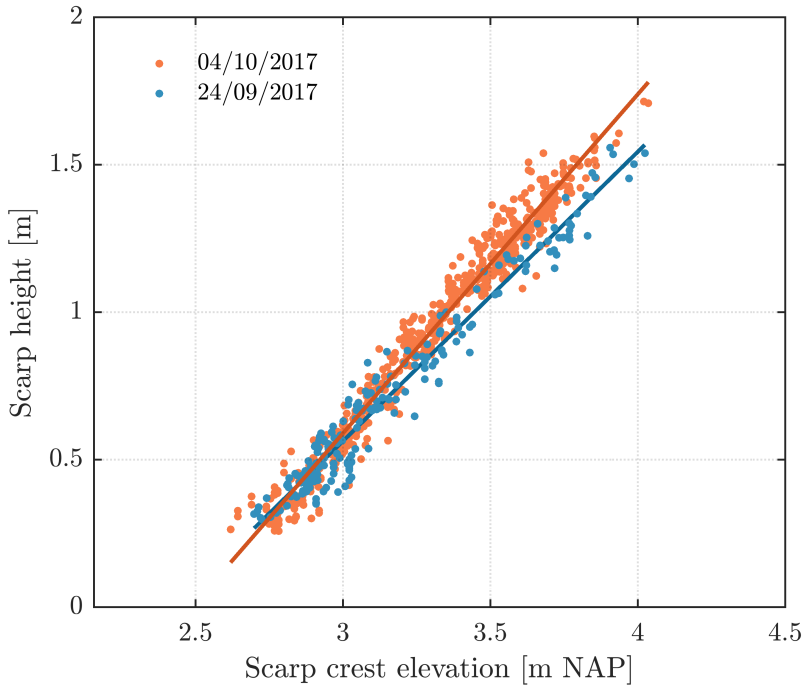

Figure 4.12: Relationship between the scarp crest elevation height S_c and scarp height S_h for the measurements performed on 24/09/2017 and 04/10/2017. The respective best linear fits between crest and scarp height follow $S_h = 0.98 * S_c - 2.38$ (RMSE = 0.066 m, $R^2 = 0.96$) and $S_h = 1.15 * S_c - 2.86$ (RMSE = 0.061 m, $R^2 = 0.97$).

The measurements presented in Figure 4.13 show that the scarp toe is rather constant around its mean value ($\mu_{S_t} = 2.38$ m NAP, $\sigma_{S_t} = 0.081$ m). The scarp crest on the other hand shows a large variation around its mean ($\mu_{S_c} = 3.30$ m NAP, $\sigma_{S_t} = 0.31$ m). This strong variability was also found in the scarp height, which is therefore mainly influenced by the undulating platform height for beach scarps with a 'fixed toe'.

The scarp toe elevation for both surveys has remained at the same level for both measurements (2.5 m NAP), which is very comparable to the combined maximum water level and wave runup $R'_{2\%} = 2.53$ m NAP ($\beta_f = 0.023$, $H_{s,0} = 2.16$ m, $T_{m02} = 5$ s). Local changes in topography or hydrodynamic conditions could lead to an alongshore variation in toe elevation, but this is considered to be significantly smaller than the variation in crest (platform) elevation. As such, the spatial variability in beach scarp height is mainly governed by variations in the nourishment platform. This spatial variability can be readily seen in Figure 4.10, which shows the largest variability in scarp height at the southern part of the 'head' ($y = 825$ m to 1000 m). For this section, the platform elevation shows a similar behaviour, but a slight variation in toe elevation can also be observed. This might be related to changes (e.g. sandbanks) in local topography,

which can partly be observed from the lower panel. On the northern side of the beach scarp, it can be observed that the height decreases somewhat gradually. This is directly related to lower elevation of the Sand Engine 'spit' (y = 1300 m to 1800 m).

The observations done in the field match the measurements performed at the beach scarps; the scarp toe location seems to be fixed around the maximum swash elevation with minimal variation around this value, whereas the scarp crest elevation (platform height) varies significantly in the alongshore direction resulting in a spatial variability of beach scarp height.

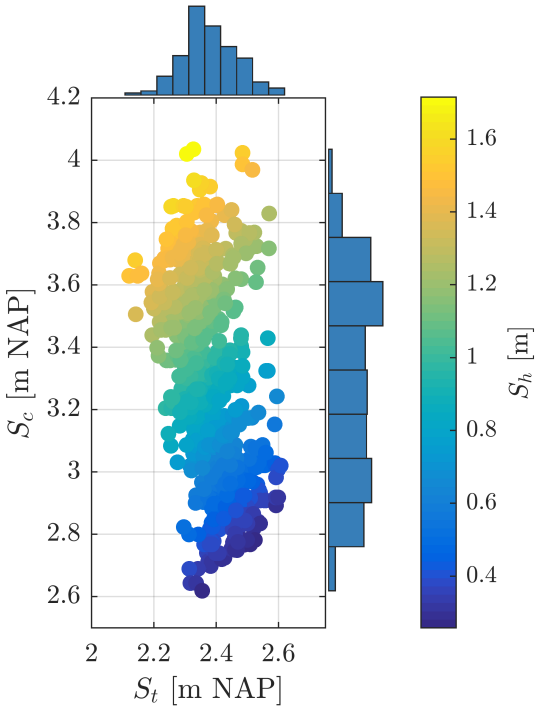

Figure 4.13: Scarp toe S_t versus scarp crest S_c of the alongshore measurements performed on 25/09 and 04/10. Colours indicate the corresponding scarp height S_h.

4.8. Argus video imagery

In order to pinpoint the moments in which beach scarps are formed and destroyed, frequent topographical measurements would have to be performed (on a day-to-day basis). This would provide excellent insights into the formation of beach scarps and their response to various environmental conditions. As this information is not available, it is interesting to see whether video observations can be used to detect beach scarps. Continuous monitoring of the hydrodynamic and morphodynamic changes around the Sand Engine is done using an Argus station. This station consists of eight 5-megapixel cameras, covering the most dynamic areas of the nourishment (Figure 4.14). These cameras provide for an almost birds-eye view as they have been mounted on top of a 40 meter high tower in the middle of the Sand Engine. The Argus system has proven to be valuable in determining the bathymetry (Wengrove et al., 2013) and aeolian transport at the Sand Engine (Weerd et al., 2016). Wodzinowski (2004) stated that beach scarps could be detected using a system inspired by the Argus system. His study does not describe the method used to detect these features and is most likely based on visual inspection of the images. During a study into the applicability of 'Surfcam' infrastructure along the SE Australian coastline, beach scarps were reported to obstruct the view on the shoreline (Turner et al., 2015). Detection of beach scarps at the Sand Engine based on Argus images would provide a very valuable source of

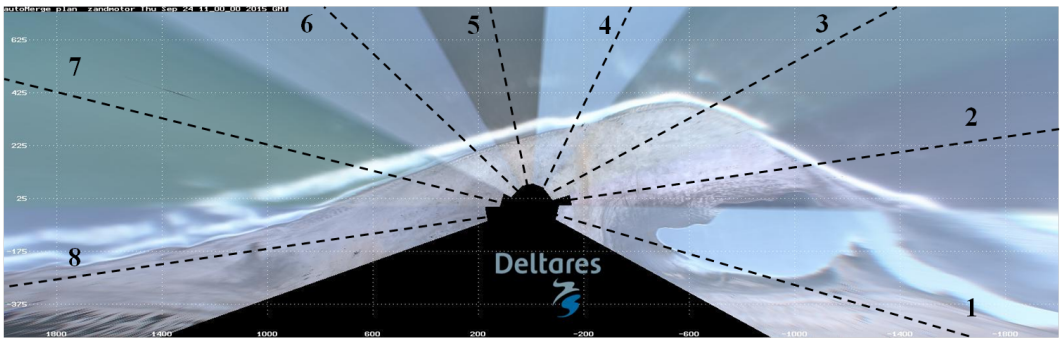

Figure 4.14: Plan-view of the Sand Engine 24-09-2015 constructed from 8 individual images. Central focus of each camera (1-8) is given with a dashed line. Adjusted from: argus-public.deltares.nl, retrieved 17/12/2017.

information for this study. The publicly available Argus images are taken with an interval of 30 minutes. After extracting the Argus images from argus-public.deltares.nl (retrieved 17/12/2017), a comparison was made to the scarp data obtained from the topographical surveys also referred to as 'ground truth' (Figure B.6).

Detection of beach scarps using the Argus system proved to be rather challenging. The shoreline is located far away from the camera tower for the first years after construction, making it impossible to recognize a scarp (Figure B.6a). Although mounted on top of a 40 m tower, the Argus cameras still overlook the vertical beach scarps. This results in a high uncertainty for the visual assessment of beach scarp presence, note however that the detection of beach scarps became easier over time. This can be attributed to the shoreline retreat at the Sand Engine, decreasing the distance towards the scarps over time and providing the cameras with a better (top)view of the scarps.

Aside from the geometric limitations, the lighting plays an important role in determining the presence of beach scarps. Under most lighting conditions, differences in sand colours can either be attributed to two sources; the soil moisture content (1) or to the presence of a beach scarp casting a shadow on the foreshore (2). Under the correct lighting conditions (sunrise at the Sand Engine) a beach scarp will cast a visible shadow on the foreshore which can be distinguished from the differences soil colour in this region of the beach profile (Figure B.6b,c).

Despite the shortcomings presented, it is possible to detect beach scarps at the Sand Engine in some cases (Figure B.6b,c). From the assessment performed on images between 2013 and 2017, it was found that 'Camera 4' is best suited for beach scarp detection due to the combination of an oblique view on and close proximity to the shoreline. Due to the obstructed view towards the shoreline, determining the beach scarp height from these images is not effective and the seaward facing slope of the beach scarp cannot be determined. In sum, the detection of beach scarps from Argus images taken from the backshore is not recommended. This method is subject to human interpretation and only possible when the shoreline is close enough in combination with good lighting conditions. In the future however, Argus imagery might become more feasible due to the heads on view of the shoreline.

4.9. General conclusions

Whereas beach scarps are often associated with extreme erosion events, they have been found to form during relatively mild (storm) conditions at the Dutch Sand Engine ($\eta \sim 1.4$ m NAP, $H_{s,0} \sim 2.25$ m). The alongshore averaged behaviour showed that in general, the destruction of beach scarps at this nourishment can be explained by extreme storm events ($\eta > 2.1$ m NAP, $H_{s,0} > 3.9$ m). During these events regular overwash or even local inundation will occur, leading to a diffuse beach profile without a beach scarp. Upon analysing the destruction of individual beach scarps, it was found that not all destruction can be explained by extreme conditions. Drying and aeolian deposition in front of the scarp are required to explain ∼50% of the individual scarp destructions during relatively mild conditions.

The alongshore averaged formation and destruction of beach scarps at the Sand Engine can be directly related to hydrodynamic conditions: formation during relatively mild periods and destruction (overwash and inundation, ∼50%) during extreme conditions. The destruction of individual beach scarps on the other hand is also dependent on non-hydrodynamic forcing (drying and aeolian transport, ∼50%).

Detailed GPS measurements along the beach scarps of the Sand Engine, showed that the toe elevation is relatively constant and can be related to the hydrodynamic conditions prior to the measurements. It was found that the maximum swash elevation derived using Equation 4.1 equals the scarp toe elevation ($S_t = R'_{2\%}$). This implies that the spatial variability in beach scarp height is mainly governed by the nourishment platform elevation, one of the parameters in the design of beach face nourishments.

A 'fixed' beach scarp toe elevation around the maximum swash elevation was found for beach scarps at the Sand Engine, which implies that the spatial variability in beach scarp height is mainly governed by the nourishment platform topography.

Beach scarp detection based on Argus imagery is found to be difficult for the Sand Engine case. With photos taken from the backshore, specific lighting conditions are required to detect whether a beach scarp is present (rising sun). Without the lighting casting a shade on the foreshore, it is almost impossible to distinguish a steeper slope $\mathcal{O}(15^o)$ from a real beach scarp. A top or head-on view of the eroding shoreline would provide better opportunities for beach scarp monitoring, which might be possible in the future.

5

Geotechnical aspects

The literature review has shown that beach scarps around the world are capable of reaching heights of up to 3 meters. At the Sand Engine, the reported beach scarps have exceeded heights of up to 1.5 meters (de Schipper et al., 2017). With the findings of the previous chapter, which stated that the beach scarp height can be determined by the nourishment platform and maximum runup elevation, the theoretical maximum beach scarp height in the future could be up to 4.5 meters[1]. The question remains whether and how these beach scarps would be stable from a geotechnical point of view.

The stability of beach scarps is largely dependent on the soil stresses within the body of sand. This allows the beach scarp to attain nearly vertical slopes of $\mathcal{O}(90^o)$, even though the dry angle of repose is around 32^o. Soil suction can be divided into two components for (cohesionless) soils: matric and osmotic suction. The focus in this part of the study is on the matric suction, caused by the capillary action between the grains and water inside the material. The osmotic suction is assumed to be of an order of magnitude lower, but does aid in the overall stability of beach scarps in saline environments. In this chapter an analytical approach is used, in which the effective stresses (based on the matric suction) in unsaturated soils are combined with a Culmann-type analysis for slope stability. This analysis is performed using the data collected during field experiments at the Sand Engine. Sieve curves obtained near the scarps in 2015 were used for the geotechnical parameters in this analysis (Figure 5.1). The shell content is not taken into consideration for the stability calculations presented.

5.1. Effective stresses in (un)saturated slopes

The porosity of a soil determines the amount of 'empty' space within the grain skeleton. The presence of a liquid in this grain skeleton (usually water) affects the stresses at the contact points between the grains. For a fully saturated soil, the stresses in the particles are determined by the contact forces between the grains and the water pressure around the grains. These *effective* stresses govern the deformations in the grain skeleton, caused by rolling and sliding at the contact points between the grains. It is this theory that introduces the concept of effective stress in saturated slopes (Terzaghi, 1947). The effective stress σ' is defined as a difference between the total stress σ and pore pressure u_a,

$$\sigma' = \sigma - u_a \tag{5.1}$$

In this equation, it is assumed that the 'empty' space within the grain skeleton is completely occupied by a fluid (saturated). In the case of beach scarp stability however, the saturation during laboratory conditions was found to be in the order of 70% (Erikson et al., 2007). Therefore, this assumption is no longer valid and a different approach is needed to determine the effective stresses in unsaturated soils. The following extension to equation 5.1 was proposed by Bishop (1954),

[1] Assuming a maximum runup elevation (= S_t) of 2.5 m NAP and platform elevation (= S_c) of 7.0 m NAP

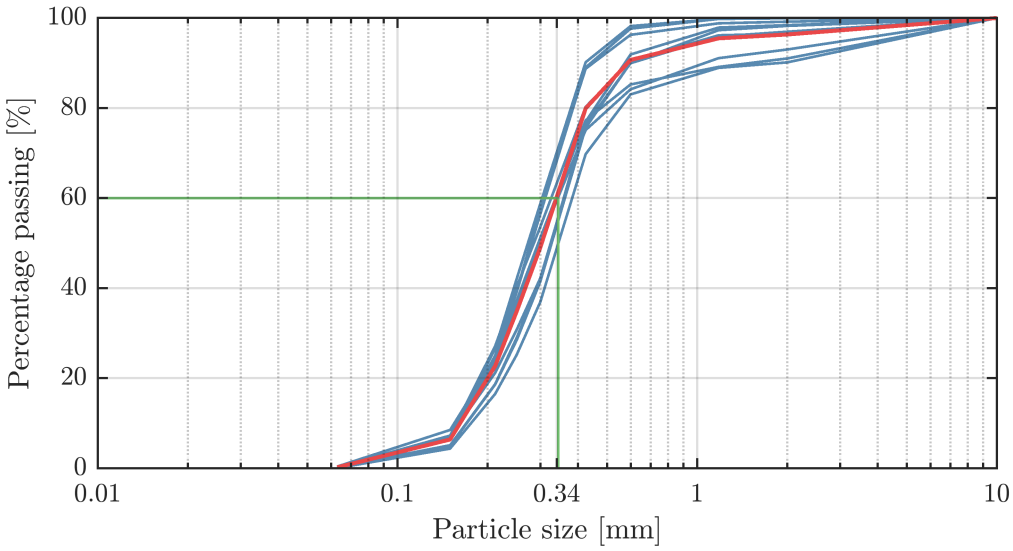

Figure 5.1: Sieving curves of sediment sampled from the beach scarp at the Sand Engine on 20-09-2015. The mean curve is given in red, in green the D_{60} of 0.34 mm is indicated.

$$\sigma' = (\sigma - u_a) - \chi(u_a - u_w) \tag{5.2}$$

In which u_a and u_w represent the pore air pressure and pore water pressure respectively. In turn, the matric suction is defined as $u_a - u_w$. After multiplying the matric suction with the Bishop effective stress parameter χ, the suction stress σ^s is obtained ($\sigma^s = \chi(u_a - u_w)$). The Bishop effective stress parameter χ can be replaced by the saturation S_e, leading to a formulation proposed by Lu and Likos (2004). This formulation is slightly modified with respect to Equation 5.2 and is based on the suction stress concept. Consistent with Equation 5.1, the effective stress can now be formulated as follows,

$$\sigma' = (\sigma - u_a) - \sigma^s \tag{5.3}$$

In which the suction stress is defined as,

$$\sigma^s = -S_e(u_a - u_w) = \frac{\theta - \theta_r}{\theta_s - \theta_r}(u_a - u_w) \tag{5.4}$$

In which the saturation (S_e), the residual volumetric moisture content (θ_r) and the saturated moisture content (θ_s) are represented. Combining Equation 5.3 and Equation 5.4 results in a more complete formula of the effective stress in unsaturated soils by Lu and Likos (2004),

$$\sigma' = (\sigma - u_a) - [-S_e(u_a - u_w)] \tag{5.5}$$

It can be seen that this equation reduces to the Therzagi formulation for saturated soils (eq. 5.1) if the pore volume is completely saturated (i.e. $u_a = u_w$).

Various models exist to determine the relationship between matric suction and saturation within soils. This relationship is referred to as the soil water characteristic curve (SWCC), which results in the soil suction characteristic curve (SSCC) when multiplied by the saturation itself. The most widely used SWCC model has been developed by van Genuchten (1980),

$$S_e = \left\{ \frac{1}{1 + [\alpha(u_a - u_w)^n]} \right\}^{1-1/n} \tag{5.6}$$

In which the fitting parameters α in kPa (air entry pressure for saturated soil) and n (pore size distribution) have to be determined in the lab, which is beyond the scope of this work. A more flexible SWCC relationship was formulated by Fredlund et al. (1994),

$$S_e = \left\{ \frac{1}{\ln\left[e + \left(\frac{u_a - u_w}{a}\right)^n\right]} \right\}^m \tag{5.7}$$

In this equation three curve fitting parameters are used; a in kPa, m (residual water content) and n. The fitting parameters a and n represent the same parameters α and n used in equation 5.6, but the flexibility of this model allows for determination of these curve fitting parameters using the D_{60} as a predictor according to Zapata et al. (2000),

$$\begin{aligned} z_a &= 0.8627(D_{60})^{-0.751} \\ z_m &= 0.1772|\ln D_{60}| + 0.7734 \\ z_n &= 7.5 \end{aligned} \tag{5.8}$$

The capillary action between fine grained soils is much larger than for that of coarse soils, resulting in a lower matric suction for the latter. The matric suction furthermore reduces with increasing amounts of saturation, until the material is fully saturated ($u_a - u_w \approx 0$) (Figure 5.2). For complete dryness ($S_e = 0$), the matric suction approaches infinity. The SSCC for both silt and sand start at zero when completely dry and reach their absolute maximum around 75% saturation, after which it returns to zero when fully saturated (van Genuchten, 1980). A major difference between the two SWCC models presented is that the Fredlund and Xing model produces a very high matric suction for low saturation values in sand, which is thus reflected in the shape of the SSCC (Figure 5.2). It can be said that the SSCC calculated with the combination of equations 5.7 and 5.8 fails for low saturation values, as the limit for the suction stresses corresponding to dry sand in reality is zero (whilst a high matric suction is present of course). For our region of interest, the zone around $S_e = 0.70$ is of most interest, as this value has also been reported to be the saturation of beach scarps during laboratory conditions (Erikson et al., 2007). It is assumed that this region is well represented by the proposed combination of the Fredlund and Xing model and the Zapata curve fitting formulas. As expected, the matric suction and suction stresses for the material found at the Sand Engine is lower than the general curve presented (Sand[a]). This is can be attributed to the relatively coarse material at the Sand Engine, leading to a lower amount of capillary action at the same degree of saturation for finer material.

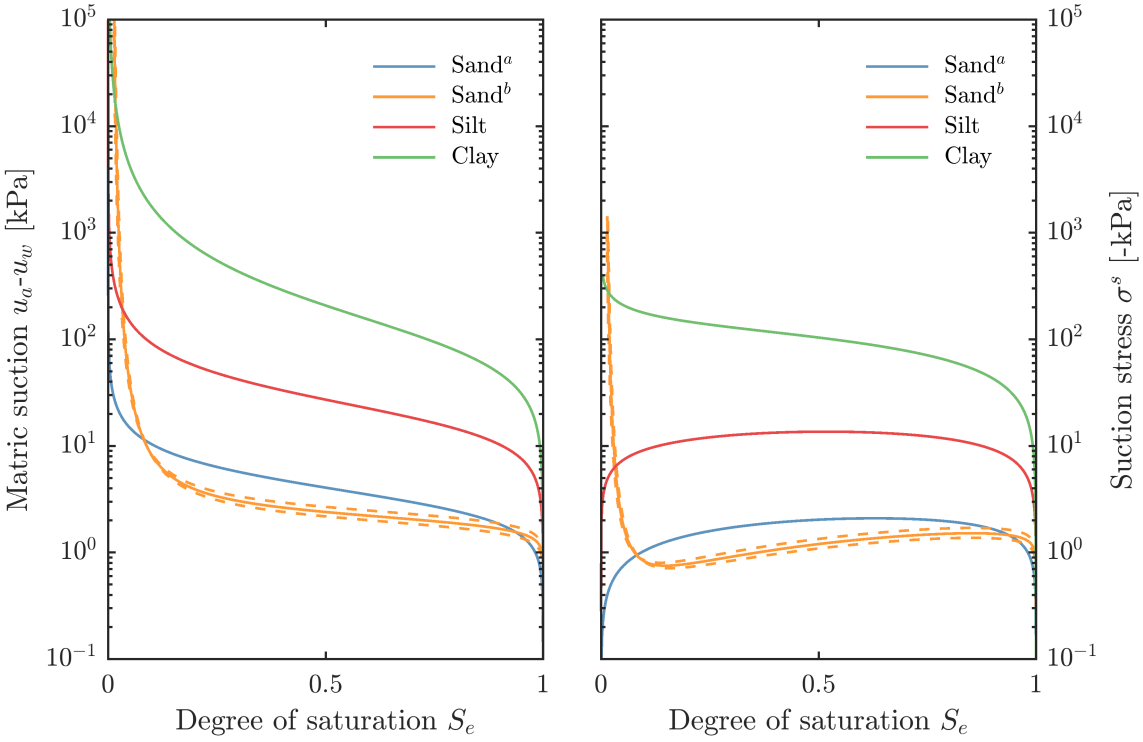

Figure 5.2: SWCC (left) and SSCC (right) based on the suction stress concept (Eq. 5.3) and the van Genuchten model for saturation (Eq. 5.6) for sand^a (α = 0.3 kPa^{-1}, n = 2.0), silt (α = 0.05 kPa^{-1}, n = 2.5) and clay (α = 0.01 kPa^{-1}, n = 1.8). The SWCC curve for the Sand Engine specific sand^b (D_{60} = 0.34 mm $\pm$ 0.05 mm) was obtained with the Fredlund et al. saturation model (5.7) and the parameter relationships based on the D_{60} presented in Zapata et al. (2000) (eq. 5.8).

5.2. Culmann-type failure analysis

Two modes of mass-failure have been defined for the migration of beach scarps in the theoretical background: shear-and beam-type failure. The first failure mode results from undercutting of the beach scarp face followed by slumping of the overhanging material. The second mode occurs when tension cracks reach an internal failure plane within the beach scarp. Shear-type failure is only initiated upon wave attack, it is therefore assumed that the geotechnical limitation to beach scarp height is determined by a beam-type failure mechanism. Although it is commonly accepted that slope failures occur on curved failure surfaces, a linearly sloping plane was assumed in the Culmann-type analysis performed for this study (Figure 5.3). This failure plane intersects with the toe of the beach scarp and fails when the average shear stress τ_s exceeds the average shear strength τ_f. After balancing τ_s and τ_f and obtaining the critical stability for a given slope, the following general Culmann-type analysis can be derived (Das and Sobhan, 2013),

$$S_{h,cr} = \frac{4\sigma_c}{\gamma}\left[\frac{\sin i \cos \phi'}{1 - \cos(i - \phi')}\right] \tag{5.9}$$

In which the critical beach scarp height is represented by $S_{h,cr}$, the beach scarp slope by i, the unit weight of the soil γ and the internal friction angle between the sand grains ϕ'. Two important aspects have to be considered when applying this type of analysis to the stability of beach scarps; the cohesionless property of beach scarp material (1) and the alongshore variability in beach scarp characteristics such as height and slope (2). The cohesive stress can be substituted by the suction stress for cohesionless soils described in the previous paragraph. This leads to a similar equation as presented in Morse et al. (2014) for the stability of a vertical cut[2],

$$S_{h,cr} = \frac{4\sigma^s}{\gamma}\left[\frac{\sin i \cos \phi'}{1 - \cos(i - \phi')}\right] \tag{5.10}$$

In which the cohesive stress σ_c of equation 5.9 is thus replaced by the suction stress σ^s. From recent surveys at the Sand Engine, it has been shown that an alongshore variability of scarp height is present at the Sand Engine (Figure 4.10). This will lead to local failures affected by non-failing parts of the beach scarp, which could lead to a higher overall stability. For the analysis presented in this study however, the effect of an alongshore variability of beach scarp characteristics is neglected. Assuming that the stability of vertical slopes is not influenced by the alongshore variation generally holds according to Taylor (1948), but at laboratory scales a different approach including the edge effects have to be taken into account (Morse et al., 2014). For the slope failure analysis presented in this study, the general Culmann-type analysis is sufficient to obtain an estimate for the geotechnical stability of beach scarp heights (at the Sand Engine).

Based on the derived Culmann-type analysis (Equation 5.10), it is now possible to determine the geotechnical limit of beach scarp height and slope combinations. To perform this analysis, the geotechnical (unit weight, internal friction angle, maximum suction stress) and geometrical (slope) properties of the beach scarp have to be determined. The specific unit weight of the material present at the Sand Engine is estimated to be 18 kN/m^3. Due to the relatively coarse material of nourished sand at the Sand Engine, the internal friction angle of the sand is estimated to be more than 32^o. In order to take the density (compaction) of the material into account, the internal friction angle was increased to 45^o. This can be seen as a *practical* approach to include the effects of dense sands, but is not theoretically robust (Winegardner, 1995). Based on these values, a large range in maximum beach scarp height can be observed as a function of suction stress σ^s and the scarp slope i (Figure 5.5). It is furthermore shown that the beach scarp height is inversely related to the scarp slope and suction stress.

The range of suction stresses has been determined using the Fredlund and Xing saturation model (Equation 5.7 and Equation 5.8) with a D_{60} of 0.34 mm is between -1.44 and -1.52 kPa. This

[2] As mentioned in Morse et al. (2014), the presented stability analysis does not take the constraints in the third dimension into account. In the case of beach scarp stability, this dimension is represented by the alongshore direction.

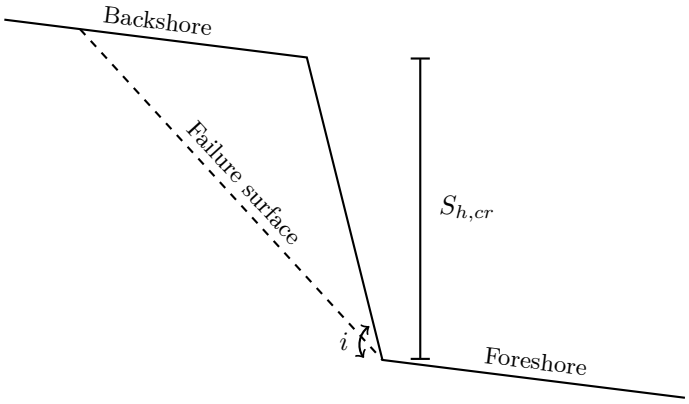

Figure 5.3: Culmann-type failure applied to the stability of a beach scarp positioned between the fore-and backshore with the critical height $S_{h,cr}$ and slope i.

was determined at saturation levels between 0.7 and 0.8, which is similar to the saturation levels found in laboratory experiments (Erikson et al., 2007; Palmsten and Holman, 2011). The calculated suction stresses are smaller, in absolute sense, than those presented in their studies ($\sigma^s \approx$ -2.41 kPa; $\sigma^s \approx$ -1.98 kPa). This is not surprising as a finer material (D_{50} = 0.13 mm; D_{50} = 0.23 mm) was used in the laboratory experiments, which is capable of producing higher suction stresses.

The range of beach scarp slopes has been determined from laser measurements performed during surveys at the Sand Engine on 24/09/2017. During this experiment, beach scarps were present at the head of the mega-nourishment. The obtained topography using a laser scanner provided useful information about the (maximum) slopes that were found for these scarps. The maximum slopes on two beach scarp sections ($S_h > 1$ m) are on average 67^o, with 62^o and 71^o being the 25th and 75th percentile respectively (Figure 5.4). The critical beach scarp heights are 3.0 m, 2.1 m and 4.8 m respectively (σ^s =-1.5 kPa), indicative of the strong relationship between the scarp slope and scarp height. A lower scarp slope allows for a much higher face to remain stable. The geotechnical limit of beach scarp heights at the Sand Engine under a slope of 67^o is in the order of 3 m, but more gently sloping scarps ($i < 60^o$) are capable of reaching heights of up to 5 m.

Based on the presented values above (referred to as the best estimate), a sensitivity analysis was performed Figure 5.6. For this test, the parameters of Equation 5.10 were increased and decreased by a maximum of 10%. From this analysis it can be seen that the various parameters produce the expected changes in critical beach scarp height. An increase in beach scarp slope results in a lower critical beach scarp height, whereas larger values for the natural angle of repose produce higher beach scarps. Increasing suction stresses provide the beach scarp with additional 'fictitious' cohesion, whereas a large specific unit weight will cause the scarp to collapse faster (i.e. lower critical height). It can be seen that the beach scarp slope has the largest impact on the critical beach scarp height based on a geotechnical analysis (Figure 5.6). The natural angle of repose furthermore has a large impact on the critical beach scarp height. Changes in suction stress and specific unit weight have a relatively small impact on the critical beach scarp height.

5.3. Cementation, compaction and shell content

In general, the stability of beach scarps can be attributed to the apparent cohesion generated by moisture inside the soil skeleton. But for some cases cementation of these features has been observed on artificially replenished beaches (Zarkogiannis et al., 2018). This can result in the formation of rather strong and persistent beach scarps, which are not easily destroyed by natural processes (wave overtopping or drying). Human intervention is therefore required to remove these beach scarps. Also referred to beach cliff formation, this process has been attributed to a compacted layer in the past. It was hypothesized that the 'bulldozing' of nourished material

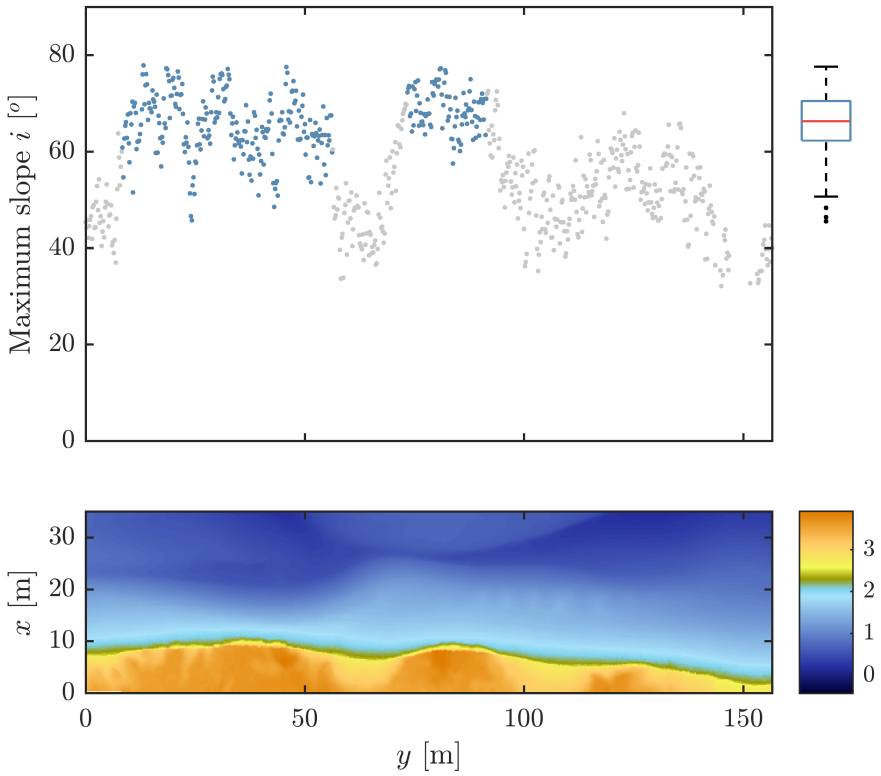

Figure 5.4: Maximum profile slopes for every 0.2 m (upper panel) of a measured beach scarp at the Sand Engine on the 24th of September 2017 (lower panel). The slopes for which the scarp height exceeded 1 m are highlighted in blue and summarized in the boxplot.

could lead to a decrease in porosity, resulting in a compacted layer susceptible to beach cliff formation (Mcfarland et al., 1994). New findings have shown that additional mechanisms (partly initiated by the 'bulldozing' of replenished material) aid in the stability of these beach scarps. Clay bridges can form between the densely-packed grains, leading to cementation of the material. These bridges are formed as a response to percolating water (which transports fine material) into the nourishment platform. These fines end up clogged in the densely packed intermediate layer, promoting the formation of cementing agents reaction with dissolved calcium[3].

Their study claims that *all* beach scarps on replenished beaches are a product of chemical processes, whereas beach scarps at natural beaches are created by physical processes (Zarkogiannis et al., 2018). This generalization can be rather misleading, as for example cementation has not been observed for beach scarps at the Sand Engine. This could be attributed to the relatively low carbonate content (as the nourished material originates from offshore). The conceptual model of nourishment cementation does allow for several mitigation measures to prevent the formation of cemented beach scarps:

- Reduction of the carbonate and fine content in the suppletion material.
- Increasing the presence of organic matter will hinder clay reactivity, and therefore reduce the amount of cementation.
- Scheduling beachface nourishments during periods with increased precipitation will lead to lowering of pH-levels and washing out of the fines.

[3]Originating from (mollusc) shells within the nourished material ions are necessary for the formation of cementing agents.

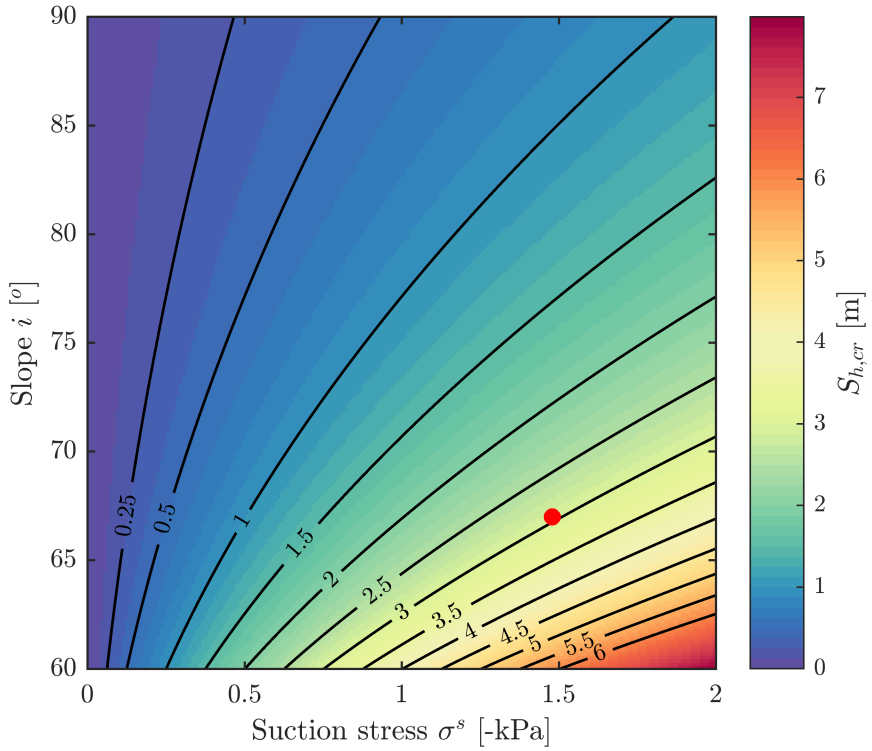

Figure 5.5: Maximum beach scarp heights at the Sand Engine as a function of the suction stress σ^s and the scarp slope i. The maximum beach scarp height for average values of the slope and suction stress is indicated in red, $S_{h,cr} \approx 3$ m.

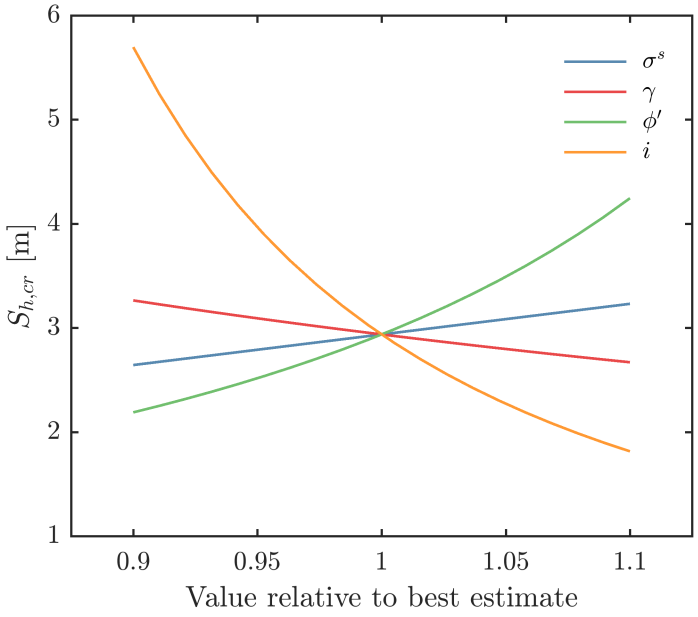

Figure 5.6: Sensitivity of the presented Culmann-type analysis (Equation 5.10) for the different parameters. Parameters plotted represent the suction stress σ^s, specific unit weight γ, natural angle of repose ϕ', beach scarp slope i.

- Subsequent 'bulldozing' is preferably avoided, but if necessary this should be performed after rain events to reduce the clogging of fines.

As previously mentioned, cementation has not been observed for the beach scarps at the Sand Engine. This leads to the need for additional mitigation methods to prevent the formation of beach scarps. A rather high shell content has been observed on some scarp sections at the Sand Engine, whereas a negligible amount of shells was present on others. The shell content might therefore aid in the stability (of dry scarps), but was thus not found to be essential.

5.4. General conclusions

The apparent cohesion produced by the suction stresses within sandy beach scarps can be used to determine the critical combination of height and slope of these features. If this height (or slope) is exceeded, mass failure of the beach scarp will occur which results in a more gentle overall slope and a sediment deposition at the scarp toe. A saturation model based on the D_{60} grainsize parameter was used to determine the maximum suction stresses for material at the Sand Engine. This apparent cohesion was used in a Culmann-type stability analysis to compute the critical combination of beach scarp height and slope dependent on a set of geotechnical and geometrical parameters.

A Culmann-type stability analysis has shown that the beach scarp slope has a large influence on critical beach scarp heights; small scarps of $\mathcal{O}(1$ m) can remain stable under almost vertical slopes of $\mathcal{O}(90^o)$, whereas scarps of $\mathcal{O}(5$ m) can only remain stable under relatively gentle slopes of $\mathcal{O}(60^o)$.

Laser measurements performed during a field survey at the Sand Engine have shown that the beach scarp slopes were on average much lower than vertical (67^o, on 24/09/2017). In order to obtain the best estimate for the maximum beach scarp heights at the Sand Engine under this slope, the natural angle of repose was increased to account for the compacted material. Based on this value, a geotechnical limit to beach scarps at the Sand Engine under the measured slope of 67^o was found to of $\mathcal{O}(3$ m).

By incorporating the findings of chapter 4, this simplified geotechnical analysis provides a practical method to determine the critical beach scarp slope associated with the scarp height. It has to be kept in mind however, that drying will affect the apparent cohesion of the material over time, possibly leading to removal of the scarp.

As the beach scarp height is determined by the backshore topography and wave runup (chapter 4), a geotechnical assessment based on the apparent cohesion of the sandy material provides insight into the corresponding critical beach scarp slope.

6

Beach scarp creation experiments

To gain a better understanding into the formation of beach scarps, field experiments have been conducted at the Sand Engine. With beach scarps forming at this nourishment during summer-storm conditions, this site provides a perfect setting for field experiments into beach scarp morphodynamics. Both the long term data and the detailed measurements (chapter 4) have been used to obtain a better understanding of the existence and characteristics of beach scarps at the Sand Engine. Field experiments, in which various geometrical parameters can be altered, are required however to further improve our understanding of the individual processes (formation, migration, destruction). Especially the monitoring of beach scarp formation will allow for the validation of conceptual models in the future. Two field experiments have therefore been performed in this study. For both experiments, artificial mounts were constructed from locally available sand on the intertidal beach at the 'head' of the Sand Engine (Figure 6.1a).

In total, five mounts with different platform heights and initial slopes were constructed using a front loader (Figure 6.1b). The first experiment (A) focussed on the profile development for mounts with different initial slopes $\tan\beta_i$ (0.1, 0.2). The second experiment (B) focussed on the profile development for mounts with different platform elevations $h_{n,p}$ (1.0, 2.0, 2.5 m NAP). After construction of each experiment, the mounts were monitored over a period of 16 tidal cycles with various wave conditions. For a detailed overview of the materials used for monitoring, the reader is referred to Appendix C.

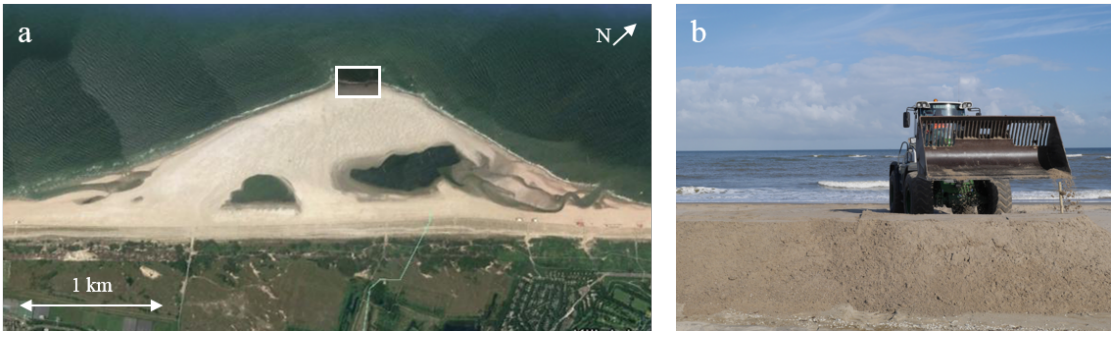

Figure 6.1: a) Location of the beach scarp creation experiments at the Sand Engine 'head'. b) The front loader used to create the artificial mounts studied for this thesis.

6.1. Experiment A: Nourishment slope

On the 21st of July 2017, two artificial mounts were constructed with similar platform heights but different initial slopes based on the design presented in Figure 6.2. These mounts were constructed on the intertidal beach at the 'head' of the Sand Engine using a front loader. Following the hypotheses presented in chapter 3, it was expected that both slopes could result in

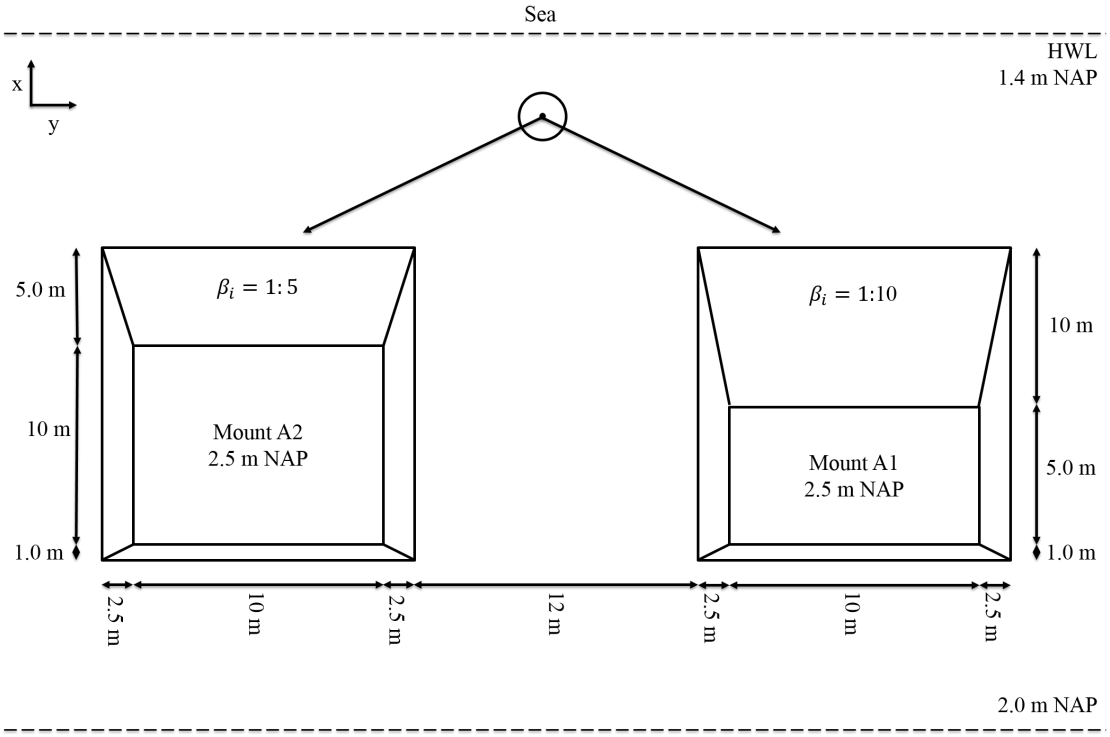

Figure 6.2: Schematic design (not to scale) of beach scarp creation experiment A. In this design, the two mounts are given with a platform elevation of 2.5 m NAP and initial slopes of 1:5 (left) and 1:10 (right). Arrows directed towards the mounts indicate the direction of the camera view.

the formation of a beach scarp under the assumption that favourite conditions persisted for long enough. These conditions can be described as wave attack on the nourished slopes ($h_{n,t} < R'_u$) without excessive overwash or inundation ($h_{n,p} < R'_d$). In order to ensure similar hydrodynamic conditions for both slopes, the toe and crest levels were constructed on similar elevations ($h_{n,t}$ = 1.4 m NAP, $h_{n,p}$ = 2.5 m NAP). The toes of the nourished mounts were thus constructed just above the high water level (MHW $\sim$ 1.2 m NAP), allowing for construction during low water and subsequent monitoring of wave attack during high water. This vertical position on the intertidal beach furthermore limited the possibility of complete inundation during mild conditions. Assuming alongshore uniform wave conditions for both mounts, the amount of overwash was expected to be similar. The mount with the steepest initial slope would then (according to the hypothetical model of chapter 3) be the first to produce a beach scarp. The most gently sloping mount (A1) was constructed with an initial slope of 1:10 whereas mount A2 was constructed with an initial slope of 1:5. Due to the very gentle slope at the intertidal beach, significantly more material was required for construction of the mounts than initially anticipated. Mount A1 was constructed according to the design with a volume of approximately 100 m^3. Construction of mount A2 had to be stopped early which lead to a smaller mount than initially designed (Figure 6.5, top right). The limited size of mount A2 (with a volume of approximately 50 m^3) made this mount more susceptible to potential edge effects (i.e. flow around the experiment).

Monitoring of this experiment was done between the 21st and the 29th of July, with topographic measurements taken on 7 days (Figure 6.4). These daytime surveys mainly consisted of taking GPS measurements and photographs during low tide. No night surveys were performed for this experiment. Daytime video recordings of both mounts under wave attack were only taken during the first and fifth day of this experiment.

6.1.1. Observations

The first days after construction of the experiment, the conditions were not energetic enough to alter the slopes of the mounts. Changes to the slope of the mounts became visible after the

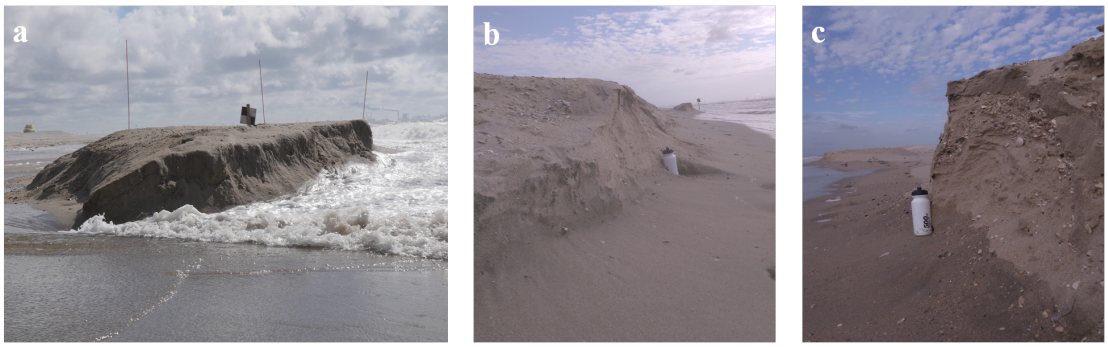

Figure 6.3: Photographs taken of the two artificial mounts constructed for this experiment. a) Mild uprush attacking the northern *scarp* of mount A2 during the survey on day 5 (25-07), accompanied by backwash/flow around the mount eroding the northern side of this mount. Note the steep profile caused by erosion on the lee side. b) Side-view of the beach scarp present at mount A1 on day 7 (27-07). c) Side-view of the beach scarp present at mount A2 on day 7 (27-07). Water bottle (0.2 m) as reference.

first high tide of day 5. The conditions led to the formation of a *scarp*[1] on the southern and the northern side of mount A2 (heights of 0.3 and 0.5 m respectively, Figure 6.3). The formation of these vertical cuts was most likely influenced by the flow of water around the mount, which was visible during the second high tide of day 5. The flow of water in a perpendicular direction to the *scarp* orientation resembles the formation of *scarps* during riverbank erosion, which was described in chapter 2. Based on these steep slopes behind mount A2, it can be concluded that water flowed around this mount during the first high tide. During the second high tide, flow around mount A2 continued and swash uprush impacted the *scarps* (Figure 6.3a). No *scarps* were observed at mount A1, but the slopes became noticeably steeper, with the steepest parts on the corners under wave attack.

A beach scarp (S_h = 0.5 m) first formed along the entire width of mount A2 during high tide between day 5 and day 6. During the high tide between day 7 and day 8, a beach scarp formed along the entire width of mount A1 (Figure 6.3b) and the height of the scarp at mount A2 increased. Both beach scarps had maximum heights between 0.5 and 0.6 m (Figure 6.3b-c).

Complete destruction of the mounts occurred during the final days (28-29) of this experiment, resulting from a summer storm. During these energetic conditions, a 'natural' beach scarp formed more landward with a length of 250 m and heights of up to 0.70 m (Figure B.4) .

Apart from these observed topographical changes, it was noted that the moisture content of the scarps remained relatively high between the surveys. Furthermore, it was observed that the scarp face of mount 2A remained stable despite the lack of a high shell content (Figure 6.3a). More shells were found on the scarp of mount A2 during the survey on day 7. These shells were not uniformly distributed along the scarp face and were not observed on mount A1 (Figure 6.3b-c). The stability of the scarps was high enough to perform GPS measurement without initiating beam-type failure (which might have resulted from the high moisture content). Shear-type failure was easily caused on the crest of the scarps, requiring the surveyor to perform measurements with minimal pressure on the crest.

6.1.2. Results and discussion

The results presented in this section focus on the topographic changes in relation to the hydrodynamic conditions during this experiment. First, an overview of the hydrodynamic conditions during this experiment is given. Second, the topographic results are presented and discussed.

[1]Note that the term used does not refer directly to a beach scarp. Edge effects might have played a major role in the formation of these features, which makes these *scarps* unsuitable to determine geometrical parameters related to beach scarp formations (e.g. toe height S_t).

Table 6.1: Detailed overview of the hydrodynamic conditions during each high tide of Experiment A: Nourishment slope. High tides during which the formation of a beach scarp occurred are given in bold.

	Date	η [m NAP]	$H_{s,0}$ [m]	T_{m02} [s]	θ_0 [^{o} N]
Day 1	21-Jul-2017 13:55	1.10	0.70	3.5	206
Day 2	22-Jul-2017 02:15	1.14	0.74	3.8	74
	22-Jul-2017 14:45	1.12	0.81	3.7	226
Day 3	23-Jul-2017 03:05	1.24	0.77	3.5	231
	23-Jul-2017 15:35	1.14	0.92	3.4	231
Day 4	24-Jul-2017 03:55	1.32	0.72	3.7	227
	24-Jul-2017 16:35	1.14	0.80	3.7	345
Day 5	25-Jul-2017 04:45	1.37	1.09	4.3	345
	25-Jul-2017 17:15	1.14	1.54	4.7	341
Day 6	26-Jul-2017 05:25**A2**	1.39	1.22	5.9	355
	26-Jul-2017 18:05	1.12	0.77	3.5	254
Day 7	27-Jul-2017 06:05**A1**	1.37	1.4	4.3	237
	27-Jul-2017 18:35	1.09	1.6	3.9	230
Day 8	28-Jul-2017 06:55	1.32	1.68	4.2	238
	28-Jul-2017 19:35	1.05	2.83	4.9	228
Day 9	29-Jul-2017 07:45	1.23	2.34	5.3	230

Hydrodynamics

The measured offshore wave conditions were taken from Europlatform and water levels were measured at Scheveningen. For the analyses presented in this chapter, the water level time series was shifted by 15 minutes in order to accommodate for the difference of the tide between Scheveningen and the Sand Engine. Furthermore, the offshore waves were transformed to Sand Engine specific conditions (Figure 6.4). The method used for this transformation was explained in section 4.3. When transforming wave conditions using a transformation matrix, the values outside of the domain are not processed. This means that waves originating between 30 to 180^o will not result in a transformed wave height using this method. Wave runup was therefore calculated using the transformed wave conditions where available, but otherwise the offshore wave conditions were used.

The first days of the experiment (1-4) conditions were rather mild, with a maximum $H_{s,0}$ of 0.92 m and a maximum water level of 1.32 m NAP. These conditions gradually changed to energetic between the day 4 and day 7, with transformed wave heights reaching a maximum offshore wave height of 1.60 m. The conditions from day 8 to day 9 can be considered a summer-storm for the Dutch coast. As stated in the observations, a 'natural' beach scarp formed along certain parts of the SE perimeter.

The formation of a 'natural' beach scarp during experiment A was the result of (typical) summer storm conditions; max $H_{s,0} \sim 2$ m (transformed) and max $\eta \sim 1.5$ m NAP which is in-line with the findings of chapter 4 (Figure 4.6).

Topographic changes

For this experiment, the formation of beach scarps is dependent on the wave attack on the mounts. During the first days (until day 5) the mounts were not eroded by wave attack. On the contrary, the measurements show swash deposition in the region below 1.5 m NAP, which approximately equals the $R'_{2\%}$ during the high tide of day 4 (1.32 m NAP + 0.19 m = 1.52 m NAP). Minor erosion of each mount could be observed at the lee-sides during the calm conditions. Not caused by wave attack, this 'erosion' originates from human disturbance during the GPS measurements. The first erosion caused by wave attack started during high water on day 5 (Table 6.1). The topographic response behind mount A2 from this erosion event shows the formation of a 'gully' of which its orientation is in-line with the northerly waves on day 5 (Figure 6.5).

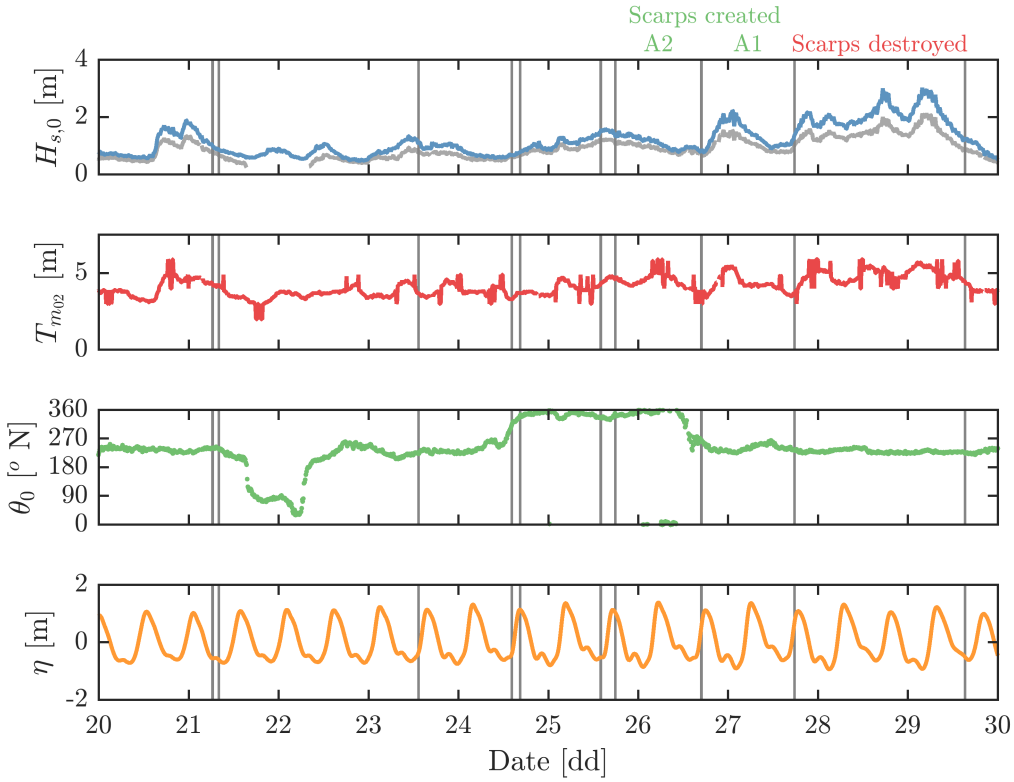

Figure 6.4: Offshore significant wave height ($H_{s,0}$, grey = transformed), mean wave period (T_{m02}) and offshore wave direction (θ_0) measured at the Europlatform presented in the top panels. The measured water levels at Scheveningen (η) are presented in the bottom panel, shifted by 15 minutes to account for tidal differences. Grey vertical lines indicate the survey moments during this experiment.

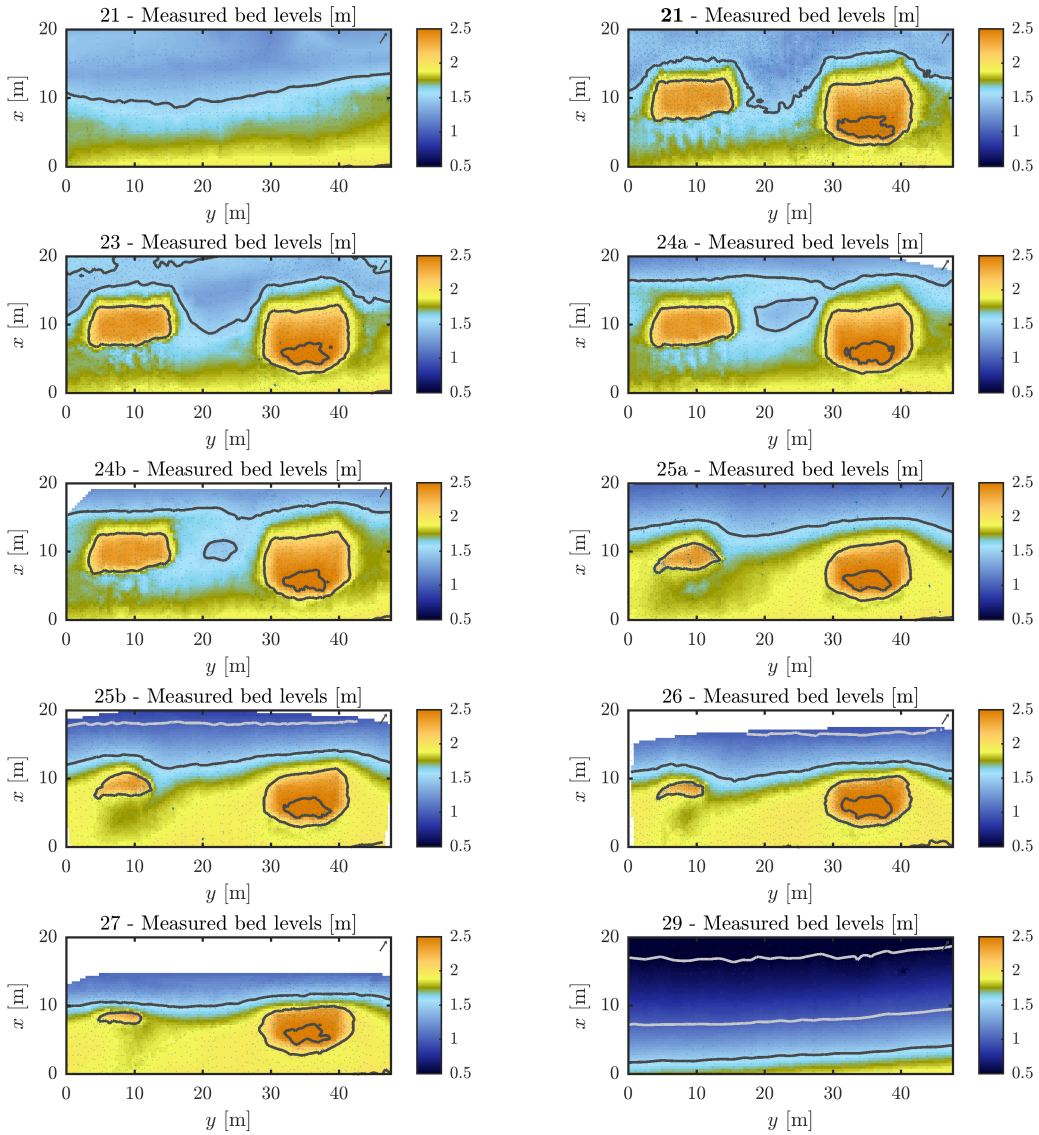

Figure 6.5: Measured topographies (GPS) for experiment A on the 21st, 23rd, 24th, 25th, 26th, 27th and 29th of July 2017. North arrow is given in the top right corners.

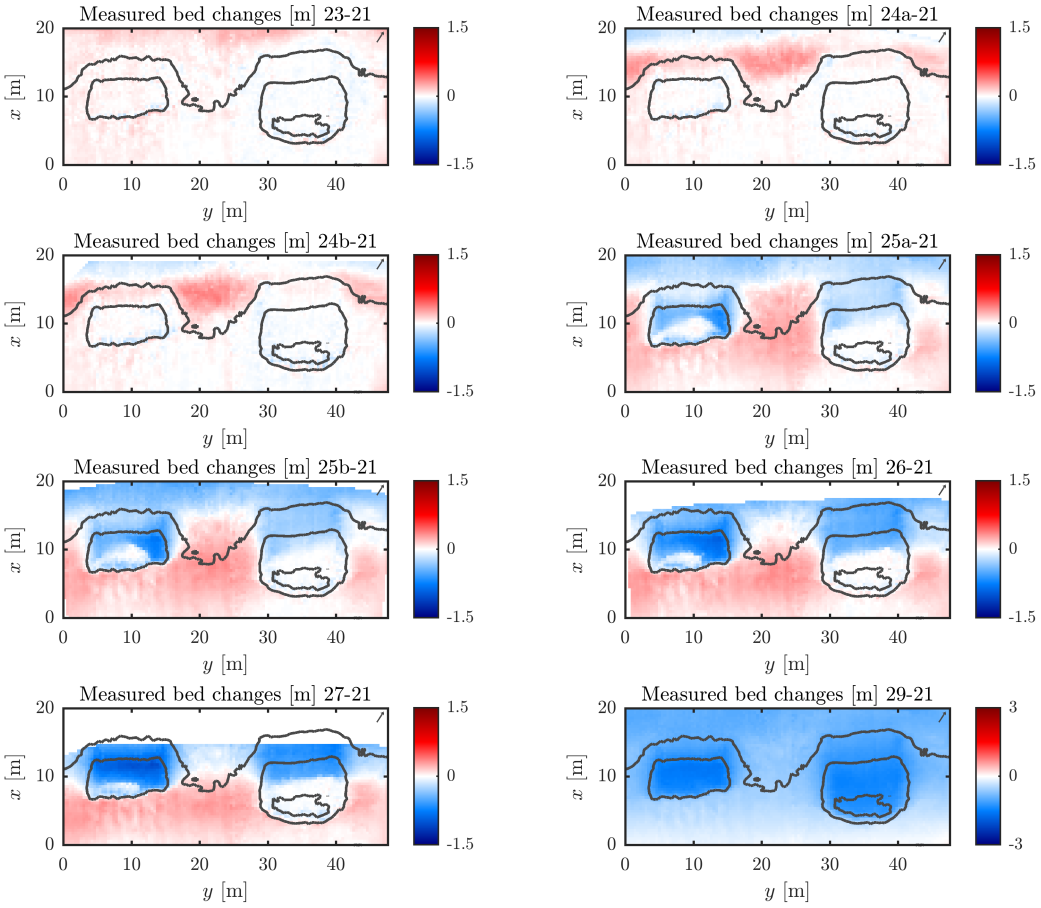

Figure 6.6: Bed level changes for experiment A on the 21st, 23rd, 24th, 25th, 26th, 27th and 29th of July 2017. North arrow is given in the top right corners.

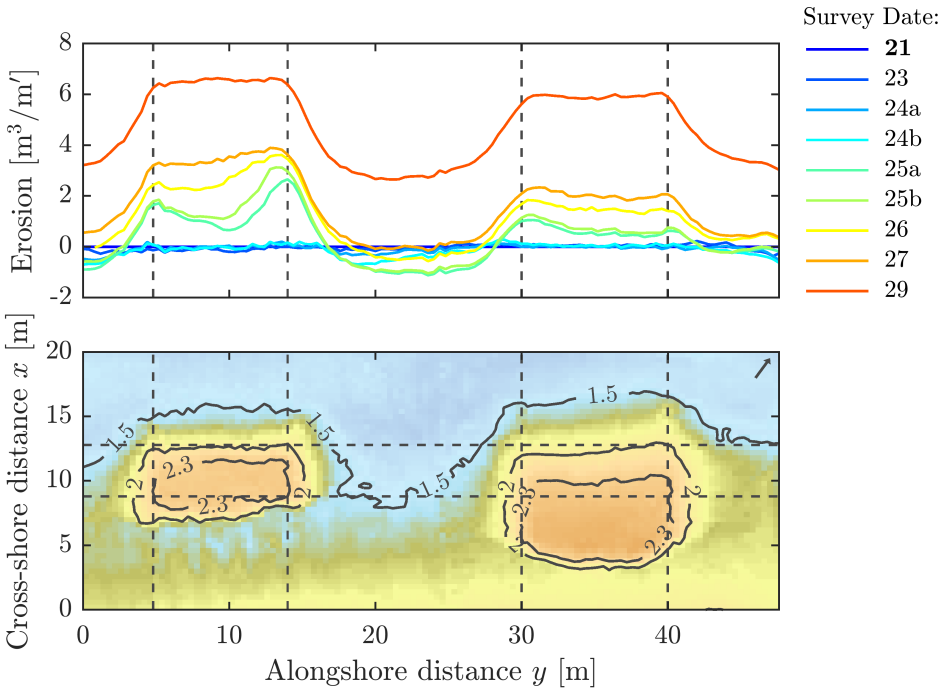

Figure 6.7: Visual representation of the cumulative erosion per running meter between $x = 9$ and $x = 13$ m for experiment A. Dashed vertical lines indicate the sides of each platform

Based on the measured topographies, the 2D effects can be assessed by means of integrating the bed level changes between two alongshore transects (Figure 6.7). For this experiment the following transects were chosen; $x = 9$ m and $x = 13$ m. These transects are bounded by the measurements performed on day 7 ($x = 13$ m) and the landward limit of mount A2 ($x = 9$ m). Based on the presented erosion patterns it can be clearly seen that the mounts started to erode on day 5 in an *alongshore non-uniform* manner. More erosion occurred on the sides of each mount when compared to the centre. For mount A1 this corresponded to 1.0 m^3/m' at ($y = 30$ m), 0.6 m^3/m' ($y = 35$ m) and 0.8 m^3/m' ($y = 40$ m). For mount A2 the edge effects were more severe, which was expected from this slimmer profile; 1.7 m^3/m' ($y = 4$ m), 0.7 m^3/m' ($y = 10$ m) and 2.7 m^3/m' ($y = 13$ m). The main cause for these severe edge effects were the uprush and downwash along the sides of each mounts. The seaward facing corners ($x = 12$ m) of both mounts were most affected as a result of the combined edge effects and regular swash attack. As a result, steep corners formed on mount A1 and *scarps* were present on the corners of A2 (Figure 6.3).

Cross-shore transects provide a good insight into the various stages of profile development of each mount (Figure 6.8). For this figure, the associated wave runup is calculated using equation 2.1 and the transformed wave conditions from the Europlatform (Figure 6.4). During the first days, the mild conditions did not erode the mounts as sedimentation (0.15 m) can be seen in front of mount A1. The reported *scarps* on either side of mount A2 observed on day 5 are not represented by the profiles taken from the centre, indicating that these features did not extend along the entire width of the mount.

The observed scarps on mount A1 (day 7) and A2 (day 6-7) are represented in the GPS profiles (Figure 6.8, black circles). These measurements clearly show that the beach scarps developed quicker for mount A2 than for mount A1, despite very similar hydrodynamic and geotechnical conditions.

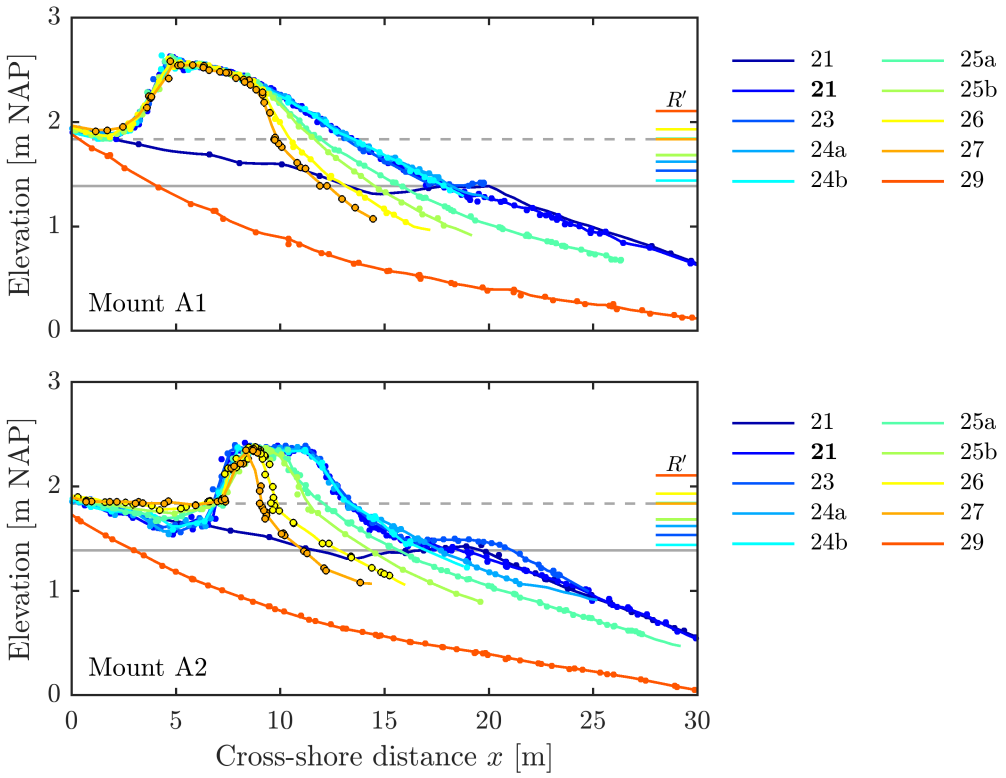

Figure 6.8: Profiles of mount A1 at $y = 35.5$ m (top panel) and mount A2 $y = 9.5$ m (bottom panel). Profiles measured in which a beach scarp was present are given with black outlined dots. The maximum water elevation η_{max} and maximum R' until the 27th of July 2017 are given in solid and dash-dot horizontal lines respectively.

Based on the cross-shore profile developments measured during experiment A, it can be stated that the rate of beach scarp formation (steepening of the upper slope) is related to the initial slope of the beach or nourishment.

The profiles of mount A1 overlap until a 'rotation point' at $x = 9$ m and $y = 2.3$ m NAP is reached. Interestingly, this is not observed for mount A2. For this mount we can see a retreat of the $y = 2.3$ m NAP platform level without the formation of a beach scarp between the 24th and 25th of July. This is could be related to overwash events between the two surveys, leading to a diffuse profile, although no evidence of the required hydrodynamic conditions for overwash was found. Another explanation could be human interference with the experiments which was observed during some of the field visits. The elevation behind mount A1 is quite constant, whereas sedimentation (0.3 m) occurred at the back of mount A2. Eroded material from the sides was deposited in these calmer zones behind the mount, resulting in a local increase in bed level (Figure 6.8).

For both beach scarps formed during this experiment, the toe elevation S_t equals 1.8 m NAP and the crest elevation S_c equals 2.3 m NAP. This resulted in similar beach scarp heights in the centre of both mounts of 0.5 m. Migration of the A2 beach scarp can be seen from the figure; a landward retreat of 0.78 m (measured from toe to toe) with negligible elevation differences of both crest and toe.

As mentioned in the observations, a summer storm caused complete removal of experiment A. This summer storm led to the formation of a 'natural' 250 m long beach scarp at the Sand Engine (with heights exceeding 0.7 m, Figure B.4). The scarp toe elevation was measured for this scarp, a mean elevation of 1.8 m NAP was found. This level is closely related to the $R'_{2\%}$ during the summer storm, which equalled 1.73 m NAP ($\eta = 1.05$ m NAP, $R_{2\%} = 0.68$ m).

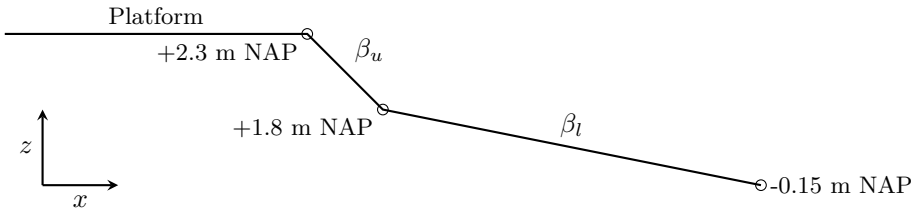

Figure 6.9: Visualization of the upper and lower slope (β_u and β_l) as defined for Experiment A: Nourishment slope.

Slope development

The cross-shore profiles show that the upper slope β_u steepened during the experiment until a beach scarp formed. The evolution of the lower slope β_l is not as straightforward however. Based on the cross-shore profiles presented, one might state that this slope remained almost constant throughout the experiment (Figure 6.8). The lower slope is defined as the slope between the offshore intersection point of the profiles (P, Figure C.2) and the MHW profile intersection. From this figure it is clear that before the experiment, mild summer conditions created a rather steep lower slope $\tan\beta_l = 0.079$ at the site. The following energetic conditions resulted in more gentle lower slopes $\tan\beta_l = 0.065$ (day 5) and $\beta_l = 0.043$ (day 9). Only the three presented datasets were suitable for determining point P, as the other measurements were limited to $x = 20$ m.

The upper and lower slope development of both mounts can be plotted over time (Figure 6.10). The lower slope β_l was calculated between point P (-0.15 m NAP) and the intersection of the profile with the 1.8 m NAP line (Figure 6.9). The upper slope β_u was calculated between the intersection of the profile with the 1.8 m NAP line (final scarp toe elevation) and the intersection with the 2.3 m NAP line (Figure 6.9).

For both mounts the upper slope steepened from the 25th of July until the 27th of July. The lower slope of both mounts decreased over time, but remained quite constant during the first days of the experiment after construction. The energetic conditions that followed reduced the slope gradually from 1:13 to 1:19. The upper profile (β_u) of both mounts steepened from the 25th of July until the end of this experiment (Figure 6.10). After the small summer storm during the end of the experiment the (lower and upper) slopes became more gentle due to the complete removal of the mounts. The calculated upper slopes which exceed the natural angle of repose of 32° are in-line with the observations and presented cross-shore profiles, in which three beach scarps are reported (1*day 7, 2*day 8).

6.1.3. Video observations

During the second high tide, cameras were used to capture the mass failure types of the northern *scarp* on mount A2. The majority of failures during these recordings were classified as shear-type (51), beam-type failure was less frequent (3). This could be attributed to the lack of compaction of both mounts after construction (Bonte and Levoy, 2015). Shear type failures were initiated by undercutting and the deposited material in front of the *scarp* was quickly removed by swash action. Partial beam-type failures were initiated by thorough wetting caused by overwash. The slumped material from these failures maintained its shape, which did not allow for quick removal by swash action. These partial beam-type failures are caused by the reduction in overturning moment, allowing for the shear stresses to find a new balance and stop the slumping of the material.

6.1.4. Summary - Experiment A

A prototype field experiment has been performed in which the topographical development of two artificial mounts with different initial slopes was monitored. The monitoring of these mounts lasted for 16 tidal cycles, during which both calm and energetic conditions were present. Beach scarps formed on both mounts but at different speeds; the rate of beach scarp formation is governed by the initial beach or nourishment slope. Beach scarps of reasonable size formed on these

uncompacted mounts, indicating that the suction stresses within the unsaturated soil provided enough stability. The type of mass-failures observed were mostly of the shear-type, which can be attributed to this same lack of compaction. It was found that for both beach scarps, the toe elevation could be approximated by the 2% exceedence runup elevation. Due to the fact that both mounts were constructed with similar platform heights, both beach scarps were of the same height; $S_h = 0.6$ m. These results support the finding that final beach scarp height is determined by the maximum runup elevation and the backshore topography (section 4.7).

This experiment showed that these type of experiments (morphological development from a linear slope) are suited to study the various phases of beach scarp morphodynamics. GPS measurements could only be performed during the day for this experiment. No data could therefore be obtained during the actual formation of the beach scarps (which happened during high tide at night). Very frequent measurements (preferably every high tide) are required to capture the complete beach scarp morphodynamics.

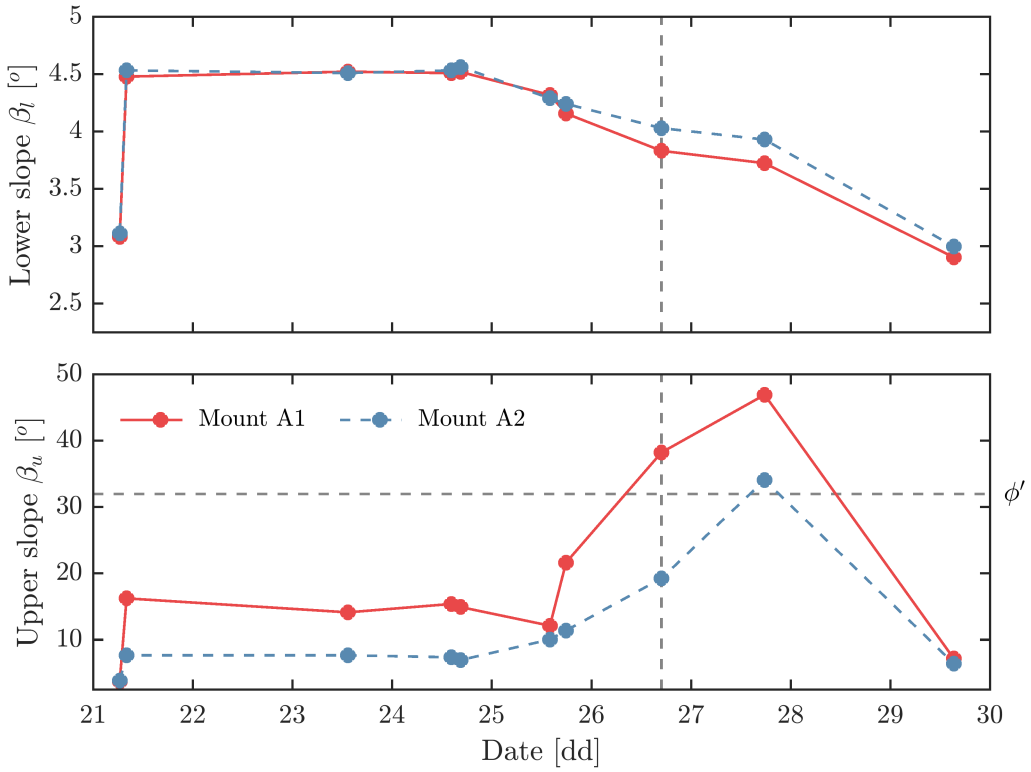

Figure 6.10: Slope development of both mounts in experiment A; lower slopes β_l (upper panel) and upper slopes β_u (lower panel). The horizontal grey dashed lines indicate the natural angle of repose for sand and the vertical dashed lines indicate the moment a scarp was first observed. Note that the upper slope exceeding the natural angle of repose match with the observations for this experiment.

6.2. Experiment B: Platform height

The platform height of a nourishment could be of great importance in the formation of beach scarps. This parameter was therefore studied in the second field experiment of this study. On the 25th of September, three artificial mounts were constructed with different platform heights and initial slopes (Figure 6.11). According to the hypotheses presented in chapter 3, scarps were expected to form on mounts where the overtopping is limited and no inundation occurred. The flow around mount A1 during the previous experiment turned out to have a significant impact on the alongshore erosion patterns in the previous experiment. In the design for this experiment, small cross-shore dams were therefore constructed which connected the edges of the experiment to the higher parts of the existing beach profile (Figure 6.14, top right).

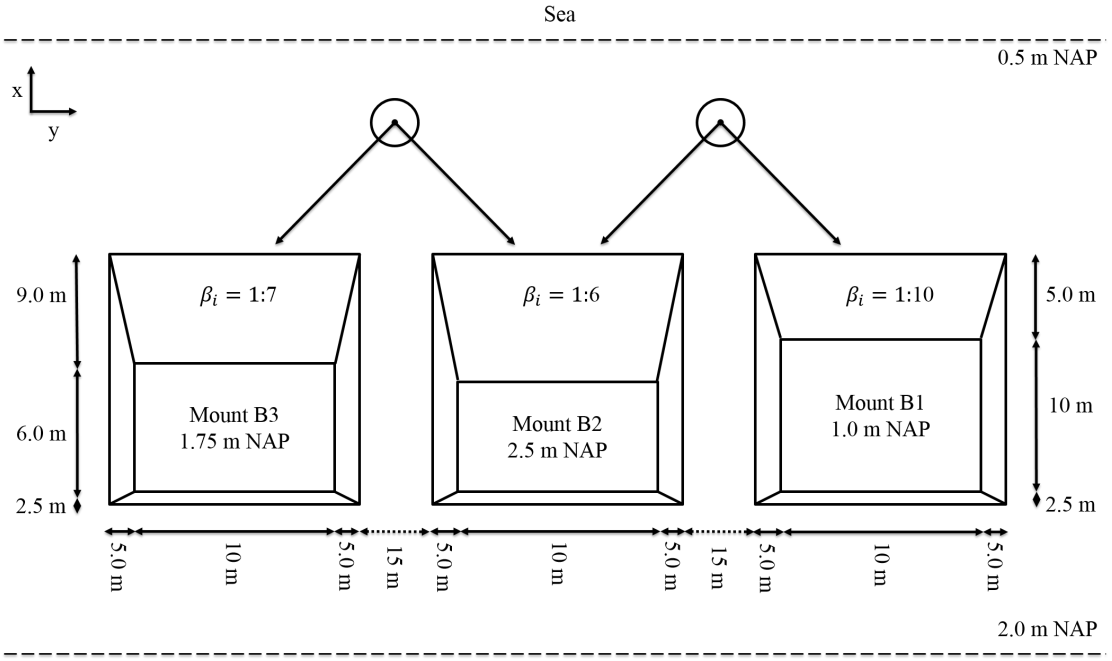

Figure 6.11: Schematic design (not to scale) of beach scarp creation Experiment B: Platform height. In this design, the three mounts are given with platform elevations of 1.0, 2.5 and 1.75 m NAP and initial slopes of 1:10, 1:6 and 1:7. Arrows indicate the direction of the camera view.

This experiment was constructed on top of a shoal on the intertidal beach in front of existing 'natural' beach scarps at the Sand Engine (Figure C.3). The toes of the mounts were constructed at $h_{n,t} = 0.50$ m NAP with platform heights $h_{n,p}$ of 1.0, 2.0 and 2.5 m NAP. The initial slopes of these mounts were 1:10, 1:6 and 1:7 respectively and were named from north to south; B1 (61 m^3), B2 (218 m^3), and B3 (161 m^3). It was expected that these mounts would result in different amounts of overtopping under the assumption of alongshore uniform hydrodynamic conditions. This would then result in different types of profile retreat; no scarp formation was expected for mount B1, whereas mount B2 was very likely to produce a beach scarp. For mount B3 alternating profiles were expected, during relatively mild conditions beach scarps might form, whereas these could easily be destroyed during the next energetic conditions.

Topographical monitoring of the mounts was done for 16 tidal cycles. Full low tide GPS and laser scan surveys were performed and cross-shore GPS measurements (10 minute interval) were done during each high tide. Video recordings were taken during every high tide for the first six days.

6.2.1. Observations

Erosion of the mounts started on the first high tide of this experiment (25/09/2017 18:00). During this high tide it was observed that mount B1 faced large amounts of overwash, whereas mounts B2 and B3 were not overtopped. The resulting profiles for these mounts were also very different; the profile of mount B1 retreated without large changes in its slope, on mount B2 a beach scarp ($S_h \sim 0.30$ m) formed, the cross-shore profile on mount B3 was found to become very steep without a beach scarp.

During the next high tide (26/09/2017 06:30) it was observed that mount B1 further eroded without beach scarp creation. The beach scarp on mount B2 was observed to migrate landward and grew to a height of approximately 0.50 m. A beach scarp formed on mount B3 with a height of approximately 0.30 m and migrated similarly to mount B2. During the described scarp migration of the mounts, sedimentation in front and between the mounts was observed. The cross-shore dams limited the flow behind the mounts for the first days of the experiment. No

Figure 6.12: Photographs taken of beach scarps at artificial mounts B2 and B3. a) Overview of the two scarps of mount B2 and B3 (left and right within image) on 26/09/2017 08:05. b) Detailed side-view of the beach scarp present at mount B2 on 26/09/2017 19:05. c) Swash impact and reflection on mount B3 on 26/09/2017 19:10. Water bottle (0.2 m) as reference.

signs of erosion from the back of the mounts could be observed.
From the 26th of September until the 2nd of October, the conditions were not energetic enough to alter the mounts. The formation of a sand bar in front of the mounts, caused the waves to dissipate most of their energy before being able to reach the mounts. No severe wind conditions were present during these days of the experiment, but the layer of shells on the platforms became more noticeable over time as a result of aeolian transport.

During the last measurements of this experiment (02/10/2017), a summer storm completely removed the remaining mounts. Mount B1 was already mostly eroded during the previous high tides and was now quickly inundated. Mount B2 remained until the beach scarp had reached the landward limit of the mount. This mount faced only occasional overwash, which was able to initiate beam-type failures of the beach scarp. Mount B3 faced significantly more overwash than B2, but the beach scarp persisted for most of the measurements. During these very energetic conditions, water was flowing between and behind the mounts with significant speeds. Erosion of the sides of mount B2 could be observed as a consequence of the water flowing between around the mounts; on the sides *scarps* were formed. A final check of the beach state was performed on the 4th of October. Upon arrival, a uniform beach profile could be observed and the existing 'natural' beach scarps had migrated and regained a steep scarp face (Figure B.5).

6.2.2. Results and discussion

Hydrodynamics

The same sources for the hydrodynamic data were used as in the analysis of experiment A; measured offshore wave conditions at the Europlatform (transformed according to section 4.3) and measured water levels in Scheveningen. Similar to the first experiment, the wave conditions were rather mild during the first days (25-09 to 29-09) of the experiment, with a maximum $H_{s,0}$ of 0.92 m. The waves became more energetic during the last days (01-10 to 04-10) of the experiments and can be classified as a summer storm conditions for the Dutch coast.

The migration of a 'natural' beach scarp during experiment B was the result of (typical) summer storm conditions; max $H_{s,0} \sim 1.9$ m and the max $\eta \sim 1.6$ m NAP which is in-line with the findings of chapter 4 (Figure 4.6).

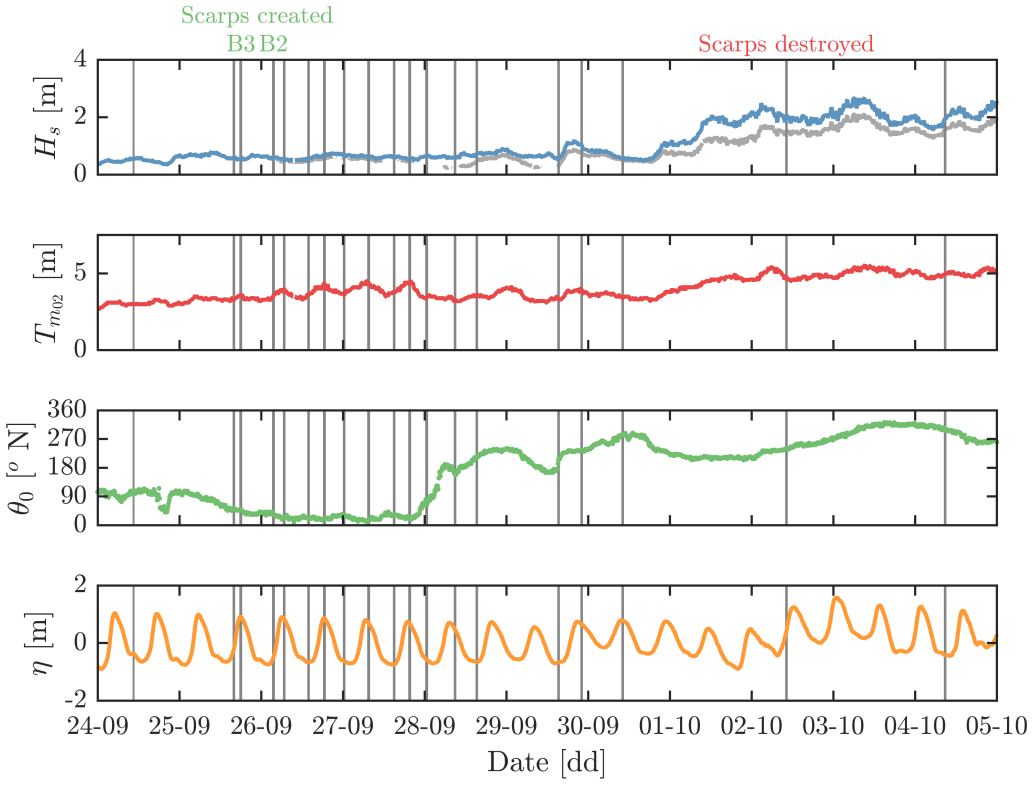

Figure 6.13: Offshore significant wave height ($H_{s,0}$, grey = transformed), mean wave period (T_{m02}) and offshore wave direction (θ_0) measured at the Europlatform are presented in the top panes. The measured water level at Scheveningen (η) is presented in the bottom pane, shifted by 15 minutes to account for tidal differences. Grey vertical lines indicate the survey moments during this experiment.

Topographic changes

As stated in the introductory section of this experiment, two types of topographic measurements were performed. A LiDAR laser scanner was used to obtain a detailed elevation map of the entire experiment field during low water and a GPS was used to obtain cross-shore profiles during wave attack at every high water. The results of the laser measurements[2] in which the beach scarp formation took place are discussed first. This is followed by the analysis of GPS measurements during wave attack for high tides.

Although similar to the mild conditions present during the first days of experiment A, erosion started on the first day of this experiment (Figure 6.14). This can be attributed to the fact that the slopes were placed lower in the profile ($h_{n,t} \sim 0.5$ m NAP). The plan view of the low tide topography between the 25th and 26th of September show that the initially rectangular nourishments reshaped into more diffuse forms (Figure 6.14). During the first high tide, mount B1 and the cross-shore dams faced large amounts of overwash, which explains some of the removed material at the lee side of this mount and the lowering of the dams. The bed level differences show that during the first high tide the removed sand from the mounts was mainly deposited between the mounts and on the stoss sides of the cross-shore dams (Figure 6.14). The accumulated sediment at the lee side of the southern dam is most likely material originating from the overtopped dam itself, whereas the sediment deposited behind the northern dam partly originates from mount B1. Some of the eroded material from the mounts has to have ended up in the lower beach profile, as a net loss of 40 m^3 was measured during the first high tide (calculated between $x = 40$ to 120 m and $y = 20$ to 55 m). This most likely initiated the formation of

[2]The reader is referred to Appendix C for an overview of all measured topographies with the laser scanner during this experiment.

a sand bar seaward of the mounts, which can be seen to migrate landward in Figures C.6 and C.7.

The plan view measurements obtained using the laser scanner provide very valuable (and detailed) insight into the spatial differences between each low tide, but the GPS measurements provide us with more data about the actual profile development during wave attack. The GPS measurements show that the profile development of mount B1 is in-line with the described overwash on the 25th, a profile retreat was measured during the first high tide without the formation of a beach scarp (Figure C.5). Compared to B1, the cross-shore profiles of mounts B2 and B3 developed differently; the retreating face of the mount resulted in sections that became much steeper over time (Figures 6.15 and 6.16). The presented GPS measurements are in-line with the observations; a beach scarp (S_h = 0.30 m) formed on mount B2 during the first high tide. The final scarp height S_h on mount B2 during the first high tide was 0.5 m. For mount B3, steepening of the profile was also observed during the first high tide (Figure 6.16). This did not result in the formation of a beach scarp, which can be attributed to the hypothesis that more gentle slopes require more erosion for a beach scarp to form.

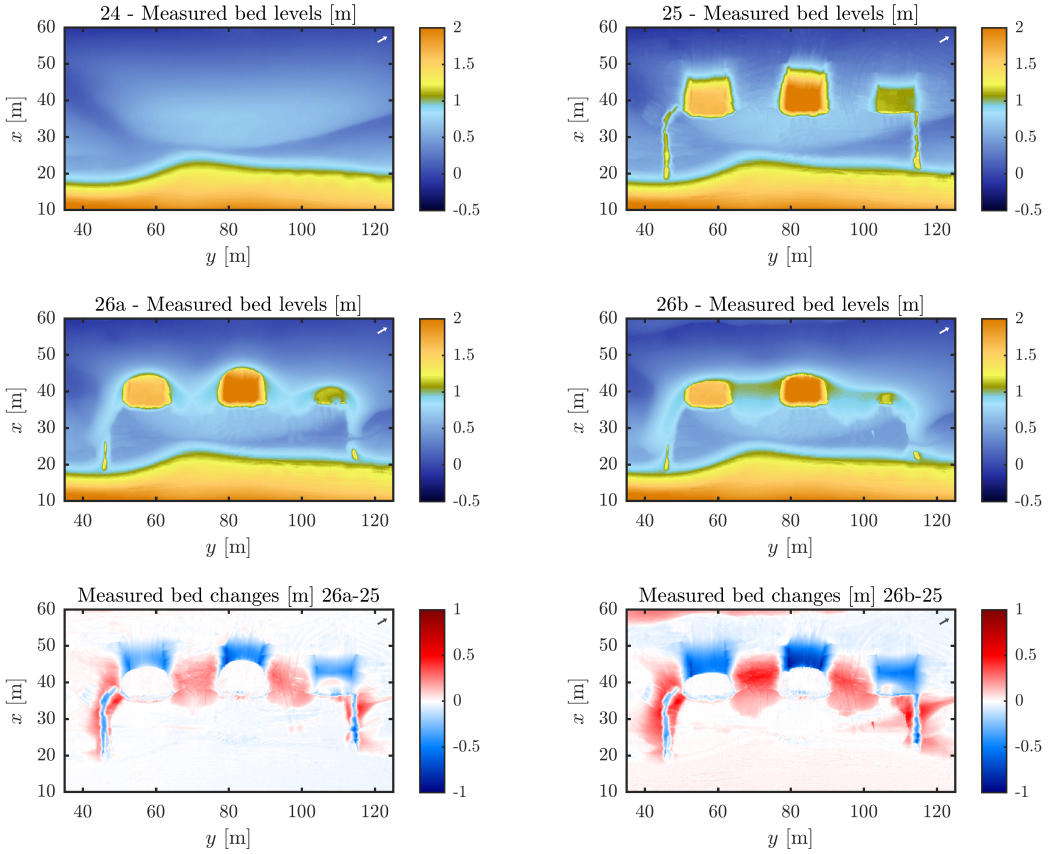

Figure 6.14: Measured bed levels for consecutive low tides (upper panels) and corresponding bed level changes with respect to the constructed mounts (lower panels). North arrows are given in the top right corner.

The following high tides on the 26th, mount B1 was again faced with large amounts of overwash which resulted in a very similar profile retreat and flattening as previously described. The beach scarp on mount B2 migrated, until it reached a height of 0.66 m. The total landward migration of this beach scarp was measured at 2.26 m, with the scarp retreating 1.50 m between 06:46 and 07:53 corresponding to a landward migration rate[3] v_{sc} of 0.022 m/min. Interestingly, the toe elevation increased whereas the wave conditions remained approximately constant ($H_{s,0}$= 0.55

[3]The migration rates are calculated from the centre of each scarp face as the toe could be influenced by slumped material.

m, T_{m02}= 3.8 s and θ_0= 25^o N) and the water levels dropped (from 0.91 m NAP to 0.62 m NAP). This behaviour can be explained from the fact that measurements were started during the peak of the tide, after the first waves had already reached the mounts. The scarp toe during these conditions would have formed lower in the cross-shore profile, resulting in a different toe elevation between the last measurement on the 25th and the first measurement on the 26th (ΔS_t = 0.20 m). The hydrodynamic conditions between these days were very similar, which resulted in the final S_t of 1.20 m NAP (compared to the final S_t on the 25th of 1.25 m NAP). On mount B3, a beach scarp formed just before the measurements started. The first beach scarp that was measured at 06:49 had a toe elevation of 1.1 m NAP (10 cm higher than the toe measured on mount B2 at 06:46). This beach scarp migrated 1.94 m landward, of which 1.75 m occurred between 06:49 and 07:55 resulting in a faster migration rate v_{sc} of 0.027 m/min.

Between the 26th of September and the 2nd of October, the scarps were not affected by wave attack. On most days the waves were just short of touching the scarp toes, and no major changes to this part of the experiment were therefore recorded. The previously described landward migration of the sand bar occurred during these calm days. The sand bar migrated with speeds of $\mathcal{O}$(0.1 m/hr) and came close to merging with the scarps (Figures C.6 and C.7). This method of destruction by swash bar migration (and merging) has been described previously in the theoretical background, but has not been observed to actually cause removal of a beach scarp during field experiments thus-far.

During the first high water of 2 October (η = 1.25 m NAP), the mounts were attacked by very energetic waves compared to the previous days (transformed $H_{s,0}$ = 1.5 m). During these conditions, the remainder of mount B1 was completely inundated. Mount B3 faced an occasional overwash, but the beach scarp remained stable during the first minutes of migration (12:05 to 12:27). After the scarp had migrated landward with a speed v_{sc} of 0.012 m/min (1.5 m between 10:15 and 12:24), the water level had increased further, whereas the wave conditions remained relatively constant. This resulted in large amounts of overwash leading to a more gentle cross-shore slope (12:32) and finally complete destruction (12:39). The beach scarp migration of mount B2 was faster compared to B3; the scarp retreated 3.4 m landward between 10:16 and 12:27 resulting in v_{sc} = 0.026 m/min. This beach scarp continued to migrate landward and attained a maximum height of 1.3 m on 12:24 until there was no material left to erode. Only very occasional water splashed up the scarp leading to large beam-type failures. Against all expectation, the scarp toe did not migrate upward as the water level increased. This behaviour can be explained in two ways; the reflected swash attacks could have led to increased backwash erosion (1), or the slumped material was not deposited in front of the scarp but was moved between and behind the mounts (2). The final destruction of this scarp is related to the limiting width of the mount, which is a direct consequence of the experimental setup used in this field experiment.

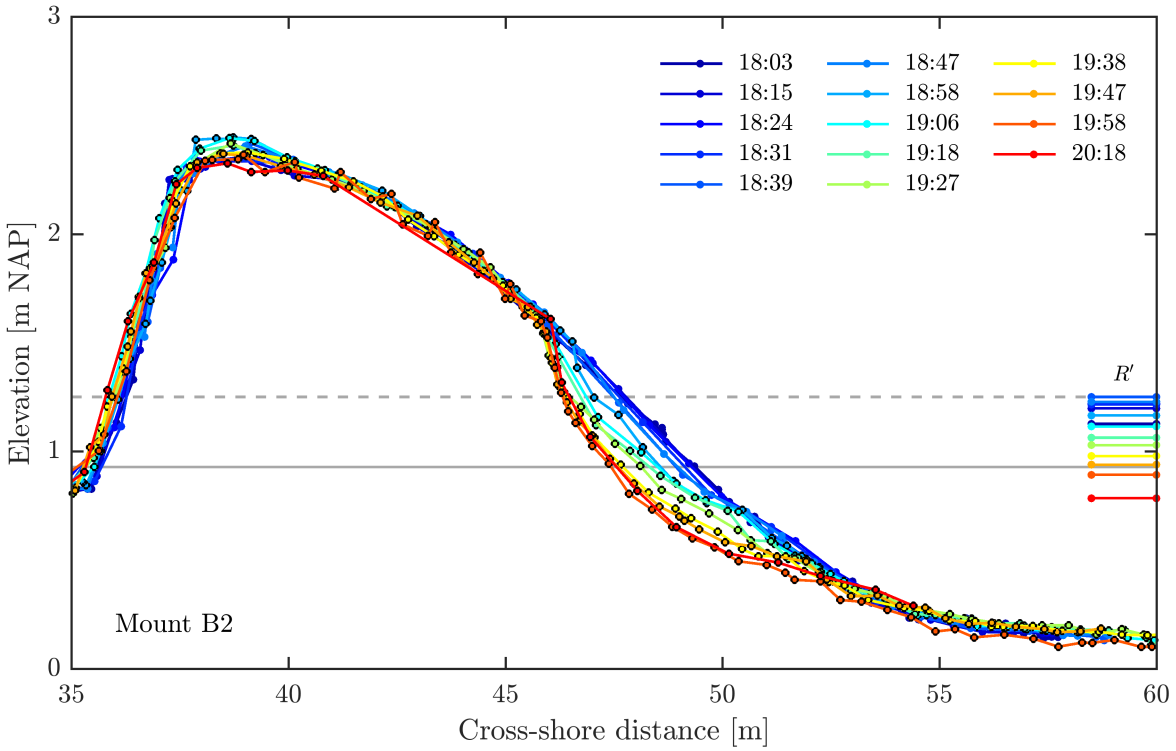

Figure 6.15: Profile development of mount B2 at $y = 83$ m during high water wave attack on 25-09-2017 (scarped profiles are black outlined). R' lines on the right indicate the runup elevation for all profiles, maximum water elevation η_{max} and maximum R' during the high water on the 25th are given in solid and dash-dot horizontal lines respectively.

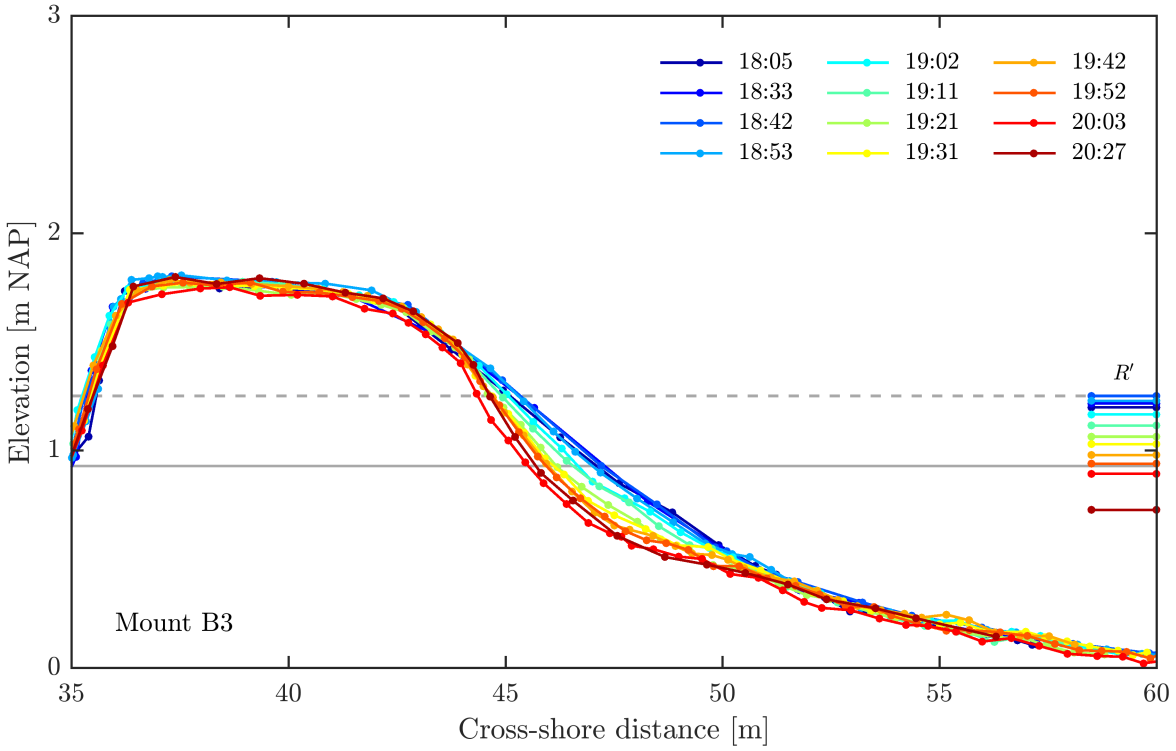

Figure 6.16: Profile development of mount B2 at $y = 57$ m during high water wave attack on 25-09-2017 (scarped profiles). R' lines on the right indicate the runup elevation for all profiles, maximum water elevation η_{max} and maximum R' during the high water on the 25th are given in solid and dashed horizontal lines respectively.

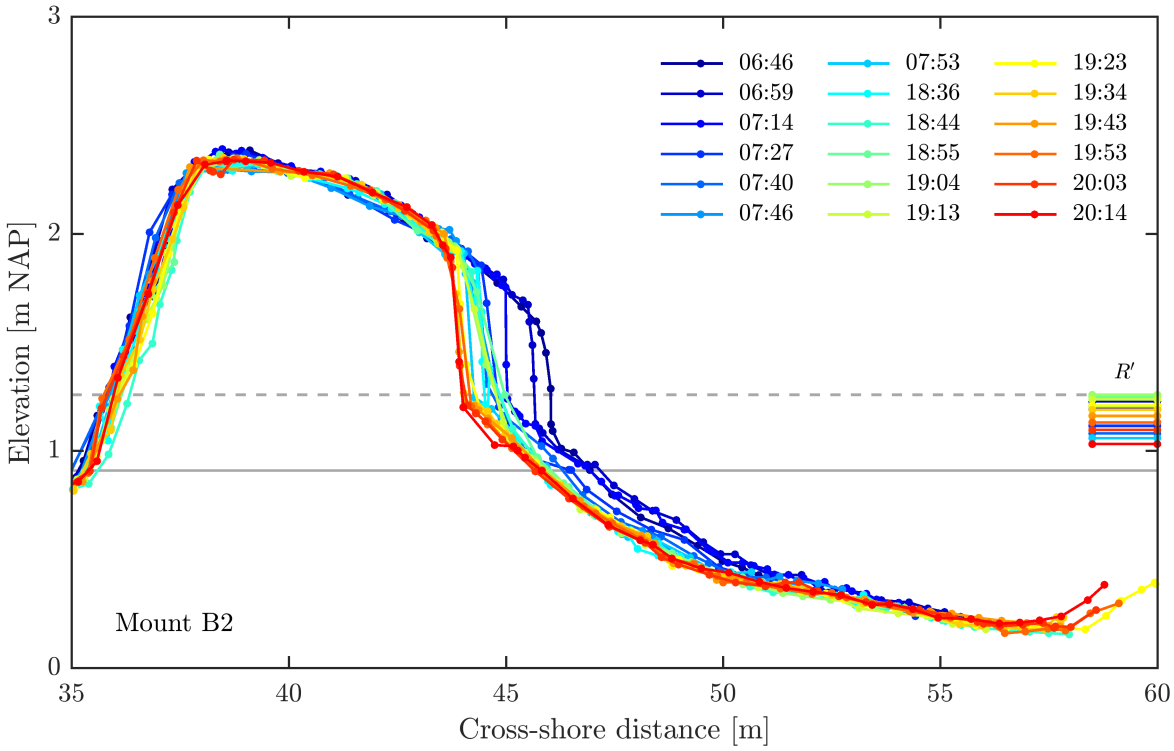

Figure 6.17: Profile development of mount B2 at $y = 83$ m during high water wave attack on 26-09-2017 (scarped profiles). R' lines on the right indicate the runup elevation for all profiles, maximum water elevation η_{max} and maximum R' during the high water on the 26th are given in solid and dashed horizontal lines respectively.

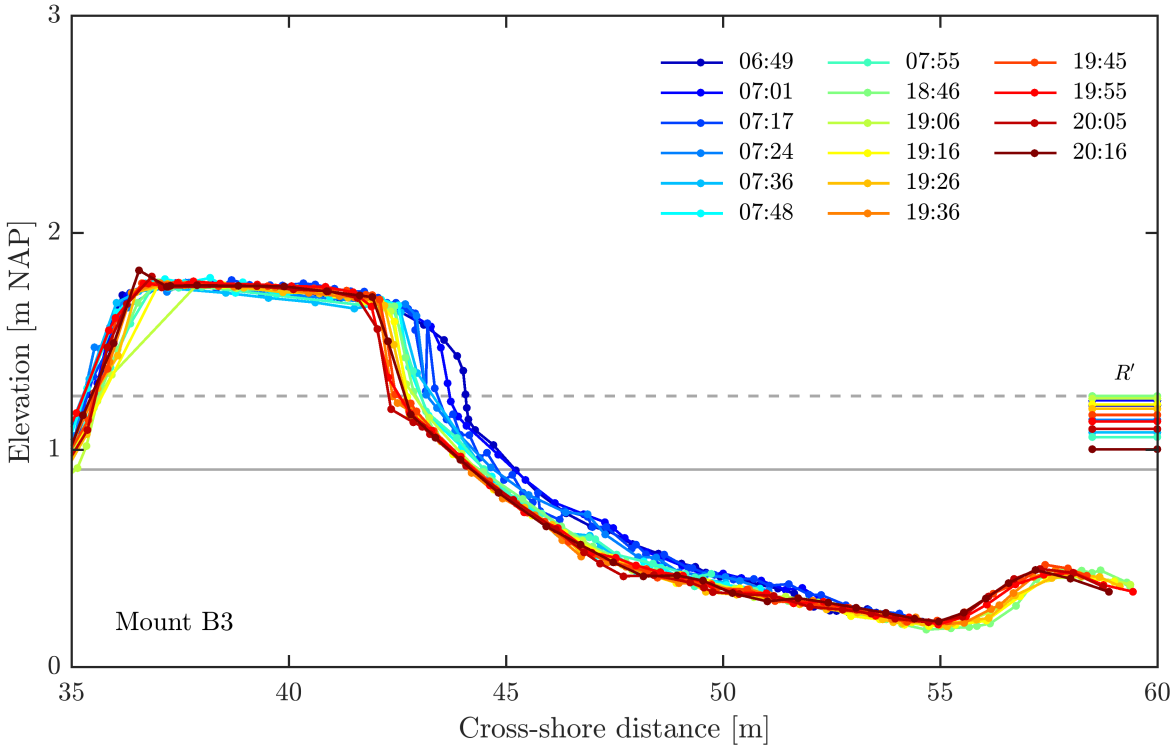

Figure 6.18: Profile development of mount B2 at $y = 57$ m during high water wave attack on 26-09-2017 (scarped profiles). R' lines on the right indicate the runup elevation for all profiles, maximum water elevation η_{max} and maximum R' during the high water on the 26th are given in solid and dashed horizontal lines respectively.

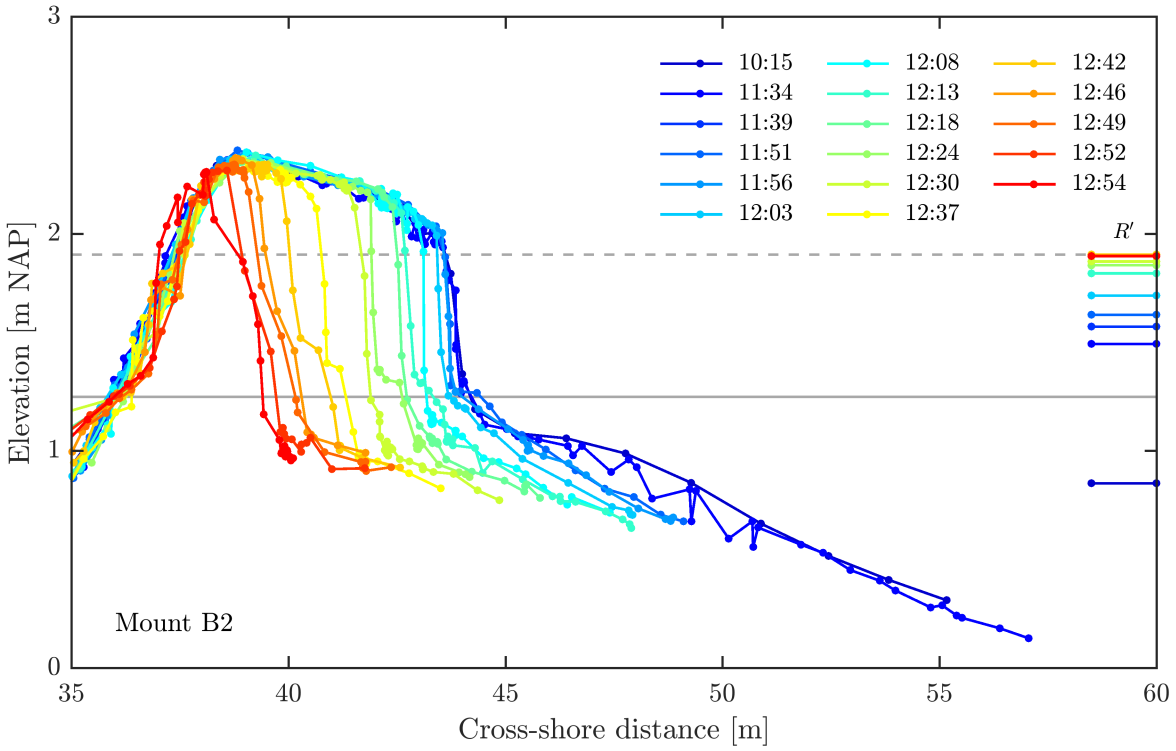

Figure 6.19: Profile development of mount B2 at $y = 83$ m during high water wave attack on 02-10-2017 (scarped profiles). R' lines on the right indicate the runup elevation for all profiles, maximum water elevation η_{max} and maximum R' during the high water on the 2nd are given in solid and dashed horizontal lines respectively.

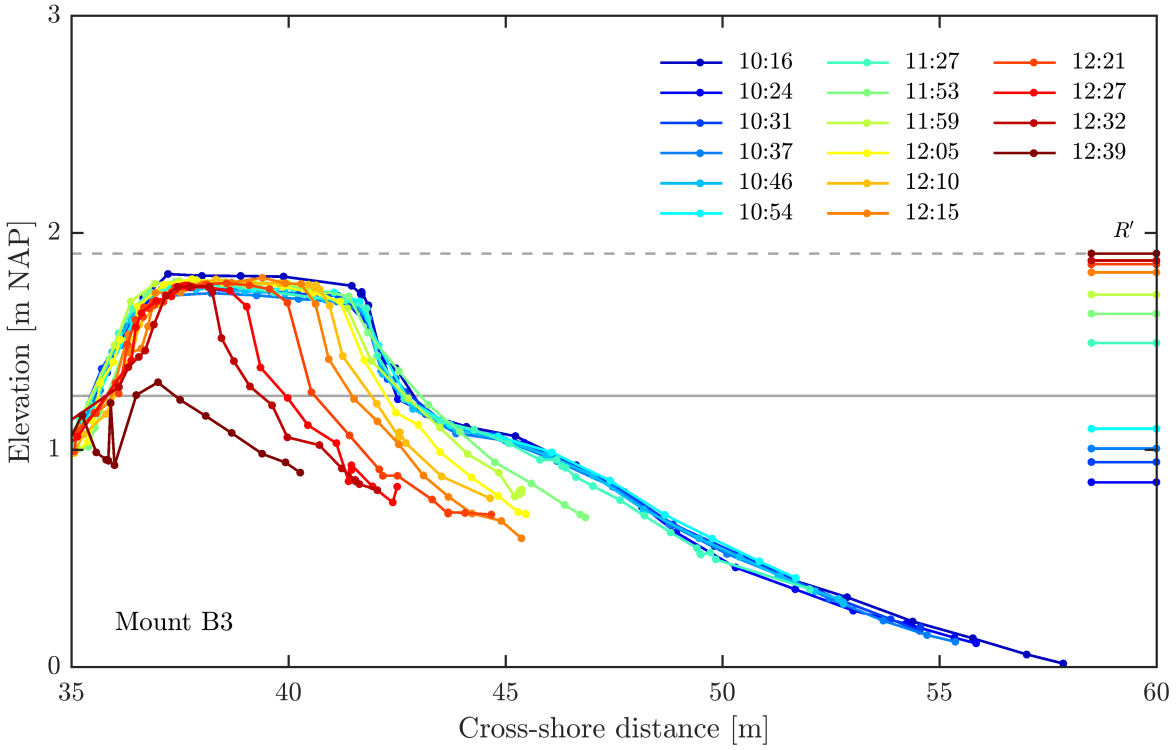

Figure 6.20: Profile development of mount B2 at $y = 57$ m during high water wave attack on 02-10-2017 (scarped profiles). R' lines on the right indicate the runup elevation for all profiles, maximum water elevation η_{max} and maximum R' during the high water on the 2nd are given in solid and dashed horizontal lines respectively.

Slope development

To document the formation of beach scarps, the slope development of mount B2 and B3 are of our interest. From the cross-shore profiles of these mounts it could be seen that the upper slopes (between 1.25 and 1.55 m NAP) steepened over time, whereas the lower slopes (between 0.30 and 1.25 m NAP) became more gentle. This can be represented in a slope development plot over time, which is presented in Figure 6.21. This figure shows that the GPS measurements are in-line with the observations; a beach scarp formed on mount B2 ($\beta_u > \phi'$) whereas none was present on mount B3 ($\beta_u < \phi'$). In general, we can see a similar slope development compared to experiment A; the lower slope decreases and the upper slope increases over time.

Interestingly, the upper beach slope of mount B2 remained under the natural angle of repose until the 19:38 whereas a beach scarp was already reported at 18:58. This discrepancy can be attributed to the fact that the 18:58 measured beach scarp was approximately 10 cm high, which was averaged out over the upper slope region (1.25-1.55 m NAP). This upper slope region in-line with the definition of a beach scarp proposed in this study, which has a minimum height of 0.30 m. The measurements between 18:58 and 19:38 were done with a lower spatial resolution; 1 m between the data points as compared to the aimed 0.20 m. These considerations explain the suboptimal representation of the beach scarp just after formation.

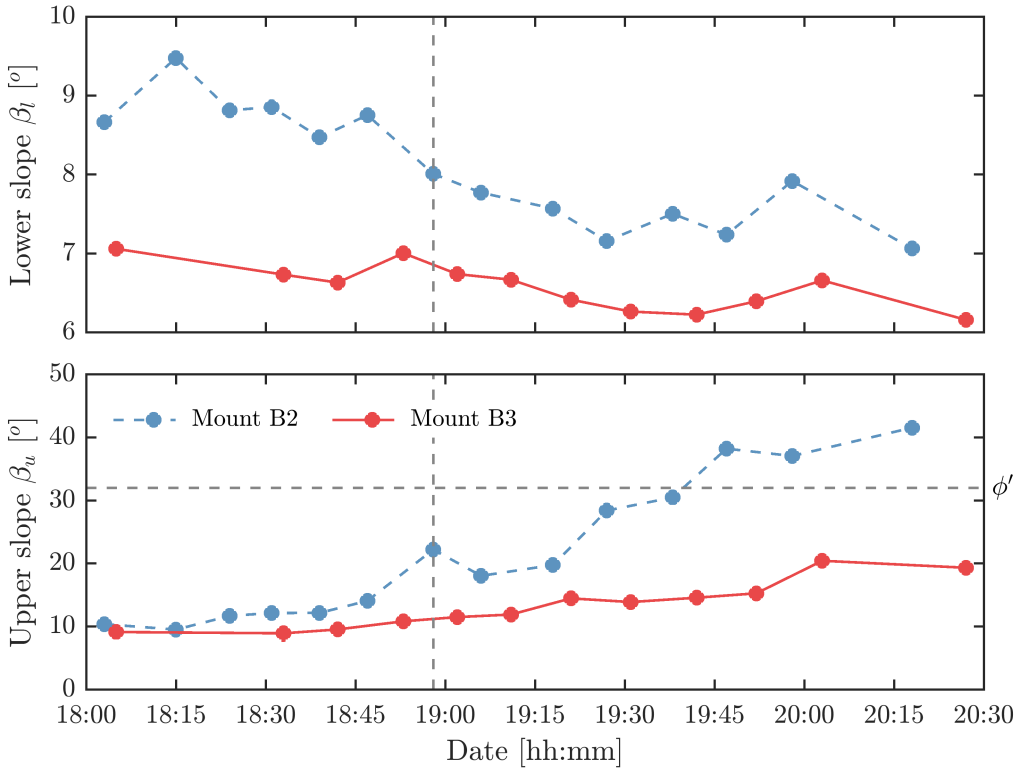

Figure 6.21: Slope development of both mounts in experiment B; lower slopes β_l (upper panel) and upper slopes β_u (lower panel). The horizontal grey dashed lines indicate the natural angle of repose for sand and the vertical dashed lines indicate the moment a scarp was first observed. Note that the upper slope exceeding the natural angle of repose match with the observations for this experiment.

6.2.3. Video observations

Despite the relatively high resolution with which the cross-shore measurements were taken, aspects such as the zone in which the formation takes place and the speed at which this occurs still remain unknown. During the formation of the beach scarp at mount B2 on the first day, video recordings were taken from a 3 m high camera pole (Figure 6.22). These recordings were used to gain additional insight into the formation of beach scarps.

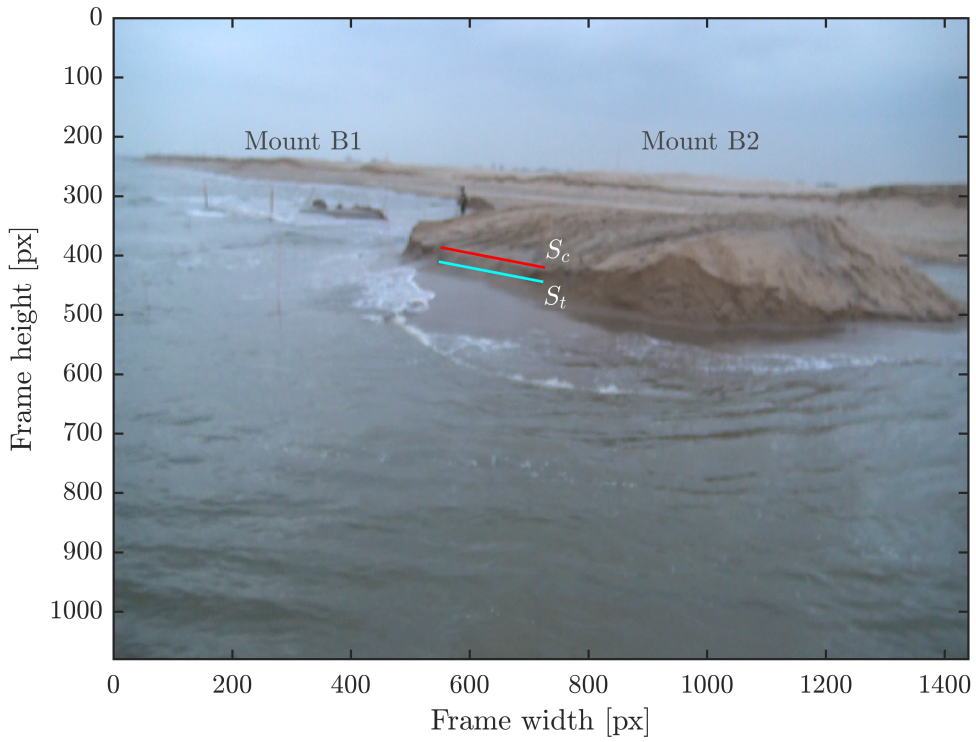

Figure 6.22: Image still of mounts B1 and B2 under wave attack taken from the video recordings on 25-09-2017 18:58. Red and cyan lines indicate the scarp crest and scarp toe elevation respectively.

The video recordings showed that it was difficult to pinpoint the exact moment of formation. The hypothetical steepening of the 'upper slope' is therefore considered a rather gradual process (i.e. no sudden changes in beach slope). This gradual steepening is then followed by slumping of the scarp face, which initiates the migration process as a result of swash collision.

By means of creating timestacks of the swash excursion relative to the constructed mounts, the zone in which the formation takes place can be further analysed. First, the scarp crest and toe were determined from a still image including the beach scarp (Figure 6.22). Second, the pixel rows during 20 minutes of wave attack prior to this frame were extracted from the center of the mount ($y = 410$ px). To obtain a timestack of the swash excursion, these pixel rows were concatenated as shown in Figure 6.23. Third, the number of swash excursions passing the scarp toe indicator were counted.

Video analysis of the formation process during experiment B showed that the scarp formed around the $R_{48/334} \approx R_{15\%}$ (Figure 6.23). This finding indicates that the formation of a beach scarp occurs slightly below the maximum runup.

After the formation, swash impacts on the scarp persisted although the water level was dropping. The waves were not capable of causing enough overwash for scarp destruction (15/333 waves during the 20 minutes after the formation). In addition to the insight obtained into the formation zone of beach scarps, the video recordings show that the mounts were affected by some degree of wave focussing. This could be a possible explanation of the underestimated wave runup modelled according to Stockdon et al. (2006).

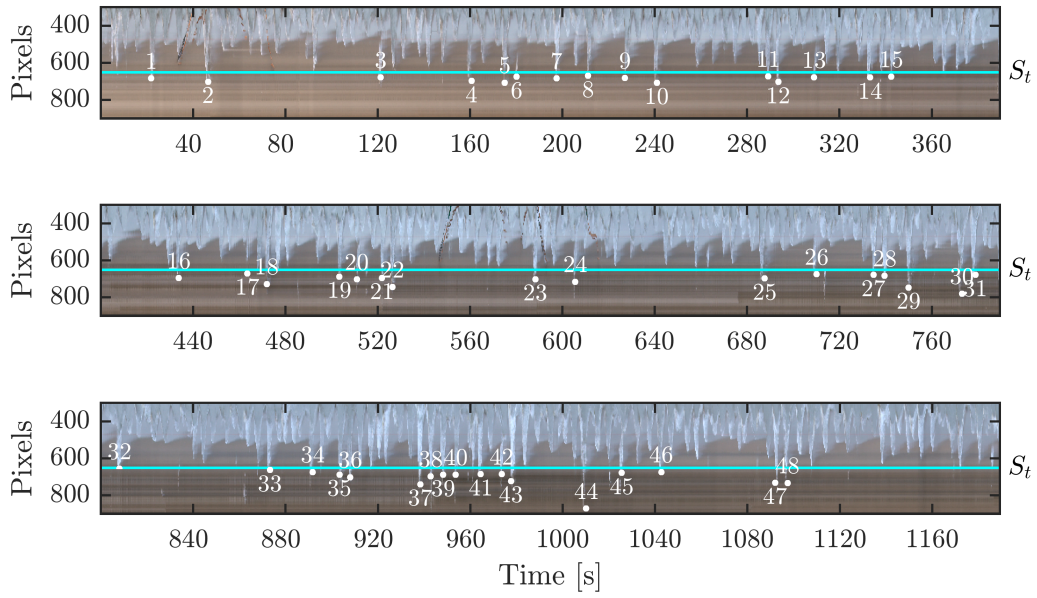

Figure 6.23: Timestack of the cross-shore location of the swash edge (in pixels) at mount B2 on 25/09/2017. The coloured horizontal line indicates the final location of the scarp toe.

6.2.4. Summary - Experiment B

A prototype field experiment has been performed in which the topographical development of three artificial mounts with different initial heights and slopes was monitored. These mounts were placed on the intertidal beach at the Sand Engine without additional compaction. The monitoring of these mounts lasted for 16 tidal cycles, in which both calm and energetic conditions were present. Beach scarps formed on the two highest mounts, with the first scarp observed at the initially steepest slope. The smallest mount was regularly overwashed during high tide, which resulted in an eroded profile without scarp formation.

During this experiment, the formation of a beach scarp on the largest mount was captured in more detail than presented in experiment A. Both GPS measurements and video observations show that the formation of a beach scarp takes place just below the maximum runup elevation. From analysing the video images, it was found that the first scarp toe formed between the $R_{15\%}$ and the maximum runup elevation. During relatively mild conditions, it was found that the largest beach scarp (S_h = 0.66 m) migrated at a rate v_{sc} = 0.022 m/min whereas the smaller scarp (S_h = 0.40 m) migrated at a slightly faster rate of 0.027 m/min. During energetic conditions, the smallest scarp (S_h = 0.55 m) migrated rather rapidly (v_{sc} = 0.026 m/min) and was destroyed by consecutive overwash. The largest scarp (S_h = 1.2 m) migrated slower landward (v_{sc} = 0.012 m/min) during these conditions until the mount was completely eroded.

The beach scarps created during this experiment faced upward migration of the scarp toe under continued wave attack and rising water levels. A down-ward shift in toe elevation between measurements can be explained by large changes in (tidal) water levels. During the most energetic storm conditions however, a non-upward migration of the beach scarp toe was observed during rising water levels. This was most likely caused by increased backwash erosion or a lack of cross-shore redistribution of sediment.

6.3. General conclusions

Field experiments have shown that it is possible to study the different stages in beach scarp morphodynamics on a prototype scale. Artificial mounts were constructed with different initial geometries (height and seaward slope) without additional compaction. After monitoring the morphological development of each mount, it can be said that the initial geometry in relation to the hydrodynamic conditions has a large influence on the formation of beach scarps.

Field experiments have shown that the formation of beach scarps on beach nourishments is related to the (lack of) overwash on the platforms. Furthermore, steep beach slopes increase the rate at which beach scarps form.

GPS measurements and video observations have indicated that the formation of a beach scarp is a rather gradual process and takes place within a narrow band; between $R'_{15\%}$ and $R'_{2\%}$. In the formation process, the upper beach slope increases over time until the undercutting and slumping indicate migration. In order to detect these initially small scale beach features, high resolution measurements $\mathcal{O}$(minutes, cm) are required.

The formation of beach scarps during the field experiments conducted for this study took place between the $R'_{15\%}$ and $R'_{2\%}$. Upon formation of a beach scarp, migration is initiated by swash elevation exceeding the scarp toe. The migration of beach scarps seems to be inversely related to the height of the scarp.

Beach scarp detection based on a slope exceeding the natural angle of repose has shown to agree with the observations during both experiments. The height criterion ($S_h \geq 0.25$ m) might present classification errors directly after the formation, when the scarp height is of $\mathcal{O}$(10 cm).

7

Developing a conceptual model

As coastal models become more and more complex, it is important to have a basic understanding of individual beach features within coastal systems (e.g. beach scarps). The individual morphodynamics of these features can provide insight into the coastal response to (soft) interventions. Furthermore, insight into the interactions between various processes and these beach features (e.g. swash reflection and sediment trapping by beach scarps) can be obtained. In this chapter, a conceptual model of beach scarp morphodynamics is presented. Three stages in the development of beach scarps have been pointed out previously; formation, migration, and destruction. The presented conceptual model aims to represent these stages as good as possible.

Based on the literature review, it was concluded that beach scarps form both at natural and nourished beaches, but can also appear under laboratory conditions. This model aims at explaining the beach scarp formation at prototype scale. The conceptual model builds upon the hypothetical model presented in chapter 3 and tries to incorporate the results of the previous chapters. An initial linear beach slope is assumed, comparable to a beach face nourishment in which the platform height $h_{n,p}$ and initial beach slope β_i determine the cross-shore geometry. This initial condition furthermore resembles the performed beach scarp creation experiments, in which the morphological developments of linearly sloping mounts were studied on a prototype scale. The long term data analysis of beach scarps at the Sand Engine showed that these features form and migrate under relatively mild storm conditions (wave attack on the nourishment face). Very energetic storm conditions result in complete removal of beach scarps at the Sand Engine (large amounts of overwash onto the nourishment platform). Based on this information, a very simple flow chart for the beach scarp life cycle at the Sand Engine can be constructed (Figure 7.1).

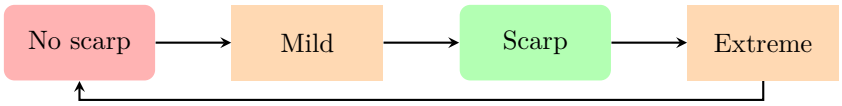

Figure 7.1: Initial flow chart for the life cycle of beach scarps at the Sand Engine

This preliminary model does not explain why beach scarps are more frequently found on nourished beaches than on naturally eroding ones. Additionally, this model neglects two important methods of scarp destruction; drying collapse and sediment deposition (aeolian and swash). Despite the fact that these methods have not been directly detected in the nourishment scale analysis of the Sand Engine, they have been observed during the field surveys performed for this study (Figure B.5). To address these shortcomings, the findings of the beach scarp creation experiments have to be included. Additionally, the model has been split into two parts; the morphological development of a linear beach slope under wave attack (*formation*) and beach scarp response to hydrodynamic forcing (*migration* and *destruction*).

7.1. Model description

For the overall description of beach scarp dynamics, three types of parameters can be distinguished; hydrodynamic, geotechnical, and geometrical. The hydrodynamic conditions are represented in this model by the maximum and 15% exceedence runup elevation ($R'_{2\%}$ and $R'_{15\%}$). These elevations are based on the superposition of the water level (astronomical and surge) and the wave runup height (Stockdon et al., 2006). The hydrodynamic conditions and geotechnical parameters are furthermore represented in the equilibrium beach slope β_{eq}, which is considered to be a function of the wave height (H), the wave period (T) and the D_{50},

$$\beta_{eq} = f(H, T, D_{50}) \tag{7.1}$$

Within this function, calm conditions (low H and T) will produce steep beach slopes, whereas energetic conditions will produce gentle slopes. Large values for the D_{50} tend to result in steeper slopes, whereas gentle slopes are expected for low values of the grain size diameter. Within the proposed conceptual model, accretive and erosive conditions are indicated by relatively steep and gentle equilibrium slopes respectively. The geometrical parameters within this model are represented by the nourishment platform elevation $h_{n,p}$ and the initial nourishment slope β_i. Erosion of the nourishment is schematized as the retreat (Δx) of the profile at $R'_{15\%}$, resulting in the separation of β_i into two geometry parameters; the upper slope β_u and the lower slope β_l. It is assumed that a beach scarp is present if the upper slope exceeds the natural angle of repose ($\beta_u > \phi'$). The changes in the upper slope can be determined from geometry,

$$\beta_u = \frac{R'_{2\%} - R'_{15\%}}{\frac{R'_{2\%} - R'_{15\%}}{\beta_i} - \Delta x} \tag{7.2}$$

Based on these parameters, the formation of a beach scarp from a linear slope can be conceptualised (Figure 7.3). This part of the model is concerned with the processes influencing the formation of a beach scarp. First, the hydrodynamic conditions with respect to the initial profile have to be determined ($\beta_{eq} \geq \beta_i$ or $\beta_{eq} < \beta_i$). This is referred to as the *initial slope response* within the model. If the equilibrium beach slope is larger than the initial beach slope, accretion of the profile is expected. This does not result in the formation of a beach scarp during these conditions, but this steeper slope aids in the formation of a scarp during future erosive conditions. If the equilibrium beach slope is smaller than the initial beach slope, erosion of the profile expected. This will produce a beach scarp if either the initial profile is very steep, or the profile retreat (Δx) is relatively large on a more gentle profile. On the other hand, no scarp will form if the upper slope does not exceed the natural angle of repose. This is referred to as the *upper slope constraint* within the model.

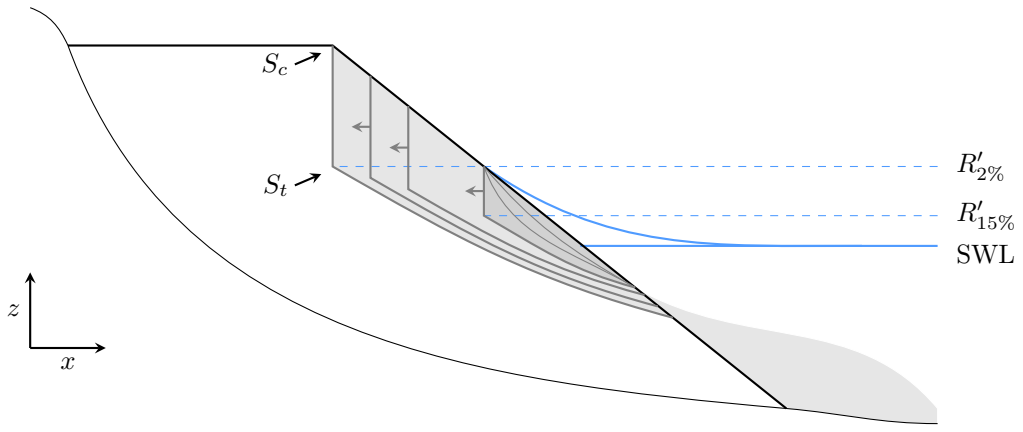

Figure 7.2: Conceptual model of beach scarp formation from a linear nourishment slope during constant conditions. The thin solid line represents the initial profile and the thick solid line represents the nourished profile slope with slope β_i.

Upon scarp formation, new parameters concerning the scarp geometry are introduced; the scarp toe S_t and scarp crest S_c. From the analysis of detailed longshore measurements of these scarp parameters, it was shown that the final scarp toe can be related to $R'_{2\%}$ and the scarp crest is directly related to the nourishment platform height. For the conceptual model presented below, it is therefore important to note that the beach scarp crest level can be replaced by the nourishment platform elevation ($S_c = h_{n,p}$). If a beach scarp is affected by swash action ($R'_{2\%} \geq S_t$), three responses can follow; migration, overwash destruction, and accretion. This is referred to as the *collision check* within the model. Migration and overwash destruction can occur during 'severe' conditions ($\beta_{eq} \leq \beta_l$) with the destructive runup elevation (R'_d) respectively smaller and larger than the scarp crest. This is referred to as the *overwash check* within the model. Hypothetically, accretive conditions ($\beta_{eq} > \beta_l$) could cause 'destruction' of the beach scarp by means of swash deposition. This is referred to as the *lower slope response* within the model. If a beach scarp is not affected by swash action ($R'_{2\%} < S_t$), no major changes will occur on a short timescale (hours). On a larger timescale however, aeolian transport and drying of the scarp could lead to destruction of this feature. Aeolian transport could result in an increase in scarp toe elevation, which could potentially cover the entire scarp within the order of several days. Drying of the beach scarp causes the material to lose its suction stress ($S = 0$), leading to a dry slope under the natural angle of repose.

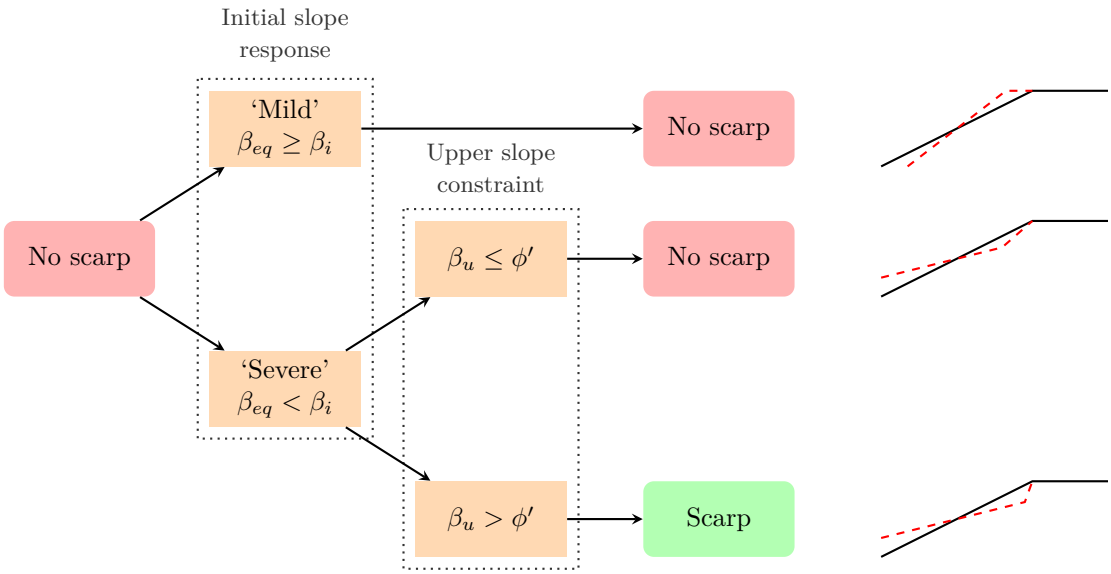

Figure 7.3: Conceptual diagram of the conditions (hydrodynamic and geometric) required for beach scarp *formation* from a linear slope. A visual representation of the profile development is given on the right, in which the initial and resulting profiles are indicated with a solid black and dashed red line respectively.

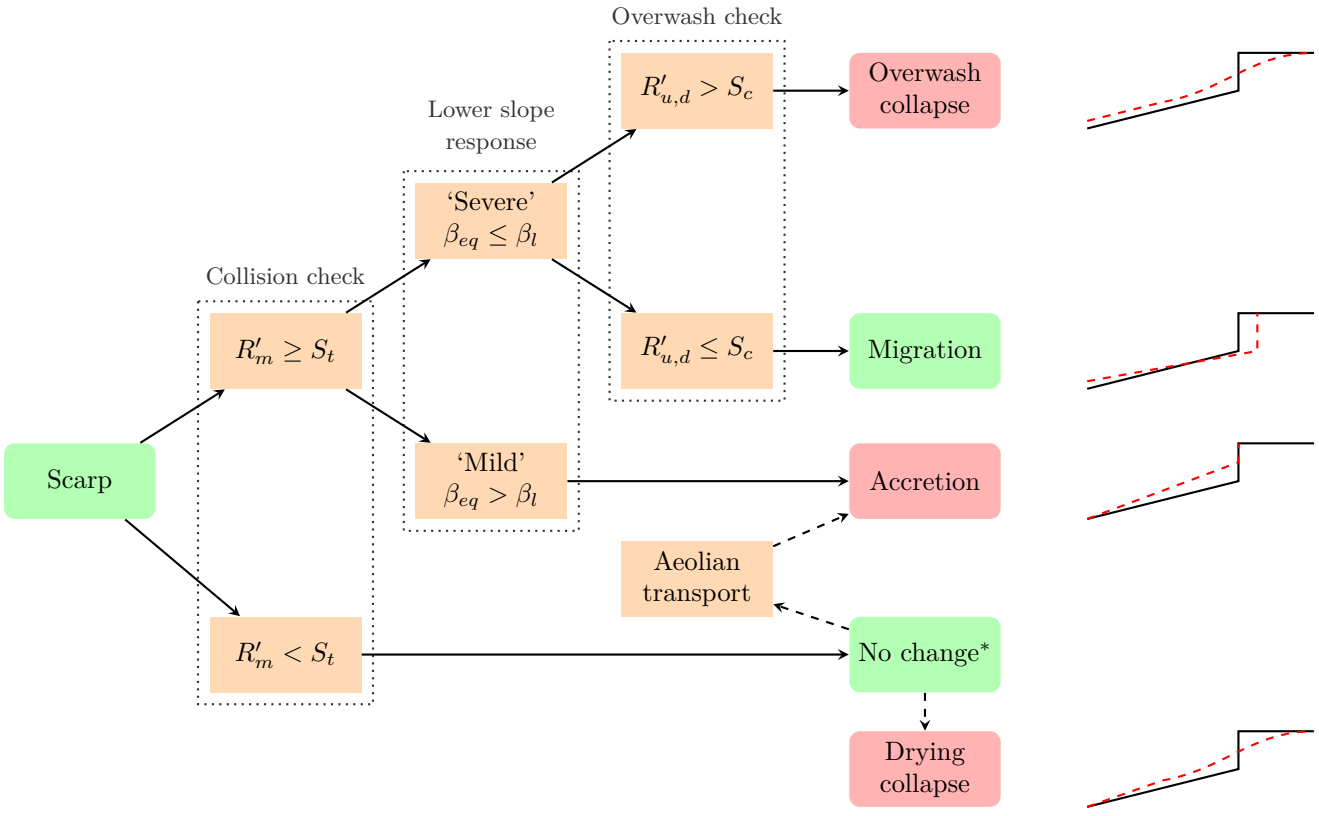

Figure 7.4: Conceptual diagram of the conditions (hydrodynamic and geometric) causing beach scarp *migration* and eventual *destruction*. A visual representation of the profile development is given on the right, in which the initial and resulting profiles are indicated with a solid black and dashed red line respectively. On a short timescale (hours) no large changes* in the beach scarp geometry will occur, but on larger timescales (days) aeolian transport and drying of the beach scarp will result in destruction.

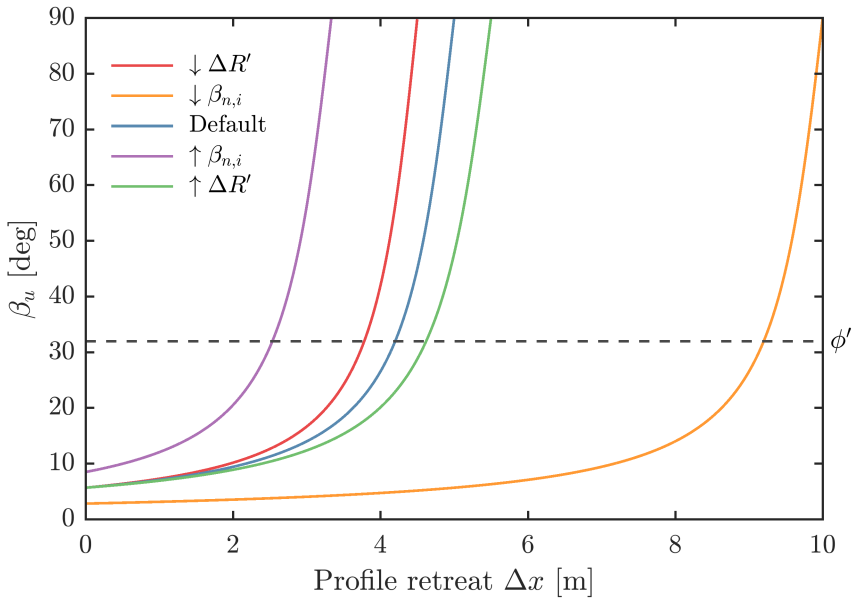

Figure 7.5: Conceptualised upper slope development between β_u from an initially linear slope β_i as a function of the profile retreat Δx at $R'_{15\%}$ after Equation 7.2. The upper slope is defined between $R'_m - R'_{15\%}$ $(= \Delta R')$. Chosen values are arbitrary but indicate the relationship between scarp development and β_i and $\Delta R'$.

7.2. Conceptual model analysis

The presented models allow for the assessment of effects different parameters will have on beach scarp morphodynamics. First, the implications of the proposed formation diagram (Figure 7.3) are discussed. Second, the implications of the proposed beach scarp response diagram (Figure 7.4) are treated. Third, some case studies are analysed with respect to the proposed conceptual model.

7.2.1. Beach scarp formation

From the presented conceptual model it can be seen that beach scarps will tend to form quicker when a steep (nourished) profile is present (i.e. large β_i values). This is in-line with the scarp creation experiments and long term data analysis of this study. During the field experiments, it was observed that beach scarps form faster on steep slopes. From the long term data analysis of beach scarps at the Sand Engine, it was observed that scarps tend to form under summer storm conditions. Before these storm conditions, steep slopes are generally present at the Sand Engine as a result of accretive (summer) conditions. This sediment is then quickly removed during energetic storm conditions, leading to the steepening of the upper profile and eventually beach scarp formation. The evolution of the upper beach slope under erosive conditions is dependent on the retreat rate Δx, initial beach profile and the difference between maximum and 15% exceedence runup (Equation 7.1). This means that beach scarp formations are not limited to initially steep profiles; large amounts of shoreline retreat on gentle beach profiles can potentially produce beach scarps. A 'narrow' upper beach slope (small $R'_{2\%} - R'_{15\%}$) is also capable of producing beach scarps faster (Figure 7.5).

7.2.2. Beach scarp migration and destruction

The conceptualised response diagram of beach scarps shows that a beach scarp can only migrate or face destruction by overwash if the maximum runup reaches the present scarp toe. As we often face changing environmental conditions, it is important that this check precedes the type of beach scarp response. During the field surveys, large beach scarps were present at the Sand Engine landward of the constructed mounts. The toe elevation of these scarps remained well above the maximum runup during the experiments. This caused the beach scarp to remain in place, with drying collapse of the beach scarp occurring after some time.

This model furthermore suggests that migration of the beach scarp (and therefore its presence) could continue for quite some while. In time, the beach scarp toe will most likely increase in elevation due to the fact that only 'more' energetic conditions affect the migration of the beach scarp. If other beach scarp responses are neglected, the final toe elevation of a beach scarp is determined by the most energetic condition within this migration loop. Assuming a horizontal nourishment platform, it follows that the height of the beach scarp associated with these conditions would be smaller than those after milder conditions ($S_h = S_c - S_t = h_{n,p} - R'_{2\%}$).

7.2.3. DUROS+ adaptations

To incorporate the conceptual model into an existing empirical storm erosion model, an adjusted version of the DUROS+ model is presented in this thesis (Figure 7.7). The DUROS+ model has been used to determine the effects of storm erosion at the Dutch coast, and was aimed at predicting dune erosion. Originally developed by Vellinga (1986), this model builds upon the results of erosion profiles during large scale laboratory experiments and has been improved by van Gent et al. (2008). Based on the storm surge level (SSL), wave height $H_{s,0}$, wave period T_p, the grainsize diameter (represented by the settling velocity w_s) and the pre-storm coastal profile, this model is capable of determining the approximate post-storm profile. This profile is generated by a straightforward cross-shore redistribution of the sediment, with erosion and sedimentation above and below the SSL respectively (Figure 2.7).

The adjusted model presented in this thesis uses the model of van Gent et al. (2008) as a basis to predict the beach scarp toe elevation, height and slope. Based on the findings presented in this study, it can be assumed that the final beach scarp toe is positioned around the maximum wave runup elevation ($R'_{2\%}$). A slight modification to the original DUROS+ equilibrium profile model was therefore necessary (Equation 7.7, bold). In order to start the initialization of the DUROS+ calculations, the parameters x_{max} and z_{max} have to be calculated (Figure 2.7). These parameters determine the maximum seaward extent of the equilibrium profile as follows,

$$x_{max} = 250\left(\frac{H_{s,0}}{7.6}\right)^{1.28}\left(\frac{0.0268}{w_s}\right)^{0.56} \tag{7.3}$$

$$z_{max} = -\left[0.4714\left\{250\left(\frac{12}{T_p}\right)^{0.45} + 18\right\}^{0.5} - 2.0\right]\left(\frac{H_{s,0}}{7.6}\right) \tag{7.4}$$

Apart from this starting point, the adjusted DUROS+ model requires the maximum wave runup elevation. For this, the wave runup is calculated using the Stockdon et al. (2006) formula as a function of the foreshore slope, wave height and wave length,

$$R_{2\%} = 1.1\left(0.35\beta_f(H_0L_0)^{1/2} + \frac{[H_0L_0(0.563\beta_f^2 + 0.004)]^{1/2}}{2}\right) \tag{7.5}$$

With the foreshore slope defined as,

$$\beta_f = \frac{2\sigma_\eta}{x_{(z=\eta-\sigma_\eta)} - x_{(z=\eta+\sigma_\eta)}} \tag{7.6}$$

Based on the starting point (x_{max}, z_{max}), the calculated maximum wave runup elevation, the user-defined hydrodynamic and the geotechnical parameters, the equilibrium profile of the DUROS+ model can be calculated. The following equation is used to calculate the equilibrium profile with the scarp toe positioned at the maximum wave runup elevation (analogous to Equation 7.1),

$$\left(\frac{7.6}{H_s}\right)z = 0.4714\left[\left(\frac{7.6}{H_s}\right)^{1.28}\left(\frac{12}{T_p}\right)^{0.45}\left(\frac{w_s}{0.0268}\right)^{0.56}x + 18\right]^{0.5} - 2.0 + \mathbf{R_{2\%}} \tag{7.7}$$

After calculating the equilibrium profile, the seaward part of the DUROS+ profile is added. It should be noted that this linear slope cannot be more gentle than the initial beach slope, as the

cross-shore redistribution of sediment will then no longer be possible. The following relationship is used to obtain the seaward profile,

$$z = x/\beta_{seaward} \tag{7.8}$$

The profile above the $R'_{2\%}$ (or SSL in the default DUROS+) is usually estimated with a slope of 1:1. Based on the findings presented in chapter 5, this could lead to an underestimation of the beach scarp slope. Instead, a Culmann-type analysis (derivation presented in chapter 4) can be used to determine the critical combination of scarp height and scarp slope. The following relationship between these two parameters has been implemented in the model,

$$S_{h,cr} = \frac{4\sigma^s}{\gamma}\left[\frac{\sin i \cos\phi'}{1-\cos(i-\phi')}\right] \tag{7.9}$$

In order to calculate this critical relationship between scarp height and slope, one needs to define the specific unit weight γ, the angle of internal friction ϕ' and the grainsize parameter D_{60}, which is used to determine the associated suction stress σ^s. Now that the relationship between the scarp slope and height has been established, the beach scarp part of the DUROS+ model can be added as follows,

$$z = x/i \tag{7.10}$$

After obtaining the final storm profile produced by the adjusted model, a volume check is performed to determine whether the profile is volume conservative. When this check is passed, the final storm profile is presented according with the final scarp toe elevation. This toe elevation can be used to determine the beach scarp height for a horizontal platform. For undulating platforms, the scarp height is highly dependent on the actual landward retreat of the profile. It has been shown that the DUROS+ model generally overestimates the retreat distance, which limits the predictive capabilities of this model (Brandenburg, 2010). The beach scarp slope according to the Culmann-type stability analysis is presented (Equation 7.9). This will give the user an estimate about the scarp toe elevation, height and associated slope.

General simulations performed with the adapted model show a behaviour that seems to be typical for beach scarp morphodynamics on beach nourishments; formation during mildly erosive conditions and destruction during highly energetic storm conditions (Figure 7.6). It can furthermore be seen that the beach scarp toe elevation increases with increasing offshore energy and water levels. As the height of a beach scarp is directly related to the toe elevation and the nourishment topography, it can be said that the highest beach scarps will form during mildly erosive conditions for a horizontal nourishment.

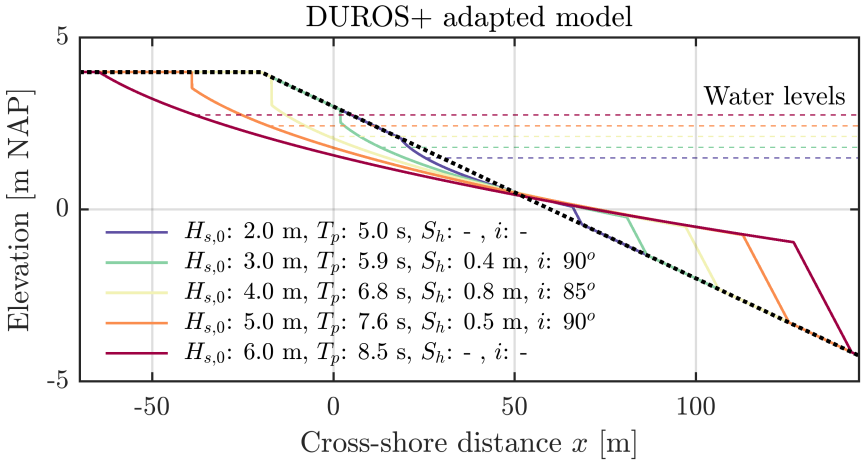

Figure 7.6: General results of the DUROS+ adapted model applied to a nourishment with a platform elevation $h_{n,p}$ of 3.75 m NAP, an initial beach slope β_i of 1/15 (dotted) and a settling velocity w_s of 0.025 m/s for various hydrodynamic conditions (legend).

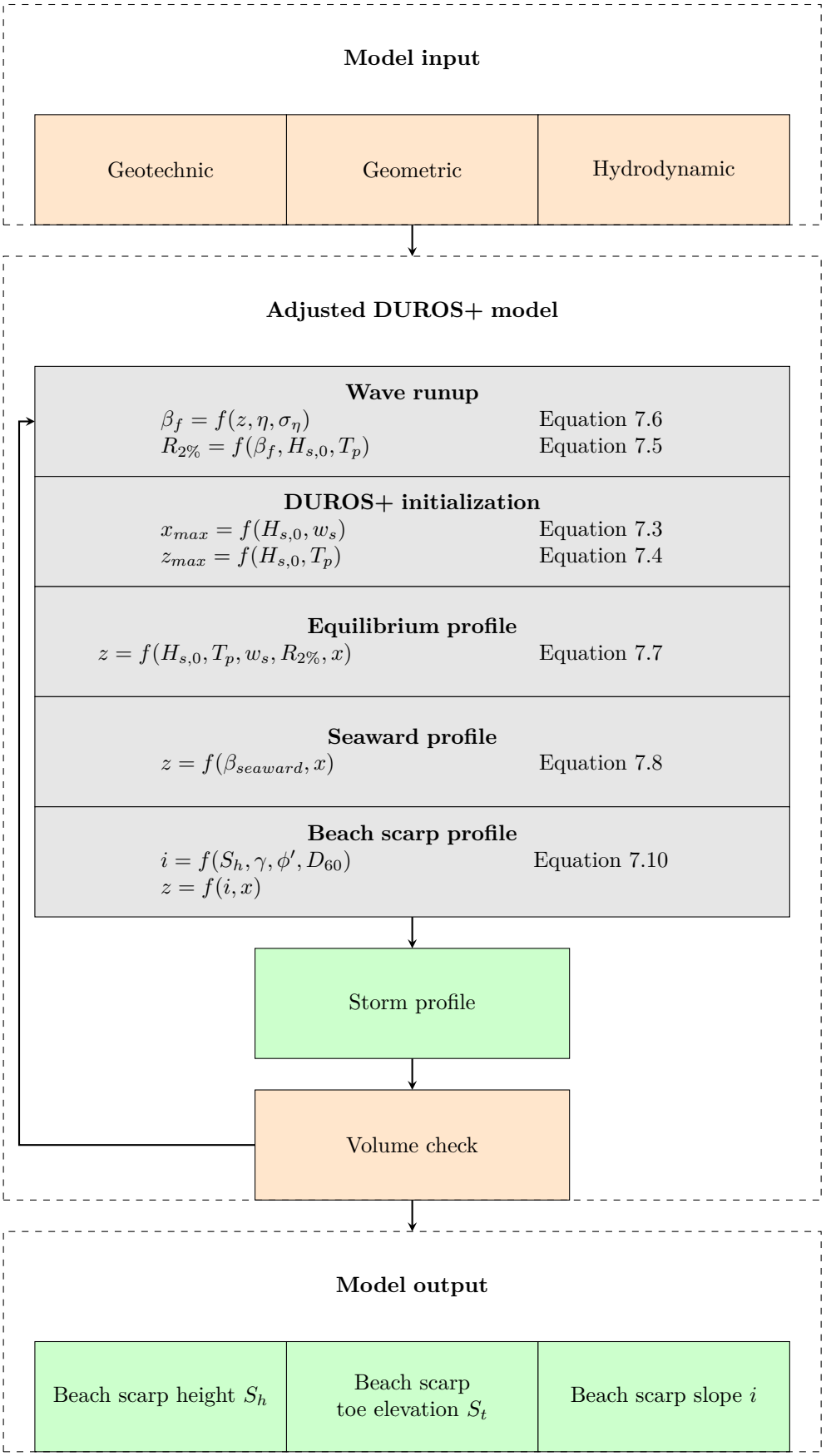

Figure 7.7: Flowchart of the adjusted DUROS+ model developed for beach scarp prediction.

7.2.4. Application to case studies

To test the presented beach scarp prediction tool, it was used to predict the formation on two nourishments faced with beach scarp formation; Cancun Beach in Mexico and the Sand Engine in the Netherlands.

Cancun Beach, Mexico

The microtidal barrier beach of Cancun is located on eastern tip of Mexico at the border between the Gulf of Mexico and the Caribbean Sea (Figure 7.9 top left). As this beach is mainly used for recreational purposes, a wide beach is desired by most of the stakeholders and has been ensured by several beach nourishments. With spring and neap tidal ranges of 0.32 m and 0.07 m, the tidal oscillations within this study area are small (Ruiz de Alegria-Arzaburu et al., 2013). Waves typically approach from the east-southeast, whereas a large part of the energetic waves originate from the northerly directions during winter storms. Most waves are of relatively low energy approaching from the southeast with significant wave heights of 0.5 - 1.5 m and mean wave periods of 6.0 - 8.0 s (Figure 7.9, wave rose).

Large beach scarps of up to 2 meters high and extending for several hundreds of meters have been reported to form along various parts of this beach after the nourishment works of 2009 (Ruiz de Alegria-Arzaburu et al., 2013). A typical cross-section of the (nourished) Cancun Beach is given in Figure 7.9 (bottom panel), which shows the presence of a 2 m high beach scarp and a nourishment platform at an elevation of approximately 3.5 m MSL.

To apply the adjusted DUROS+ model, an initial beach profile is required. No profiles of Cancun Beach directly after the nourishment works could be found. The design proposed by Bodegom (2004) was therefore combined with the platform found in Ruiz de Alegria-Arzaburu et al. (2013); an initial slope of 1:15 and a platform height of 3.5 m MSL. In addition, the sediment fall velocity of 0.04 m/s measured at Cancun Beach was used (Gabriel et al., 2008).

The results show that the model is capable of predicting the scarp toe elevation after typical energetic wave conditions ($H_{s,0}$ = 3.0 m, T_p = 8.0 s). The modelled scarp toe elevation is positioned at 1.31 m above MSL (Figure 7.8), whereas the measured scarp toe elevation was situated around 1.25 m MSL. The predicted beach scarp height at Cancun Beach can therefore be roughly estimated around 2 meters ($h_{n,p} - S_t$), which matches the measured profile in March 2010 (Figure 7.9). Comparing the beach slope seaward of the scarp shows that the modelled profile is slightly more gentle (1:10) than measured (1:8). This could be related to the assumption that had to be made for the sediment fall velocity and wave conditions. The value obtained from Gabriel et al. (2008) was for the non-nourished beach whereas Ruiz de Alegria-Arzaburu et al. (2013) report that the nourished material was more coarse than the natural material.

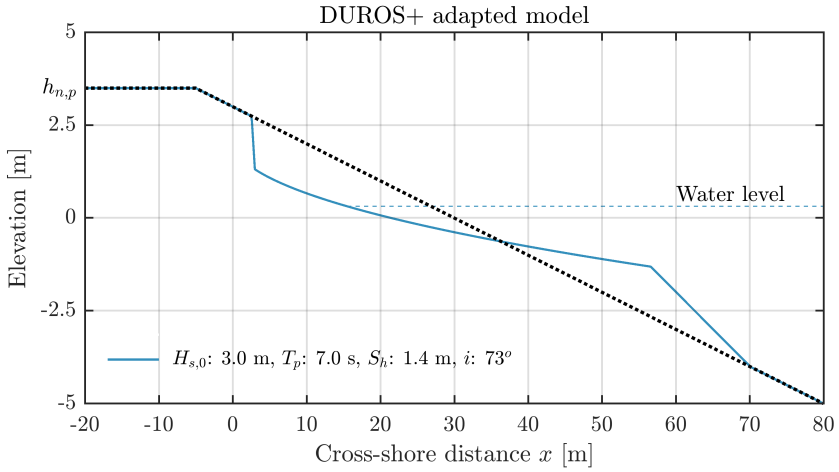

Figure 7.8: Predicted beach scarp formation at Cancun Beach after a beach nourishment with $h_{n,p}$ = 3.5 m.

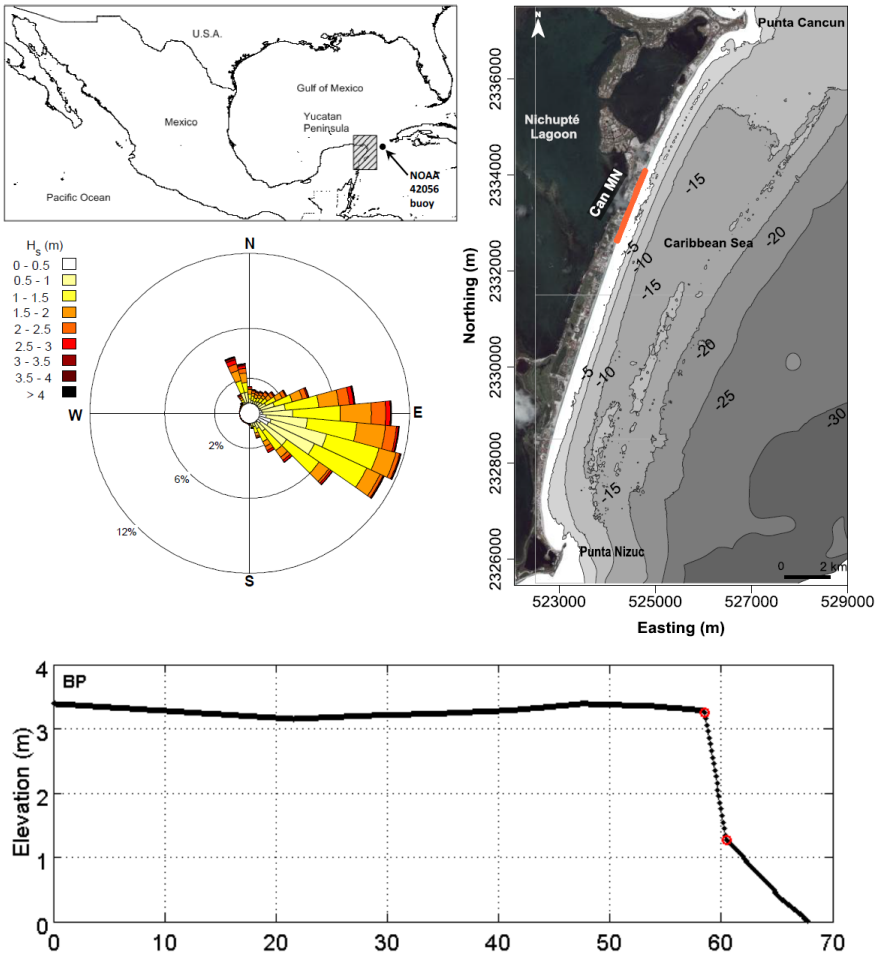

Figure 7.9: Case study location Cancun Beach within the Mexican Caribbean coast. NOAA offshore wave measurements between September 2007 and May 2011 are presented in the bottom left wave rose. Source: Ruiz de Alegria-Arzaburu et al. (2013).

Sand Engine, The Netherlands

As the Sand Engine has been extensively treated in chapter 4, this section directly focusses on the beach scarp morphodynamics at this mega-nourishment. Based on the long term data analysis, it was found that beach scarps form during mildly erosive (summer) storm conditions at this nourishment. Cross-shore transects have been measured before and after storm conditions in the summer of 2017 (Figure 7.10). The scarp height measured at this cross-shore transect was measured at approximately 1 meter, with a corresponding toe elevation of 2.36 m.

Application of the adapted DUROS+ model for this case was done with an initial slope of 1:10 (slope between 1 to 3 m NAP, Figure 7.10) and platform elevation of 3.5 m NAP (x = -10 m). Both typical summer storm conditions ($H_{s,0}$ = 2.0 m, T_p = 5 s, η = 2 m NAP, also observed in the days before 04/10/2017) and winter storm conditions ($H_{s,0}$ = 3.0 m, T_p = 8.0 s, η = 3 m NAP) were used as input for the model. The results show that the beach scarp prediction is in-line with the measurements; a beach scarp with a toe position around 2.46 m and a corresponding height of 1.04 m. The prediction based on winter storm conditions show that the maximum runup elevation exceeds the nourishment platform, leading to a (diffuse) storm profile without beach scarps.

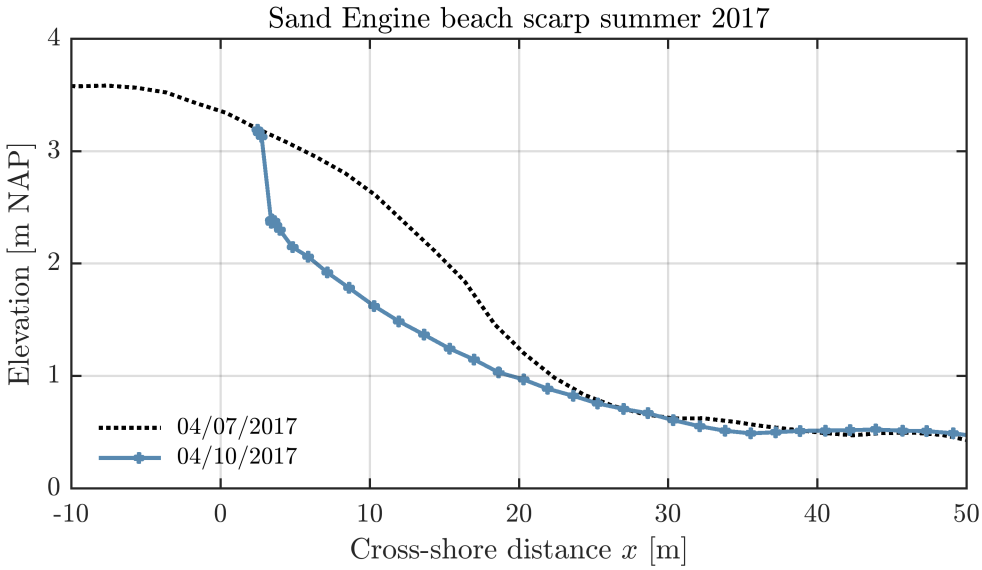

Figure 7.10: Measured cross-shore beach profiles at the Sand Engine with and without a beach scarp.

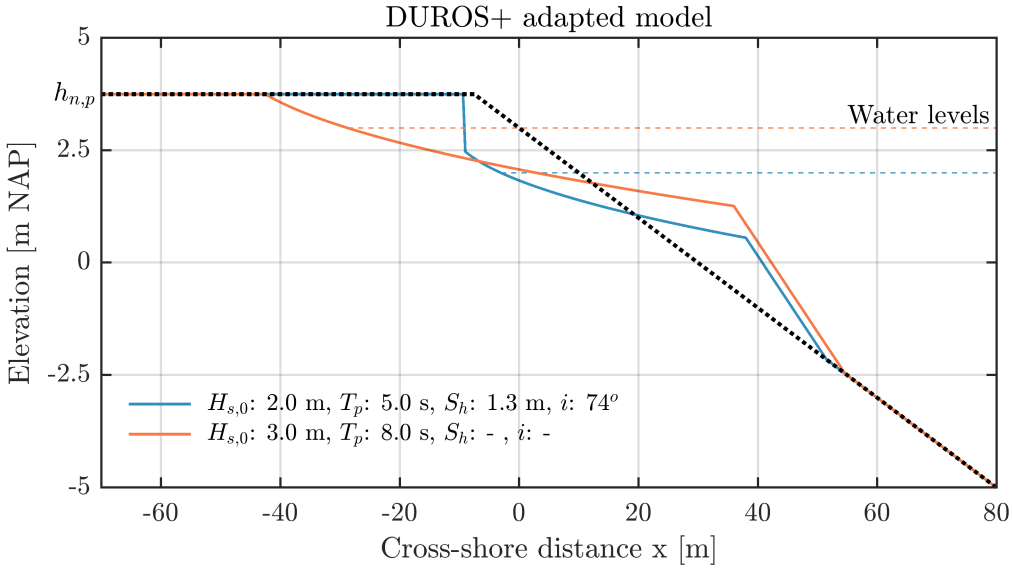

Figure 7.11: Modelled cross-shore beach profiles after typical summer (blue) and winter (orange) storm conditions at the Sand Engine with a platform elevation $h_{n,p}$ of 3.50 m NAP

7.3. General conclusions

A conceptual model has been developed in which the various stages of beach scarp morphodynamics are represented. The formation of beach scarps is conceptualized to occur between the $R'_{15\%}$ and $R'_{2\%}$, after which landward migration of the beach scarp is initiated by undercutting and slumping. Beach scarp migration will continue until the scarp toe reaches the maximum runup elevation ($R'_{2\%}$). The (natural) destruction of beach scarps has been included in the conceptual framework in four ways; hydrodynamic controlled overwash (1), drying collapse (2), burying by aeolian transport (3) and swash deposition (4).

Based on these concepts, the DUROS+ model was adjusted to provide a relatively simple (empirical) tool for beach scarp prediction in the future. By incorporating the empirical Stockdon wave runup formula and a Culmann-type stability analysis into this model, a first estimate of beach scarp characteristics (toe elevation, height and slope) on (nourished) beaches can be made.

By comparing results of the model predictions to case studies at Cancun Beach and the Sand Engine, it was shown that the scarp toe elevation can be predicted with reasonable accuracy ($\pm$ 0.1 m). Predicting the actual beach scarp height was found to be challenging, as variations in the platform topography can cause massive changes in beach scarp height. This requires accurate modelling of the landward profile retreat during erosive conditions, which is not correctly implemented in the model. In conclusion, this tool can be used to get a first impression of the beach scarp heights for horizontal nourishment platforms. For undulating nourishment platforms, it is suggested that a 'worst-case' scenario is modelled, in which the maximum platform elevation is given as input to the model.

8

Discussion

In order to critically reflect on the results presented in the previous chapters and to contrast these findings to prior beach scarp studies, the discussion has been separated into four sections. First, the findings regarding beach scarp morphodynamics are discussed. Second, general properties of beach scarps are treated (e.g. positioning in beach models and definition). Third, the geotechnical analysis and beach scarp creation experiments are discussed. Fourth and final, the presented conceptual model of beach scarp morphodynamics is discussed alongside the implications for end-users.

Beach scarp morphodynamics

Formation of beach scarps

The findings of this study show that beach scarps form as a result of landward coastline retreat with respect to the initial beach slope. For beachface nourishments, the formation of beach scarps has to be paired with relatively low swash elevations (with respect to the nourishment platform) to ensure steepening of the upper beach profile. Beach scarps are likely to form within these systems due to the generally steep cross-shore profiles associated with beach nourishments. Video observations during the field experiments showed that the formation of beach scarps is a gradual process, which took place between the 15% exceedence and maximum wave runup elevation. This suggests that beach scarps start as a small $\mathcal{O}$(cm) vertical discontinuities in the cross-shore beach profile, but can grow in height $\mathcal{O}$(m) during landward migration dependent on the backshore geometry and hydrodynamic conditions.

The long term data analysis showed that the formation of beach scarps on beachface nourishments occurs during relatively mild storm conditions. For the Sand Engine mega-nourishment it was found that these conditions are present during summer months. During these erosive conditions the overwash of the nourishment platform has to remain limited, allowing for the steepening of the upper beach slope until a beach scarp forms. This dependency on erosive events is similar to dune scarp formation, which has generally been linked to extreme hydrodynamic (winter) storm conditions (Carter et al., 1990; Nishi et al., 1995; Kobayashi et al., 2008).

The field experiments presented in this study have shown that steep beach slopes increase the speed at which beach scarps form, which was also observed during laboratory experiments (van Rijn et al., 2011). The relation between beach scarp formation and steep beach slopes furthermore supports the finding that beach scarps tend to form during summer storms; steep summer profiles after accretive conditions are more susceptible to beach scarp formation than gentle winter profiles. The relationship between steep slopes and the formation of beach scarps also explains the existence of beach scarps on cusp horns (Johnson, 1919; Antia, 1989; van Gaalen et al., 2011), which are generally steeper than the beach cusp embayments.

Migration of beach scarps
The documented migration of beach scarps during the field experiments showed that the toe elevation is directly linked to changes in hydrodynamic conditions (with a strong dependency on the water level). This is similar to the findings presented in Bonte and Levoy (2015), but their described upward migration of the scarp toe cannot always be expected. During slowly rising tide, a beach scarp might form relatively low in the cross-shore profile (just below the maximum wave runup at high tide). This will cause an upward migration of the scarp toe as the tide keeps rising. During the next high tide, the hydrodynamic conditions might be milder which can result in the formation of a second beach scarp just below the original one (Figure B.4). After some landward migration of the second scarp, intersection with the original scarp could occur, essentially leading to a decrease of toe elevation.

Destruction of beach scarps
Based on the long term data analysis, the destruction of beach scarps is generally caused by extreme conditions (winter storm). These conditions cause large amounts of overwash leading to smoothing of the beach profile, which has been described previously as a type of beach scarp destruction (Sherman and Nordstrom, 1985; Bonte and Levoy, 2015). This type of destruction was also observed during the field experiments, which led to the idea that a certain amount of overwash is required for complete removal of a beach scarp. The value for the runup elevation associated with beach scarp destruction remains unknown, but could be an important parameter in predicting beach scarp behaviour (and possible nourishment design choices). The destruction of mount B2 was unlike the types described in the theoretical background. Its destruction was namely related to the horizontal extent of the experiment, the scarp was destroyed upon complete removal of the mount.

Despite the correlation between the destruction of beach scarps and severe storm conditions, not all destruction can be explained by extreme events. Drying of the scarp and aeolian deposition in front of the scarp are required to explain the observed destruction periods without these extreme hydrodynamics. These destruction methods have not been extensively reported in scientific literature, but have been mentioned by Sherman and Nordstrom (1985) as a possible type of destruction and were observed during the field experiments conducted during this study. The time scales on which these processes take place and the parameters influencing these destruction mechanisms still remain unknown, but could be studied in the future.

General properties of beach scarps

Beach scarp positioning in beach models
Beach scarps have often been positioned inside the foreshore within various beach models (e.g. Engineers, 2002; Sorensen, 2005; Longhitano, 2015). This position is not sustainable on a long term, with swash impacts causing migration of the beach scarp. After the formation of a beach scarp, migration of this feature will cause the scarp toe to be positioned around the maximum runup elevation. The final position of the beach scarp is of course time dependent, as changing hydrodynamic conditions alter the rate of migration. We therefore suggest that beach scarps are to be positioned inside the backshore, with the toe elevation positioned on the maximum runup during MHW (Figure 8.1). Synonymously, the position of dune scarps has been suggested to align with the maximum wave runup limit at the peak storm surge (Kriebel and Dean, 1985).

The definition of beach scarps
The definition proposed in the theoretical background of this study has been adjusted from Ruiz de Alegria-Arzaburu et al. (2013) and was found to fit the newly observed beach scarps at SE and the scarps created during the field experiments,

> A **beach scarp** is defined as a non-vegetated, subaerial beach feature with a slope larger than the critical angle of repose of 32^o and a minimum height of 0.30 m.

Despite the fact that this definition is theoretically sound, some unwanted implications can arise

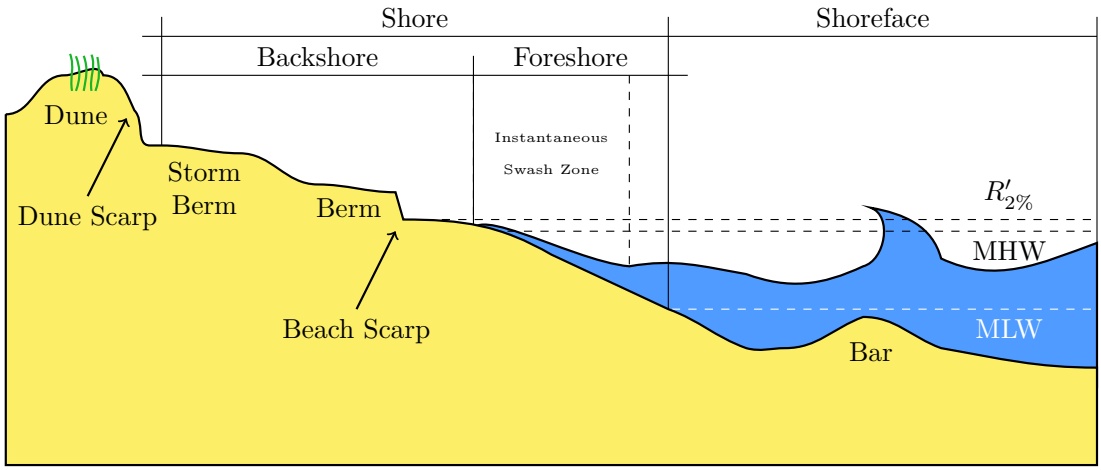

Figure 8.1: Proposed graphical representation of the coastal region, adapted from the Coastal Engineering Manual 2002 and Sorensen (2005)

when dealing with its implementation. Slopes just above the natural angle of repose will remain stable due to the apparent cohesion of the unsaturated material. Theoretically, this definition thus implies that beach scarps can reach infinite heights under relatively mild slopes. These 'beach scarps' with slopes just above the natural angle of repose will neither cause dangerous situations nor nuisance to beach visitors. A classification based on the scarp slope is therefore proposed: 'mild' beach scarps between 32-60 degrees, 'severe' beach scarps steeper than 60 degrees. Laser measurements of an existing beach scarp at the Sand Engine showed an alongshore variability in scarp slope. From these measurements, slopes exceeding the 60 degree boundary were found to representative for 'severe' beach scarps. Beach scarp height could be incorporated in this classification, which would result in a definition of beach scarps based on a combination of height and slope (from a beach visitors point of view).

Beach scarp toe elevation
Detailed measurements of beach scarp toe and crest elevations at the Sand Engine have shown that the spatial variability in beach scarp height is related to the platform height. This is caused by a rather constant ('fixed') toe at the maximum runup elevation, similar to the reported beach scarp toe elevation in literature (Figure 8.2). For this figure, both field observations (Ruiz de Alegria-Arzaburu et al. (2013), this study) and experiments (Bonte and Levoy (2015), this study) and laboratory studies were included (van Gent et al. (2008), Palmsten and Splinter (2016)) were included. The wave runup has been calculated according to Stockdon et al. (2006) and shows a direct correlation to the beach scarp toe elevation ($R^2 = 0.80$ and RMSE = 0.07 m).

In the alongshore direction, local variations in wave runup could therefore lead to changes in beach scarp height. But as shown from the detailed measurements at the SE, the spatial variability in scarp height is mostly governed by changes in crest elevation (i.e. undulating nourishment platform). On the contrary, the spatial variability in dune scarping elevation has been shown to be largely dependent on vegetation and soil development (Carter et al., 1990).

Beach scarp height
Nishi et al. (1995) showed that the height of beach scarps formed on a continuous linear slope is related to the steepness of the beach profile; steeper slopes will result in higher beach scarps. This is not the case for scarps on beach face nourishments, which are bounded by the platform elevation and maximum swash elevation. It could even be argued that the scarps on these nourishments are smaller when formed on steeper slopes as the maximum wave runup is positively correlated to the beach steepness (Stockdon et al., 2006).

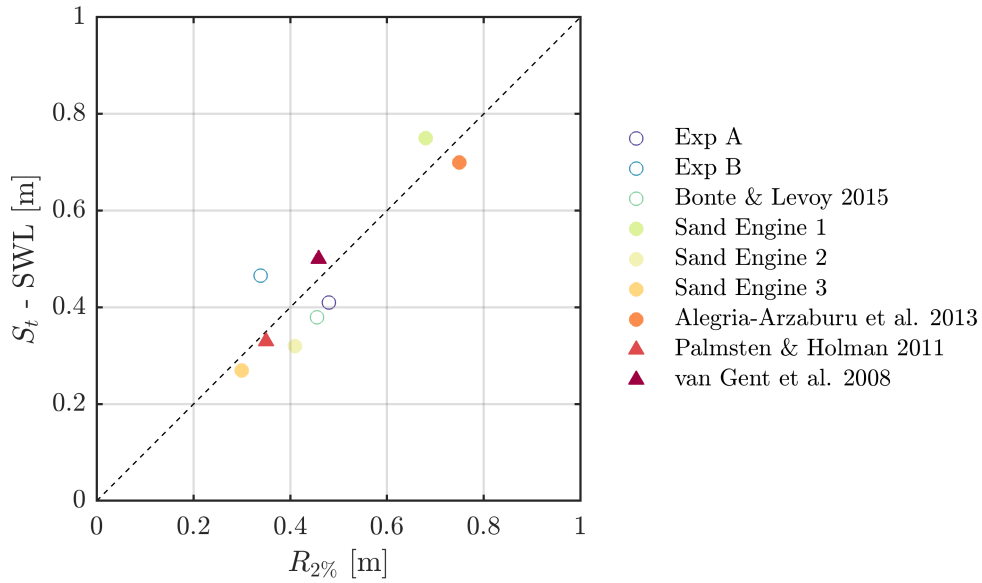

Figure 8.2: Beach scarp toe elevation with respect to SWL compared to the wave runup according to Stockdon et al. (2006) for various field experiments (crosses), field observations (circles) and laboratory experiments (upward triangles) reporting beach scarps ($R^2 = 0.80$, RMSE = 0.071 m)

Geotechnical analysis and field experiments

Culmann-type analysis

To perform the beach scarp stability analysis presented in chapter 5, several assumptions and simplifications had to be made which are discussed in this section. The Culmann-type analysis is based on the cohesive strength of a material. As treated in the introduction, two forces provide the apparent cohesion required for beach scarp stability; the matric and osmotic suction. For the presented analysis, only the matric suction was taken into consideration as the osmotic suction was assumed to be an order of magnitude lower. Although this assumption seems to be valid, inclusion of the osmotic suction could lead to an increase in beach scarp stability. Computing the apparent cohesion solely on the matric suction stress for unsaturated slopes can therefore not be considered conservative; higher scarps with steeper slopes are expected when the osmotic suction is taken into account. To better understand the geometry of beach scarps (slope and height), additional measurements are needed of newly formed beach scarps. Collecting the data directly after the formation, will allow for an analysis without the effects of drying collapse or burying by aeolian transport. This data should furthermore be obtained with a high spatial resolution (e.g. LiDAR or drone imagery), as GPS measurements might result in a poor representation of the scarp slope (Darnall, 2016). This data could for example be obtained using LiDAR equipment and will provide the relationship between scarp slope and height required for validation of the geotechnical analysis.

One of the main assumptions is the beach scarp slope used in the Culmann-type analysis. Detailed measurements of a naturally occurring beach scarp at the Sand Engine showed that on average, these features are not completely vertical but had an average slope of 67^o. It was assumed that this value corresponded to the angle under which the beach scarps at the Sand Engine exist. A corresponding critical beach scarp of 3 meters was found, which implies that scarps exceeding this height will collapse under their own weight, creating a more gentle profile. It could also be posed that the slope is an output parameter of this analysis, as the beach scarp toe and crest elevations are determined by the swash elevation and platform topography (which was used in the conceptual model presented in this thesis). Based on this idea, beach scarps can be classified either as **stable** or **unstable** (Figure 8.3).

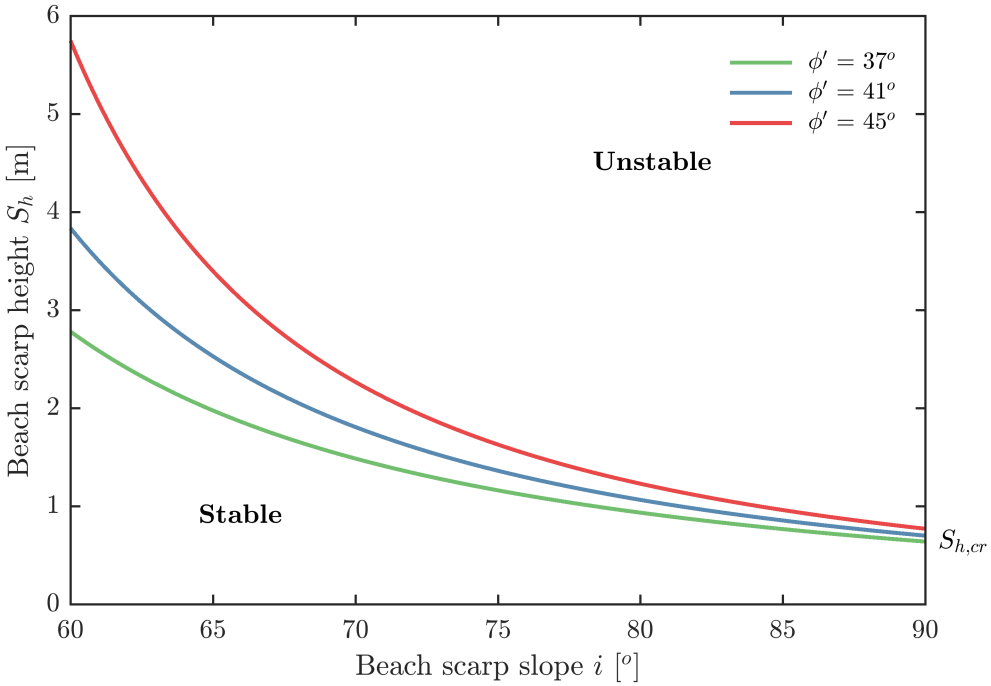

Figure 8.3: Beach scarp stability as a function of the scarp slope as derived from the Culmann-type stability analysis presented in chapter 5 (γ = 18 kN/m^3, σ^s=-1.44 kPa). Two regions can be distinguished; stable and unstable beach scarps located below and above the critical heights respectively.

Validity of beach scarp creation experiments

The experiments showed that 2D-effects influenced the erosion rates of the constructed mounts. It was found that the erosion rates were higher on the seaward corners than at the centre of each mount. The alongshore variation was found to be highest for the steepest mounts (A2 and B2), which were the first to form *scarps* on their corners. This variation in erosion rates along the mounts can be attributed to the combined swash attack and backwash influencing the corners. Despite the influence of these 2D effects on the alongshore variation in erosion rates, the formation observed is still considered a highly cross-shore dominated process as it takes place in the upper part of the wave runup zone and is observed in laboratory experiments.

During the experiment presented in this thesis, the formation took place between $R'_{15\%}$ and $R'_{2\%}$. Based on this single experiment, it cannot be determined whether this range is universal and it might vary between experiments. Additional compaction of the constructed berms was not performed, which most likely resulted in increased erosion rates (compared to the relatively compact Sand Engine).

Conceptual model and end-users

Conceptual model

Theoretically, beach scarps form when the beach slope just above the maximum swash extent exceeds the natural angle of repose. As discussed in *the definition of beach scarps*, a different classification based on the nuisances and hazards to beach visitors is proposed. This adjusted limit could be included into the conceptual model, where a beach scarp is considered to be present if the upper beach slope is steeper than 60 degrees.

Implementation of the conceptual model into a predictive model can be done in two ways; process based or empirical. According to the conceptual model, a process based model should incorporate the distinction between profile retreat with and without beach scarp formation (erosion with steepening upper profile). In addition, the ideal process based model should incorporate

the various responses of beach scarps to the environmental conditions. This not only includes hydrodynamically controlled overwash and migration events, but also the aeolian transport and drying collapse of beach scarps on longer timescales. This ideal model should also include a module to account for groundwater flow, which is required to predict the migration of beach scarps (Palmsten and Holman, 2011). The required overwash for beach scarp destruction would have to be included, a value which is not known as of now.

A first estimation on whether beach scarps will form can be made using the adapted DUROS+ model. The presented model in this study takes the elevation of the scarp toe into account, which is positioned at the maximum runup elevation as opposed to the water level used in DUROS+. Additionally, the steepness of the slope between $R'_{2\%}$ and backshore has been changed to match the critical combination of beach scarp slope and height according to a Culmann-type stability analysis. Without these adaptations to DUROS+, the height of beach scarps formed at beach-face nourishments would be over-predicted (SWL to nourishment platform) whereas the slope would be under-predicted (1:1).

Although the final beach profiles seem reasonable, the application of this tool to curved coastlines (e.g. local mega-nourishments) is doubtful as retreat distances can increase more than 100% for typical Dutch coastline curvatures (Hoonhout and den Heijer, 2011). This model is therefore not advised to determine the erosion of beach nourishments, which can be highly two dimensional. It does however, provide some insight into the expected beach scarp toe elevation (and corresponding scarp height and slope). In order to better predict the landward retreat of the profile, and thus the crest elevation of the potential scarp, more advanced process-based models could be used (e.g. XBeach). The presented Culmann-type stability analysis could be implemented as a first estimation of the beach scarp height and slope, instead of the typical user-defined slopes in these type of models. More advanced models could incorporate numerical infiltration models to better predict slope stability, but might be less practical for end-users as more (often unknown) input parameters are required (Palmsten and Holman, 2011). A correct implementation of beach scarp destruction would furthermore increase the reliability of model predictions, which has not been included in the presented DUROS+ adaptations.

End-users
In general, stakeholders in nourishment projects prefer the (dry) beachface nourishments, to directly benefit from the beach-widening. This is therefore often chosen as a soft solution to eroding coastlines by designers, contractors and decision makers (Botero et al., 2018). On the short term, a beachface nourishment will positively benefit some stakeholders (e.g. beach visitors and local businesses). On the long term however, reshaping (erosion) of the beach profile could lead to the formation of unwanted beach scarps, negatively affecting stakeholders (e.g. beach visitors, lifeguards) and ecosystems.

Based on the results presented in the previous chapters, several aspects in the design of beach nourishment schemes can be discussed. First, the type of nourishment (beach or shoreface) has to be considered carefully. The formation of beach scarps is far more likely to occur after a beach nourishment, which should be avoided if these vertical cliffs are unacceptable. Second, several geometrical and geotechnical aspects of beach nourishments can be adjusted to reduce the formation and persistence of beach scarps (Table 8.1).

The design of tourist beach nourishments can lead to the formation of beach scarps, leading to serious economic implications on tourist beaches (e.g. Cancun Beach, Mexico and Cádiz Province, Spain). Stakeholders in these replenishment projects favour the immediate widening of their beach profile, which often results in unnaturally high berms and steep slopes as a result of beach *overloading*. Upon erosion of these steep profiles, the formation of beach scarps can easily be initiated, whereas the unusually high berms limit the possibility for hydrodynamic destruction. As inundation of a tourist beach is also not preferred, a nourishment design that ensures some degree of beach scarp destruction in the form of destructive overtopping is therefore suggested for tourist beaches. This type of design includes a nourishment platform elevation just above

Table 8.1: Relative influence of geometrical and geotechnical nourishment design choices on general beach scarp morphodynamics. Other aspects could affect these processes as well (e.g. groundwater, wind speed/direction and coastline orientation), but are not included in this overview of design parameters for beach nourishments.

	Design parameters				
	$h_{n,p}$	β_{ini}	D_{50}	Compaction	Shell content
Scarp response					
Formation rate	0	+ +	+	-	0
Migration rate	-	0	-	-	0
Hydrodynamic destruction	- -	0	-	-	0
Dry collapse destruction	+	0	+	-	-
Aeolian destruction	+	0	-	0	0
Scarp properties					
Height	+ +	0	-	0	0
Slope	-	0	+	+	+

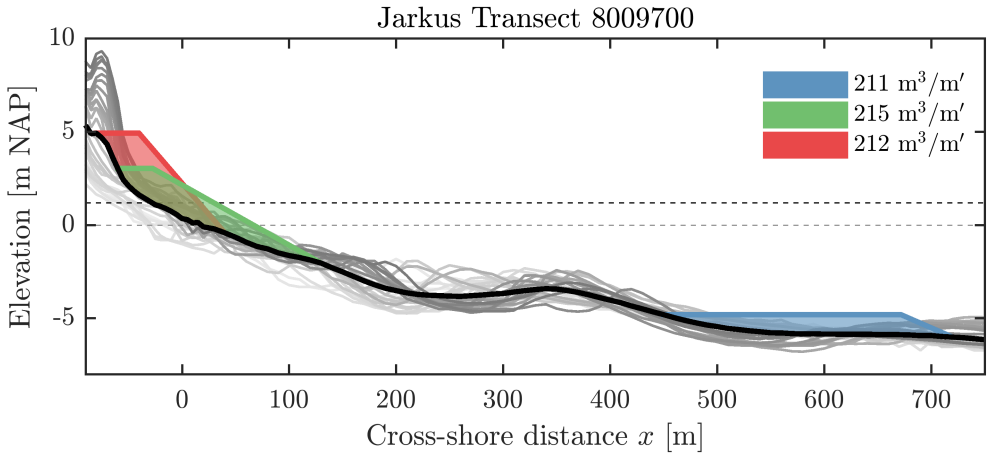

Figure 8.4: Three nourishment options for Scheveningen (Netherlands) with volumes of $\mathcal{O}(200\ \mathrm{m}^3/\mathrm{m}')$. MHW and MSL are given in dashed horizontal lines. Nourishment from least to most susceptible to beach scarp formation; foreshore nourishment (blue), beach nourishment with low platform and gentle slopes (green), beach nourishment with high platform and steep slopes (red).

the expected maximum swash elevation during MHW and relatively gentle slopes. During storm conditions, overwash of the platform will reduce the upper beach slope and remove any unwanted beach scarps without the need for (expensive) beach maintenance (e.g. 15/1 year). By reducing the nourishment platform height, additional material is available to design a gentle seaward slope or increase the nourishment extent in the horizontal plane (Figure 8.4). Apart from these geometrical design choices, material with a relatively low angle of repose (and therefore low D_{50}) should be nourished without additional compaction.

Apart from the addition of recreational areas, new environmental habitats and storm protection can be created using beach nourishments (Dean and Dalrymple, 2001). Initially, beach nourishments will result in large disturbances in the local ecosystems. On the long term the formation of beach scarps is undesirable, which calls for a nourishment design similar to the described design for tourist beaches; ensuring hydrodynamic destruction. In addition to the design rules presented for tourist beaches, these nourishments could be designed to ensure local inundation, providing continuous interaction possibilities between the foreshore and backshore. Beach nourishment projects with the aim of increasing coastal resilience to storm protection might not directly benefit from taking these design guidelines into account, as beach scarps do not increase the amount of erosion. But as these nourishments are often designed for multi-purpose use, it is still advised to alter the design accordingly.

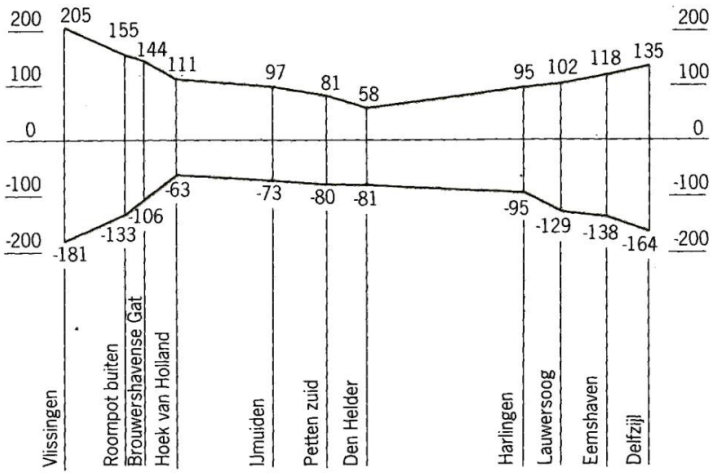

Figure 8.5: Graphical representation of average high and low waters at measurement stations along the Dutch coast (in cm NAP) adjusted from Hisgen and Laane (2004). Source: Bosboom and Stive (2013)

Due to the strong relation between the water level and the destruction of beach scarps formed on beach nourishments, an alongshore variation in tidal amplitude could result in different design guidelines for beach nourishments along a certain coastline. For the Dutch coast a maximum platform elevation of 3.5 m NAP is often enforced, with most of the beach nourishments constructed at 3.0 m NAP (Q. Lodder, personal communication, Jan 9, 2018). Some exceptions to these general platform heights exist; in 2011 a beach nourishment in Hoek van Holland was constructed with a platform elevation of 4.5 m NAP. Rapid steepening of the beach slope was reported afterwards (reminiscent of the beach scarp formation process), which required smoothing out of the profile using front loaders to ensure a swimmer safety. Taking into account the alongshore variation in tidal amplitude for the Dutch coast (Figure 8.5) and the effect on beach scarp morphodynamics, it is implied that the nourishment platform can be designed on a higher elevation for Vlissingen than for Den Helder (assuming similar wave conditions and storm surge).

9

Conclusions and recommendations

The objective of this study was to gain a better understanding of beach scarp morphodynamics, focussing on the prediction of beach scarp formation. This was studied by means of an extensive literature study, an analysis of beach scarp dynamics at the Sand Engine, an assessment of the geotechnical aspects of beach scarps, large scale field experiments and the development of a conceptual model. This chapter presents the conclusions of this study by means of answering the research questions posed in chapter 1. The main research question is answered first, followed by the subquestions.

Which combinations of hydrodynamic conditions and geotechnical/geometrical parameters will result in beach scarp formation, migration, and destruction?

This study has shown that the formation of beach scarps occurs during erosive conditions on relatively steep beach slopes. The process of beach scarp formation is characterized as the steepening of the beach profile between $R'_{15\%}$ and $R'_{2\%}$ caused by landward retreat of the beach profile. Beach scarps are therefore found to form during mildly erosive conditions on steep beach slopes (e.g. beach nourishments or cusp horns), whereas beach scarp formation on more gently sloping (natural) beaches require highly energetic storm conditions (e.g. typhoon conditions along the Japanese coast according to Nishi et al. (1995)). As the beach steepness and erosion rates are related to geotechnical parameters, these were found to influence the formation to some extent. Beaches with coarse material are generally associated with steep beach profiles, which are therefore more susceptible to beach scarp formation than fine grained beaches. Compaction and shell content were found to increase the stability of beach scarps (and therefore their persistence).

Beach scarp migration is initiated by the swash elevation exceeding the scarp toe elevation. Undercutting and slumping of the beach scarp face occurs during this collision regime, leading to a landward migration of the beach scarp. Landward migration rates of the beach scarp face were found to be dependent on the scarp height given the same hydrodynamic conditions (on 26/09 $S_h = 0.40$ & 0.66 m with $v_{sc} = 0.027$ & 0.022 m/min; on 02/10 $S_h = 0.55$ & 1.2 m with $v_{sc} = 0.026$ & 0.012 m/min). This indicates that the landward migration rate is inversely related to the beach scarp height.

The destruction of beach scarps is not only governed by extreme hydrodynamic conditions causing overwash of the beach scarp (producing a more diffuse profile), but is also related to environmental conditions leading to drying collapse and burying of the scarp by aeolian transport. Apart from destruction by overwash and inundation, these methods of destruction can therefore not be neglected in the overall life cycle of beach scarps.

What conditions cause the formation, migration and destruction of beach scarps at the Sand Engine?

The long term data analysis of beach scarp existence at the Sand Engine has shown that these features form during summer storm conditions at this mega-nourishment. Prior to these summer storms, mild conditions result in relatively steep beach slopes which have been found to be more susceptible to scarp formation. During the following summer storms, erosion occurs without excessive overwash of the nourishment platform leading to further steepening of the upper beach profile and eventual beach scarp formation. After the formation of a beach scarp, migration is initiated when the swash elevation exceeds the scarp toe in mild (summer) storms.

The alongshore averaged behaviour of beach scarps at the Sand Engine has shown that the destruction can be related to major (winter) storm events. During these events the overwash or inundation regimes caused flattening of the beach profile and removal of the beach scarp. Based on an analysis of beach scarp presence per transect it was shown however that not all beach scarp destruction can be explained by changes in hydrodynamic conditions. It was found that $\sim$50% of the removed beach scarps are related to either the drying and subsequent collapse or the burying by aeolian transport.

What causes the alongshore variability of beach scarps at the Sand Engine?

A direct relation between the alongshore non-uniform beach slope and non-uniform beach scarp presence at the Sand Engine was not found from the long term data analysis. Detailed beach scarp measurements have shown however that the toe elevation is almost constant ('fixed') around the maximum runup elevation, leading to a high correlation between the scarp height and the platform elevation. On lower parts of the Sand Engine the maximum runup elevation might have exceeded the platform, leading to a spatial variability in beach scarp presence. As beach scarp height is defined as the crest elevation minus the toe elevation ($S_h = S_c - S_t$), the spatial variability in beach scarp height can be largely explained from the undulating nourishment platform at the Sand Engine. These findings imply that the height of beach scarps can be written as a function of the nourishment geometry and swash elevation; $S_h = h_{n,p} - R'_{2\%}$.

As the scarp toe is positioned around the maximum runup level, the beach scarp height is inversely related to the maximum runup level (assuming a horizontal nourishment platform). Mildly erosive conditions with low water levels can therefore lead to the formation of relatively high beach scarps compared to those formed during more energetic conditions with high water levels.

Is there a geotechnical limit to beach scarp heights (at the Sand Engine)?

Critical beach scarp heights can be determined using a geotechnical analysis based on suction stresses and a Culmann-type stability calculation. It was found that these critical beach scarp heights were a function of the scarp slope. As the definition states that beach scarps are features with slopes larger than the angle of repose, this implies that no single value exists for the maximum beach scarp height. The critically stable beach scarp height (determined by the maximum swash elevation and platform topography) is thus highly dependent on the beach scarp slope; large beach scarps $\mathcal{O}$(5 m) are stable under slopes of $\mathcal{O}(60^o)$, whereas small beach scarps $\mathcal{O}$(1 m) can reach slopes of $\mathcal{O}(90^o)$. The major influencers of beach scarp stability are the scarp slope (negative) and the natural angle of repose (positive). Suction stresses are higher for fine grained material which increase the maximum attainable height of a beach scarp, whereas the specific unit weight has a negative influence on this limit.

How does the design (initial slope and platform height) of nourishments influence the formation of beach scarps?

Field experiments, in which the initial slope and platform height were varied, showed that it is possible to study the effects of the nourishment design on a large scale (without additional compaction). By changing the initial slopes of the artificial mounts under wave attack, it was shown that the initial beach steepness increases the rate at which beach scarps form. Whether

beach scarps form after beach nourishments is largely related to the platform elevation level, which governs the amount of overwash. By allowing enough overwash on the platform, the formation of beach scarps can be prevented. Reducing the nourishment steepness furthermore reduces the rate at which beach scarps might form, leading to a better overall prevention of beach scarp formation on beach nourishments.

To what extent and how can we predict the formation of beach scarps?

This study has shown that the toe elevation of beach scarps can be predicted using a modified version of the DUROS+ model, which was originally developed to predict dune erosion (with the dune scarp toe at the SSL). As mentioned earlier, detailed beach scarp measurements have shown that the toe elevation is almost constant around the maximum swash elevation. This has been included in this model using the Stockdon et al. (2006) empirical wave runup formula. For horizontal nourishment platforms, this model can furthermore predict the maximum height of a beach scarp for given hydrodynamic conditions. Additionally, the model uses a Culmann-type analysis to determine the associated critical beach scarp slope to the scarp height based on geotechnical parameters. By comparing results of the model predictions to case studies at Cancun Beach and the Sand Engine, it was shown that the scarp toe elevation can be predicted with reasonable accuracy ($\pm$ 0.1 m). The prediction of beach scarp heights for undulating platform levels is not advisable using the presented model, as the prediction of the landward profile retreat is only based on a cross-shore re-distribution of the sediment. The presented model does however provide a tool to gain more insight into beach scarp formation as a result of beach nourishment projects for various geometrical, geotechnical and hydrodynamic conditions.

Engineering recommendations

In the design of beach nourishment projects, the formation of beach scarps can be influenced in several ways. First, the platform elevation should be designed as such to allow hydrodynamic destruction (overwash) to occur once in a while (e.g. 15/1 year). By designing an non-overwashable nourishment, the destruction of beach scarps solely relies on drying collapse, burying by aeolian transport or human intervention. Determining the platform elevation based on the overwash occurrence will lead to lower beach nourishments in general, which might require extending the design in the horizontal plane. Other implementations of this recommendation could include the design of a wave-like nourishment platform, to prevent excessively long beach scarps to form. This type of design allows for scarp destruction on low-lying areas (as the scarp height is limited) providing possible interaction between back-and foreshore. Second, the initial nourishment slope should be chosen rather gently (e.g. 1/30), to reduce the speed at which beach scarps form. This can allow for natural diffusion of the steep beach profile during more energetic conditions before beach scarps have formed. Third, it is advised to use material with a relatively low angle of repose for the nourishment without additional compaction during construction.

Research recommendations

This study has provided more insight into the morphodynamics and general properties of beach scarps. The findings generally hold for both natural and replenished beaches by means of beach nourishments. The experimental research has shown how beach scarps form and migrate, but certain aspects of these processes remain unknown. Especially the destruction of beach scarps by means of hydraulic controls remains a poorly understood subject.

Large scale laboratory experiments to study beach scarp formation

Large scale laboratory experiments could provide additional insights into the formation mechanism of beach scarps. By conducting wave-flume experiments on an initially linear slope using with different hydrodynamic, geometrical and geotechnical settings, the formation of beach scarps can be assessed in more detail. This study has shown that beach scarps form as small scale features in a narrow band at the maximum swash extent (between $R'_{15\%}$ and $R'_{2\%}$). Whether this zone can be considered 'universal' remains unknown, laboratory studies might show that this is a function of the geotechnical parameters and the hydrodynamic conditions.

Beach scarp destruction by overwash and inundation
Further laboratory experiments could be conducted to assess the required overwash for complete destruction of a beach scarp (R'_d). By changing the hydrodynamic forcing (wave conditions, or water level) the overwash on top of an existing scarp could be adjusted until destruction occurs. The destruction of this scarp is most likely dependent on several geotechnical aspects (e.g. grainsize and compaction) and geometrical parameters and geometrical (e.g. scarp height and scarp slope). Performing these experiments using different scarp configurations could therefore provide new insights into the overwash destruction mechanism.

Long term beach scarp response: drying collapse
By constructing beach scarps with pre-defined geotechnical properties, the drying collapse mechanism could be assessed more thoroughly. This experimental research could either be done in the lab or in the field and may show the dependency of scarp drying collapse on grainsize distribution, shell content, scarp height and scarp slope.

Long term beach scarp response: aeolian transport
Field experiments could be conducted to assess the destruction of beach scarps by aeolian transport. Ideally, beach scarps would be formed during high water spring storm conditions after which the scarp remains unaffected by swash impacts for several days. Monitoring the accumulation of sediment in front of the scarp with respect to the environmental conditions (e.g. wind speed, soil moisture) may reveal valuable insights into the effect of aeolian transport on beach scarps (and vice versa).

Geotechnical aspects
In addition, LiDAR measurements of newly formed scarps (i.e. without drying collapse or burying by aeolian transport) may provide valuable data for the geotechnical assessment of beach scarps. By taking these highly detailed topographical measurements, the relationship between scarp height and (critical) scarp slope can be validated. Moreover, laser measurements could provide insight into the moisture content of 'fresh' scarp faces. Apart from these laser measurements, the general assessment of this study could be improved upon. Currently, the natural angle of repose is increased in order to account for the compaction nourished material. This was considered a 'practical' approach for this study, it is advised to look into dense sands for a more theoretically robust analysis.

Implementation into process-based models
Finally, incorporation of the found beach scarp dynamics into a process-based models such as XBeach could result in better predictions of these features in the future. As the formation of these features around the maximum swash extent is often included, it is advised to determine the according beach scarp slope based on the geotechnical assessment presented in this thesis. In addition, the overwash and inundation should be included for a proper assessment of beach scarp destruction on short timescales. To determine beach scarp response on longer timescales, the inclusion of aeolian transport and drying of the scarp is advised. For these advanced models, proper inclusion of water infiltration into the sand body might be required (as suggested by Palmsten and Holman (2011)).

Appendices

A

Literature study

The literature review presented in chapter 2 contained a brief overview of the studies reporting beach scarps under both laboratory and prototype conditions. This appendix contains additional information about the studies into beach scarp morphodynamics in a chronological order. Furthermore, several papers about dune scarp morphodynamics are included as they might produce valuable insights into their beach equivalents.

Kana (1977)

The formation of beach scarps has been related to the occurrence of beach cusps at Debidue Island, South Carolina (Kana, 1977). Beach cusps are pronounced arc-shaped shoreline formations which are typically associated with reflective beaches Bosboom and Stive (2013). These low parts of these rhythmic patterns are generally referred to as *cusp embayments* and contain relative fine sediment, whereas the higher parts are called *cusp horns* and are made of coarser sediment (Figure A.1). During a minor storm that occurred at Debidue Island, beach scarps with heights of up to 1 meter occurred along the entire study area and were found to be dependent on the beach cusp topography. The following description of a beach scarp life cycle was is given;

1. The *formation* of beach scarps was initiated by minor wave attack on the beach cusps.
2. The landward *migration* of the initial scarps occurred as a result of swash attack on these features. This swash attack caused 'undermining' (undercutting) of the vertical cliffs, which eventually caused slumping and removal of the sediment offshore. Next, the scarps coalesced into a single (uninterrupted) scarp along the entire study area. Retreat of the scarp was not found to develop any further due to the fact that high waves were out of phase with the high tide.
3. The *destruction* of the beach scarp was observed and was caused by partial recovery of the beach (i.e. accretion). A complete recovery of the beach was not observed within the study.

Figure A.1: Observation of well developed beach cusps at Trafalgar Beach in the Cádiz Province (Spain), note the very steep cusp horns with respect to the rather gentle embayments. Source: Miguel Ortega Sánchez, 2013

This study concludes with stating that five non-storm factors control the rate of beach erosion and scarp formation: sediment grain size; degree of lithification; beach slope; beach morphology; water level. The beach morphology refers to the fact that wave attack on the beach cusps triggered the formation of the scarps. The results from the study showed that the transition from plunging waves to spilling waves could be of importance when predicting beach scarp formation (beach scarps were formed when $\xi \approx 0.5$). The study finally claims that erosion (under the same wave conditions) occurs faster when beach scarps are present.

Short and Wright (1981)

During field observation at the Narrabeen-Collaroy coast, both dune and beach scarps have been observed. Based on these observations, the formation of beach scarps was associated with a combination of intermediate beach states and intermediate wave energy. It was found that short (T_p = 7 - 9 s) and moderately high waves (H_s = 1 - 1.5 m) caused the cliffs to form, whereas the highest energy waves resulted in dune scarping.

Short and Hesp (1982)

In this paper the morphodynamic classification of beaches based on cases found along the Australian coastline is discussed. The type of scarping described is mainly related to the erosion of dunes. These dune scarps are often found to form along dissipative beaches, which only show minor variation in the alongshore direction. It is furthermore stated that occasional dune scarping can be observed along reflective coasts.

Wright and Short (1984)

An overview of the beach states classification, which had been a popular topic during the 1980's, is presented in this paper. Two parameters are discussed; the surf-scaling parameter ϵ, given by $a_b\omega^2/(g\tan^2\beta)$, and the dimensionless fall velocity Ω, given by $H_b/(\bar{\omega_s}T)$. The classification of beach states was found to follow both of the classification parameters, ranging from reflective ($\epsilon < 2.5$, $\Omega < 1$) to dissipative beaches ($\epsilon > 20$, $\Omega > 6$). Typical plan an profile configurations show beach scarps to be present on the dissipative side of the intermediate states, which lies between the limits described above. As this study provides a rather general description of beach states, detailed information about beach scarp morphodynamics (formation, migration, destruction) is not presented.

Sherman and Nordstrom (1985)

This paper presents an overview of the beach scarps noted in literature and points out the need for a better understanding of these features. It is hypothesised that beach scarps are formed as a response to coastal erosion. This is in direct contrast to the common misconception that these scarps cause erosion (e.g. Kana, 1977). The formation of beach scarps into two groups; initiation by process controls (1) and initiation by structural controls (2). Process controls contain the influence of waves and currents whereas structural controls are based around natural and human impact. One could also state that process controls are the forces that govern beach scarp formation whereas structural controls (both horizontal as vertical) present the resistance.

It was found that structures perpendicular to the shoreline orientation, such as groins and natural headlands, tend to favour beach scarp formation. The beach scarps were furthermore found to be associated with beach cusps (with five examples given). This is in-line with the findings presented in prior scientific literature (e.g. Kana, 1977).

After the beach scarps have been formed, migration is mostly governed by the amount of swash reaching the toe of this vertical cliff. This will cause undercutting and slumping as expected. Migration of the scarp will come to a standstill if the swash is not able to reach the toe. This can be related to changes in water level, which happens to also play an important role in scarp destruction. When a sudden increase in water level causes waves to overtop the scarp, the structure is moulded into a diffusive shape and is no longer classified as a beach scarp. This paper concludes with the completion of a beach scarp life cycle by destruction. The following

causes for destruction are discussed;

1. Continued upward migration, until the beach scarp coalesces with its dune counterpart (which was also described in Short and Wright, 1981).
2. Onshore migration of a swash bar, which can merge with the beach scarp.
3. Retreating water levels, which cause the scarp to dry and returns the sediment to its natural angle of repose.
4. Deposition of sediment in front of the scarp by either swash or aeolian transport.
5. High amounts of overwash, which results in a collapse of the near vertical cliff and leaves a more diffuse beach profile.

Nicholls and Webber (1989)

Beach scarp formation as described in Sherman and Nordstrom (1985) is not only limited to sandy beaches, shingle beaches located in southern England have been known to form these features as well. These beaches are composed of pebble and cobble fractions, which result in a very coarse and therefore permeable lithology. This study has shown that the location and amount of sand within this coarse material is of great importance for beach scarp development and persistence.

Beach scarps have been found to develop with heights of approximately 0.1 m for non-nourished shingle beaches. After a marine-dredged shingle nourishment was performed at Hurst Beach and Hayling Island, beach scarps were found to be an order of magnitude larger with local heights up to 2 m. It was found that these nourishments resulted in a considerable amount of sand between the larger grained pebbles and cobbles. Two sources for this 'contamination' could be indicated; the composition of marine material (1) and the method of nourishment (2). The large beach scarps had to be artificially removed, but were found to reappear at the beach of Hayling Island. This suggested that the large scarps will only cease to form when sediments are sorted similar to 'natural' shingle beaches (shingles located on the back-and foreshore; sand located on shoreface).

Antia (1989)

A relationship between erosion at beach cusp horns and the formation of beach scarps has been implied in Kana (1977). An analysis of beach cusps at Ibeno Beach (Nigeria) showed a very similar relationship. From observations of 93 volumetric beach changes it was claimed that only very few accreting beaches showed a combination of cusps and scarps. These beaches were furthermore found to be associated to scarp stability (no temporal change in height), whereas eroding beaches showed more beach scarps and a wider temporal variation their height. This was found to be in-line with the observation by Sherman and Nordstrom (1985), which stated that beach scarps are typical features of eroding coasts.

Carter and Stone (1989)

Carter and Stone studied the formation of *dune scarps* in Northern Ireland. Their study showed the importance of vegetation to the stability of these vertical cliffs. Two sites were used in this study with conditional wave heights in a different order of magnitude. Their response to a storm event was very similar however; in both cases *dune scarps* were found to form. It was claimed that sand accumulating vegetation, which reportedly increased the shear strength from 10-20 kN m^{-2} to 400-550 kN m^{-2}, was of vital importance to the stability of the *dune scarp*.

Bauer and Allen (1995)

Beach steps, which are located in a different part of the lower-shoreface, have been subject of this study by Bauer and Allen (1995). These steep seaward facing features show some resemblance to a submerged beach scarp. Clear differences have to be noted however: beach steps can be formed through 'carving', 'excavation' or 'building'. These three beach step initiation mechanisms occur during eroding, neutral or accreting events respectively. The conceptual model that has been

developed in this paper could be of use when studying beach scarp formation. A link between the transition from surging to plunging waves ($t/T \approx 0.5$) and beach step formation has been made in this paper. The notation t/T has been introduced by Kemp in 1975 (as cited in Bauer and Allen (1995)) as a means of indicating the 'phase difference' between uprush duration (t, given by $3H_b^{0.5}/(g^{0.5}\tan\beta)$) and wave period ($T$). No direct evidence was found of the impact of tidal variations on beach step development in this study.

Nishi et al. (1995)

This study from 1995 showed that storm conditions caused by typhoons are able of leading to massive dune and beach scarp formations. In 1991, when a rather large typhoon passed Japan, a large *dune scarp* was formed at Kashiwabara Beach (maximum height of 7 meters). Shortly after a beach nourishment has been completed in 1993, an even larger typhoon caused extreme storm conditions at this beach. These conditions resulted in the formation of *beach scarps*, which was attributed to the different nearshore beach profile present after the nourishment. In their study a numerical model was also developed, which indicated that beach scarp height tends to increase with increasing beach steepness.

Anfuso et al. (2001)

After several nourishments had been performed at eroding beaches in the south west of Spain beach scarps were observed. The scarps formed as a result of storm conditions prior to the execution of the replenishment. Monitoring of the nourished beaches showed that beach scarps formed again in front of a berm where plunging waves ($\bar{\Omega} = 1.06$) attacked the reflective-intermediate beach profile ($\bar{\epsilon} = 2.8$). Monitoring of the non-nourished adjacent beach showed that this at this location spilling-plunging waves ($\bar{\Omega} = 0.33$) attacked a dissipative beach ($\bar{\epsilon} = 28.7$), which showed little three-dimensional variability. It was concluded that the following three factors govern the beach fill stability; gradient of the restored beach, sediment grain size and density of the nourished material.

Erikson et al. (2005)

Swash interactions, which were described in Bauer and Allen (1995), have shown to be important in beach step formation. The question remains whether the interactions between the so called up-rush and down-wash also influence the formation of beach scarps. Some insight into the mechanisms of swash interactions are presented in this study. Erosion and foreshore flattening is expected when swash duration (up-rush and down-wash) is shorter than the period of incoming waves. Steepening of the foreshore is expected when swash duration is longer than the period of incoming waves. A more complex formulation of the total swash duration (which is not repeated here) was given in this study when compared to Bauer and Allen (1995). Two types of interactions between consecutive waves in their up-rush and down-wash stages were identified in this study; 'catch-up and absorption' and 'up-rush and back-wash collision' (Figure A.2). It was found that these swash interactions play an important role in cases with gentle foreshore slopes ($\tan\beta = 0.07$). For steep slopes ($\tan\beta = 0.20$) however, swash interactions were found to be of less importance.

Pelletier et al. (2006)

From the field of hillslope geomorphology, scarp evolution has been studied previously (e.g. Hanks et al. (1984)). These scarps are often observed with a slope equal to the angle of repose and their formation has been attributed to wave cutting and a drop in water levels (Wallace, 1977). Two methods are often used to determine the retreat of these scarps and are based on assumption of a linear relationship between the slope and sediment flux (F) as follows,

$$F = \kappa \frac{\partial h}{\partial x} \tag{A.1}$$

In which the diffusivity parameter is represented by κ, the distance along a profile by x and the elevation by h. The evolution of the scarp the follows from the classic linear diffusion equation,

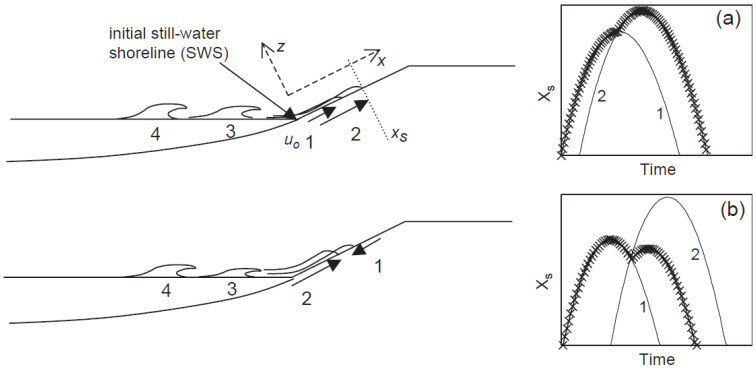

Figure A.2: Two types of swash interactions; 'catch-up and absorption' (a), 'up-rush and back-wash collision' (b). Source: Erikson et al. (2005).

$$\frac{\partial h}{\partial t} = \frac{\partial F}{\partial x} = \kappa \frac{\partial^2 h}{\partial x^2} \tag{A.2}$$

- Midpoint-slope methods
  Single scarp analysis, in which the midpoint slope of a single scarp is used within the analytic solution of the diffusion equation.
  Multiple scarp analysis, in which the midpoint slopes of a multitude of scarps are compared to their scarp offsets (vertical height).

- Full-scarp methods
  Within this the entire scarp (or its corresponding hillslope gradient) is fitted to a solution (analytic or numerical) of the diffusion equation.

The methods and equations derived within this field of science might not be of direct use for beach scarp morphodynamics due to the differences in soil types and forces causing these hillslope scarps to form. It does however provide for an interesting comparison to beach scarps and their evolution in time.

Alves and El-Robrini (2006)

A clear distinction between beach scarps and *dune scarps* is of great importance for this thesis. This paper from 2006 discusses the formation of beach scarps located on the foredunes, which seems rather contradictory. The observational field study at Ajuruteua, Bragança north Brazil, describes flattening of the beach profile and the formation of beach scarps caused by a combination of macrotidal processes and strong waves. The wave height was approximately 1.5 m whereas the tidal range at the study location equals 6 m. The influence of vegetation is not further discussed, although the included figures show vegetation and even some constructed houses at the foredunes. These will have a significant impact on the formation and stability of the *dune scarps*.

Erikson et al. (2007)

Experiments in the laboratory were done in which artificial beach scarps were constructed and their morphological response to various wave conditions was monitored. This study also presents an analytical model composed of a notch evolution part (sediment transport & conservation) and mass failure models (soil mechanics) based on these tests. The complete model was validated using the small-scale laboratory experiments and showed reasonable performance with a reported maximum absolute recession distance error of about 20%.

The notching model was developed to estimate the amount of eroded material at the *dune* foot. The erosion rate was shown to be linearly related to the hydrodynamic forcing (incident wave height) and the geotechnical properties (grain size and compaction). Whether this relationship

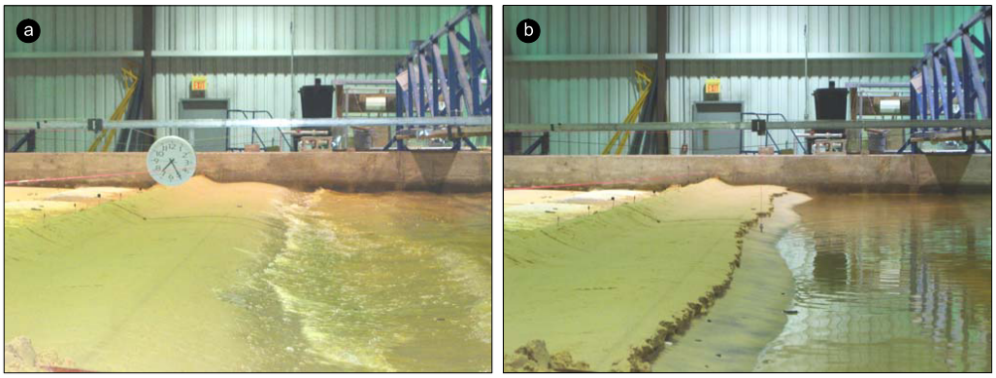

Figure A.3: The initial beach profile with a horizontal berm (a) compared to the final profile after 143 minutes of waves (b). The corresponding wave conditions were as follows; $H_{m0} = 6.50$ cm and $T_p = 1.07$ s. Source: Payo et al. (2008).

also holds for the formation of beach scarps remained unknown however.

Two modes of mass failure have been studied in this paper; shear- and beam-type failure (Figure 2.5). The first of these occurs when undercutting of the scarp causes a substantial overhang of material. If the shear force exceeds the shear strength of the sediment, shear-type failure occurs. If tensile cracking at the top of a scarp (and some distance from the scarp face) reaches an internal failure plane beam-type failure will occur. This beam-type failure can either result in sliding down or rotation of the failure block (Figure 2.5d-e).

It was noted that soil suction might be important in the stability of beach scarps. This was also one of the destruction mechanisms described in Sherman and Nordstrom (1985), 'drying of sand' is in essence the reduction (or lack of) soil suction. In this paper two types of suction are described; matric (1) and osmotic suction (2).

Although the results have shown to be reasonably accurate compared to small scale laboratory experiments, the authors acknowledge that field conditions are more complex. It is therefore suggested that the model presented in this study should be used in future studies under more complex situations.

Payo et al. (2008)

A multi-directional wave basin was used in this study to simulated the formation and migration of beach scarps. A relatively simple beach profile was created at an 18 m long wave basin in Delaware (United States). A steep foreshore slope of 0.2 is reported in the paper, whereas the figures indicate a much more gentle slope (≈0.05). The findings were later compared to a version of the model presented in Kobayashi et al. (2008), which included the effects of the bottom slope on sediment transport and scarping of the scarp face. Results showed a 'good' performance of this model with a reported Brier Skill Scores between 0.4 and 0.6.

An alongshore variability of beach scarp can be observed (Figure A.3b), which was reportedly caused by the non-uniform concrete slope used in the experiments. Similar to the discussion presented in Erikson et al. (2007), this study noted the lack of field data to validate various aspects of beach scarp behaviour.
In addition to the experiment, a model was developed, which was found to perform best with inclusion of the roller and bottom slope effects enabled. The roller effect increases the offshore return current and suspended transport in shallow waters.

Kobayashi et al. (2009)

In this study a numerical model is proposed to improve the understanding of berm and dune erosion during a storm. Relatively simple formulae are introduced and combined with a hydro-

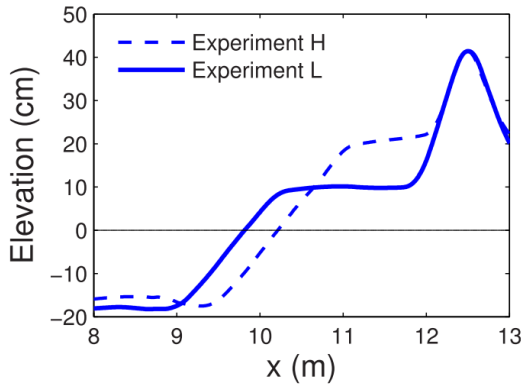

Figure A.4: Berm profiles used in small scale experiments. Source: Kobayashi et al. (2009).

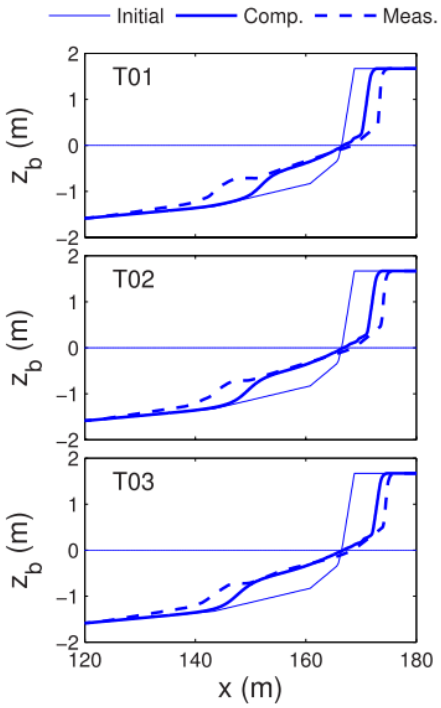

Figure A.5: Berm profiles used in the large scale experiments. Source: van Gent et al. (2008).

dynamic model presented in Kobayashi et al. (2007). This combined model is then compared to small-scale experiments performed by the authors and large scale experiments conducted by van Gent et al. (2006).

The small scale tests were performed with two different initial berm profiles. For both experiments the profile above still water level (SWL) were constructed with a slope of 30^o and a height exceeding 40 cm above SWL. According to the definitions used in other studies, this slope could already be classified as a beach scarp (e.g. **?**, Alegria-Arzaburu2013,Darnall2016)

The berm used in the first experiment was narrow and high, whereas the second was wide and low (Figure A.4). Scarping occurred during the beginning of the first experiment (referred to as Test HA). The hydrodynamic conditions that lead to the scarping behaviour were as follows; $H_{m0} = 0.19$ m and $T_p = 2.57$ s. The sediment used in this experiment had a mean diameter (D_{50}) of 0.18 mm, a fall velocity w_s of 0.02 m/s and a porosity equal to 2.6. The authors unfortunately do not present the resulting cross-shore profile after the scarping occurred during Test HA. The described scarp was removed during Test HB, in which the water level was increased by 5 cm (implying that the original scarp height was of $\mathcal{O}$(cm)).

The large scale tests have been performed by van Gent et al. (2006), which conducted experiments in the Delta Flume using various wave conditions. Above the SWL the initial profiles were constructed with slopes exceeding 32^o and a height exceeding 1 m, which can be classified as a beach scarp (Ruiz de Alegria-Arzaburu et al., 2013; Darnall, 2016). The sand used in their study was characterized by $D_{50} = 0.20$ mm, $w_f = 0.025$ m/s, s = 2.65 and $n_p = 0.4$.

The proposed numerical model showed to be less accurate for the experiments conducted by van Gent et al. (2006). The rate of erosion was clearly under predicted by the model when compared to these experiments. Despite the fact that this model was not shown to be perfect, it was further used in this study to assess the importance of the incident wave angle. Results showed that the influence of the wave angle, when comparing eroded areas, is in the order of 20%.

Table A.1: Overview of SUPERTANK wave and beach conditions; n = spectral peakedness, N = Dean number ($H_{bs}/(\omega T)$), M = monochromatic wave, H_{bs} = significant breaking wave height, ξ = surf-similarity parameter.

Wave Run ID	H_0 (m)	T_p (s)	L_0 (s)	n	N	H_{bs} (m)	$\tan\beta$	ξ	Scarp
10A_60ER	0.78	3	14	20	6.4	0.68	0.1	0.42	No
10A_130ER	0.78	3	14	20	6.8	0.68	0.09	0.38	No
10A_270ER	0.78	3	14	20	6.9	0.68	0.1	0.42	No
10B_20ER	0.71	3	14	3.3	6.6	0.65	0.14	0.58	No
10B_60ER	0.73	3	14	3.3	6.8	0.67	0.11	0.44	No
10B_130ER	0.72	3	14	3.3	7	0.69	0.09	0.36	No
10E_130ER	0.69	4.5	31.6	20	4.9	0.72	0.11	0.69	No
10E_200ER	0.69	4.5	31.6	20	5	0.74	0.12	0.77	No
10E_270ER	0.69	4.5	31.6	20	5.1	0.76	0.09	0.58	No
10F_110ER	0.66	4.5	31.6	3.3	5.1	0.75	0.09	0.58	Yes
10F_130ER	0.68	4.5	31.6	3.3	5.1	0.76	0.08	0.48	Yes
10F_170ER	0.69	4.5	31.6	3.3	5.1	0.76	0.08	0.5	Yes
G0_60EM	1.05	3	14	M	10	1.18	0.1	0.43	No
G0_140EM	1.04	3	14	M	10.5	1.04	0.1	0.41	Yes
G0_210EM	1.15	3	14	M	10.8	1.07	0.09	0.39	Yes
30A_60AR	0.34	8	99.9	3.3	1.6	0.41	0.14	2.24	No
30A_130AR	0.33	8	99.9	3.3	1.6	0.39	0.13	2.09	No
30A_200AR	0.34	8	99.9	3.3	1.6	0.41	0.13	2.02	No
30C_130AR	0.31	9	126.4	20	1.4	0.4	0.13	2.36	No
30C_200AR	0.31	9	126.4	20	1.4	0.39	0.15	2.31	No
30C_270AR	0.31	9	126.4	20	1.4	0.39	0.15	2.6	No
30D_40AR	0.37	9	126.4	20	1.4	0.42	0.13	2	No
I0_80AM	0.6	8	99.9	M	2.9	0.76	0.2	2.78	No
I0_290AM	0.63	8	99.9	M	3.1	0.81	0.17	2.35	No
I0_590AM	0.6	8	99.9	M	2.7	0.72	0.12	1.64	Yes
60A_40DE	0.69	3	14	3.3	6.2	0.61	0.12	0.55	Yes
60A_60DE	0.69	3	14	3.3	6.2	0.61	0.1	0.46	Yes
60B_20DE	0.64	4.5	31.6	3.3	4.4	0.66	0.11	0.74	Yes
60B_40DE	0.63	4.5	31.6	3.3	4.4	0.66	0.11	0.76	Yes
60B_60DE	0.65	4.5	31.6	3.3	4.4	0.66	0.12	0.79	Yes

Roberts et al. (2010)

The upper limit of beach changes and wave runup were investigated in this laboratory study. Two experiments were performed; SUPERTANK (2D wave channel) and LSTF (3D wave basin). Random and monochromatic waves with various characteristics were generated in the SUPERTANK experiment (Table A.1). These were either of the accreting kind, random (AR) and monochromatic (AM), or of the erosive kind, random (ER) and monochromatic (EM). Table A.1 displays the various wave and beach conditions used in the study. The sediment used was characterized with $D_{50} = 0.22$ mm and $w_s = 0.033$ m/s.

Beach scarps were formed during some of the tests (Table A.1). The method used to detect scarps is not presented in their study, which might have an impact on the amount of beach scarps formed during the experiments (Roberts Briggs, personal communication, 2017). These scarps had an impact on this research, as they limit the amount of wave runup. From the table presented it can furthermore be seen that both random and monochromatic waves were found to be capable of developing scarps.

No clear relationship between the formation of beach scarps and the wave or beach conditions were found in this study. The data presented could however be used to indicate the most important parameters impacting the formation of these interesting features.

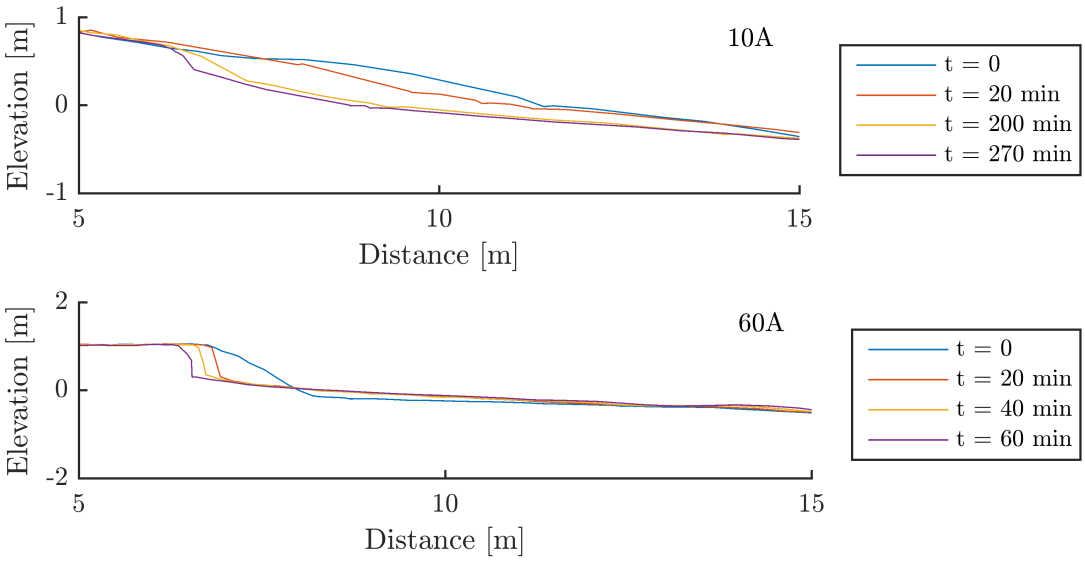

Figure A.6: Supertank profile data for two runs: 10A ($H_0 = 0.78$ m, $T_p = 3$ s, no scarp reported); 60A ($H_0 = 0.69$ m, $T_p = 3$ s, scarp reported). Data source: Roberts Briggs, personal communication, 2017.

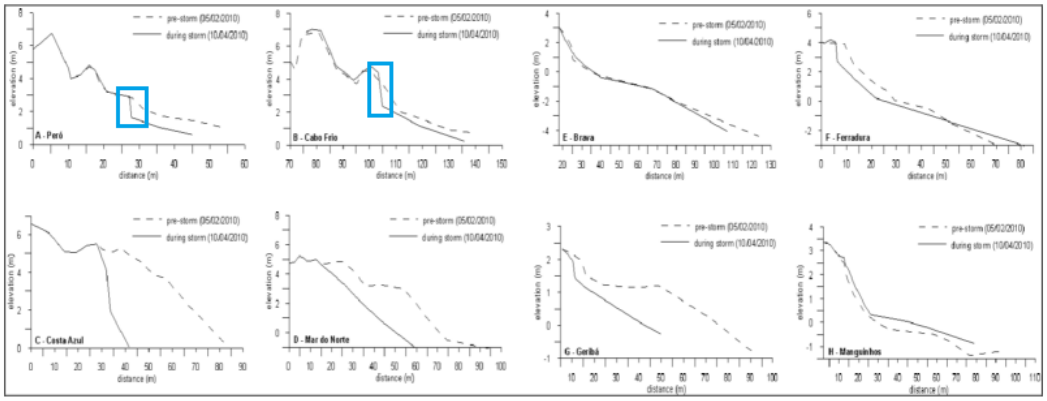

Figure A.7: Profiles measured along the Rio de Janeiro coastline, dashed lines represent pre-storm conditions and solid lines represent post-storm conditions. Source: Fernandez et al. (2011).

Jackson et al. (2010)

This study on the ecological implications of nourishments on estuarine beach systems describes beach scarps as rather common features in Delaway Bay, United States. Differences in grain sizes between the original material and the nourished material have been found to alter the form and mobility of estuarine beaches. The initial beach scarp formed as a result of a nourishment after three days. Within 6 months the scarp migrated 7 m landward and grew to a height of 0.30 m. Mechanical grading of the beach after nourishment is proposed as a measure to reduce the formation of beach scarps. If this would be performed, a profile should be shaped that is 'more compatible' with wave conditions. Furthermore, the backshore elevation could be lowered by means of human intervention to prevent scarps from forming.

Fernandez et al. (2011)

Storm impact on the coastline of Rio de Janeiro in 2010 produced a great variety of interesting beach features. The abstract of this paper describes the formation of scarps at the base of foredunes, which are according to the definition used in this thesis dune scarps. These *dune scarps* (which are mistakenly referred to as beach scarps in the paper) and were found to be the most common feature observed after the storm. Despite this misclassification, two examples (not mentioned in the paper) of beach scarps were noted (A-Pero and B-Cabo Frio in Figure A.7)

Figure A.8: Beach scarps observation at Melbourne Beach (Florida, United States), note the rhythmicity corresponding to the formation of beach cusps. Source: van Gaalen et al. (2011).

Figure A.9: Beach scarps observation at Faro Beach (Portugal), note that the beach scarp indicated by a black dot corresponds to the location of a cusp horn. Source: Vousdoukas (2012).

van Gaalen et al. (2011)

During morphological observations of beach cusp developments at Melbourne Beach (Florida, USA), it was found that beach scarps formed. The features, which grew to a height of more than 0.5 m, were found on the swash cusp horns. This finding is in line with the work of Kana (1977) and Antia (1989). No direct relation between the formation of beach scarps and the wave or beach conditions was found, but an alongshore variability in scarp height was noted. Scarps were found to be the highest at the southern part of the study area, which is where the (initial) beach slope was highest.

Vousdoukas (2012)

Intertidal topography and beach cusp systems have been the subject to this study at Faro Beach, Portugal. It was found that the intertidal topography was sensitive to changes in the wave conditions causing rapid transformation of beach cusps. The formation of beach scarps at the horns was observed, similar to Kana (1977), Antia (1989) and van Gaalen et al. (2011). Beach scarps reported at Faro Beach reached heights of up to 2 m.

Beach cusp spacing was found to be underestimated by the edge wave and self-organisation theories and was better predicted by an equation based on wave uprush and grain size. No relation between the formation of beach scarps and the specific hydrodynamic conditions was reported. The combination of steep slopes, dynamic character and tidal variation was found to impact the three-dimensional features (including scarps) on the Faro Beach. Temporal changes in wave direction (which varied between SW to SE) were suggested to cause the formation of beach scarps.

Addad and Martins-Neto (2012)

Erosion at the town of Alcobaça, eastern Brazilian coast, was the subject of this study by Addad and Martins-Neto in 2012. Escarpments between the beach and vegetated zones were described to range from 0.1 to 2.0 m. These *dune scarps* were reportedly found after a landward migration of beach scarps. During high tides, wave breaking takes place close to the beach face which then generates a beach scarp. The process of undercutting is was also observed in this study, causing the reported landward migration.

de Zeeuw et al. (2012)

In this study, the swimmer safety along the Dutch coast was assessed. Seven criteria were formulated from various sources (e.g. lifeguard interviews and detailed Lagrangian measurements). One of the criteria presented in this paper was found to be the profile gradient. Steep profiles were observed after nourishments (e.g. the Sand Engine) had been performed along the Dutch coast. At several locations beach scarps formed, impacting swimmer safety. Not only did this directly affect the bathers, but the lifeguards view on the waterline was also blocked. No information on the amount or location of scarps observed is given, but a strong hint between the

relationship of steep nourished beaches and beach scarps is given.

Ruiz de Alegria-Arzaburu et al. (2013)

Beach scarp morphodynamics at a Caribbean Mexican beach were studied in this paper. It was found that large beach scarps formed after a nourishment was performed at Cancun Beach. This beach nourishment was done with a much larger mean grain size than naturally occurring at this site. The sediment located at the beach prior to the nourishment was characterized by a $D_{50} = 0.42$ mm, whereas the dredged material had a $D_{50} \approx 0.6$ mm. The scarps that formed were up to two meters high and extended for hundreds of meters (Figure A.10). In this paper a beach scarp is defined as;

> A feature with a slope larger than the critical angle of repose of 32^o and a minimum height of 0.25 m.

Profile measurements were carried out on foot using a two-wheeled GPS trolley. This allowed for measurements close to the scarps at Cancun Beach. The method used to detect beach scarps from these profiles was based on minimum and maximum values of the second derivatives. Next, relations between the scarp morphology and hydrodynamic conditions was investigated. The authors claimed that scarp behaviour was related to three parameters; wave runup, tides and longshore energy flux.

No clear relation between the formation of beach scarps and wave conditions is given. The authors do however indicate the importance of the nourishment performed at Cancun Beach. Migration of the scarps was in 40% of the cases explained by tidal ranges, wave runup and longshore energy. Destruction of the scarps was found to coincide with energetic conditions for 50% of the scarps. Whether this method of destruction corresponds to the last cause (5) presented in Sherman and Nordstrom (1985) remains unknown.

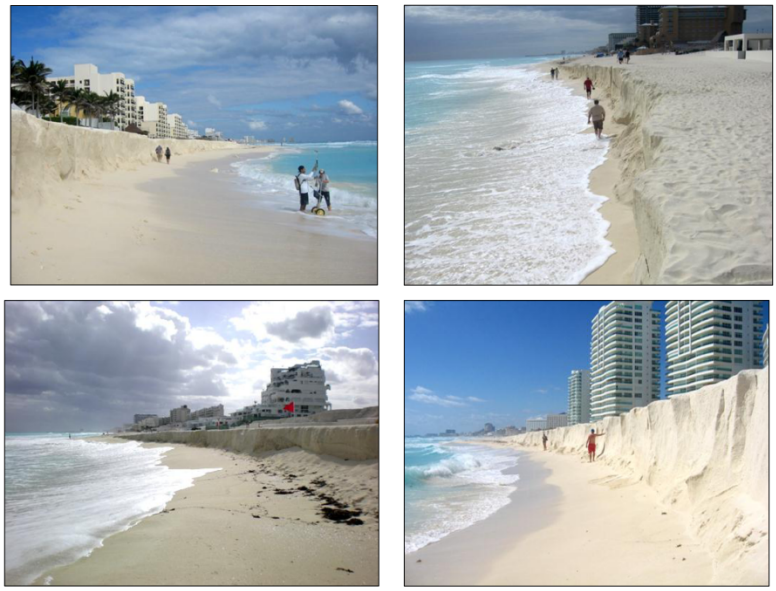

Figure A.10: Beach scarps along Cancun beach, note the height of the scarps with respect to beach visitors. Source: Ruiz de Alegria-Arzaburu et al. (2013).

Masselink et al. (2014)

During the Large-scale Barrier Dynamics Experiment II (BARDEX II) one of the wave runs resulted in the formation of a beach scarp. The laboratory experiments were performed in the Delta Flume with various wave conditions. A 1:15 foreshore slope was constructed using sedi-

ment characterized by $D_{50} = 0.51$ mm (which contained 1% gravel). The median sediment fall velocity was reported to be 0.046 m/s.

A beach scarp formed during one of the twenty tests done in this study. During the test with the lowest wave period ($T_p = 4$ s) this feature was observed. It might be of importance to note that the water level rise during this test was among the highest performed during this experiment. No further explanation on the causes of this are given in this paper, but the other (more energetic) tests did not result in beach scarp formation.

Bonte and Levoy (2015)

The evolution of a beach scarps over one tidal cycle was assessed at Luc-sur-Mer Beach, France. At this macrotidal sandy beach an artificial beach scarp was constructed and its development and nearshore hydrodynamics during rising tides and oblique waves were monitored. A variable range of grain sizes was observed at Luc-sur-Mer Beach, with fine sands characterized by $D_{50} = 0.217$ mm and coarse sands characterized by $D_{50} = 0.622$ mm. The beach scarp was constructed using local sand and compacted using a bulldozer. Compaction of the material has been shown to be of importance to the strength of sandy beaches in the SUPERTANK experiments (Nishi and Kraus, 1996). The achieved peak strength (which was measured using a penetrometer) was similar to the strength on a natural berm close to the artificial scarp. The location and shape chosen for this beach scarp matched previous scarp sightings. This artificial feature was approximately 1 m high and extended for 40 m in the alongshore direction.

Video recordings from the swash zone showed a significant impact of the beach scarp on swash dynamics, which is in line with Roberts et al. (2010). The up-rush and collision swash interaction was often observed. This swash interaction has been clearly described in Erikson et al. (2005). The video recording were transformed to an estimate of the wave spectra, which showed that in the presence of a scarp a dominant low frequency peak can be observed (around 0.05 Hz). Without the scarp the energy values are more spread over the frequencies between 0.025 and 0.25 Hz. Due to the low variability of wave conditions during the experiment, the tide is mentioned to be an important parameter to explain scarp erosion.

Topographic results showed that the undercutting and slumping mechanism (as presented in Erikson et al. (2007)) is also observed at this artificial scarp. Results showed that the scarp did not retreat in an alongshore uniform manner, which was attributed to a variable beach evolution in front of the scarp. The regime theory of Sallenger Jr (2000) is used to describe the destruction of each scarp, which occurred non-simultaneously. First, the eastern part was destroyed due to a sediment deposit in front of the scarp causing eventual overwash of the scarp. Second, the western part was destroyed during the overwash regime. The difference between the morphological activity of both sections indicates the importance of the profile development in front of a beach scarp. It should be noted that a groin was present close to the east side of the study area. This affects the longshore sediment transport and might have had an influence on the retreat rates, which was also mentioned in Nishi et al. (1995).

Darnall (2016)

To combat coastal erosion in the Netherlands, a single mega-nourishment known as the Sand Engine has been completed in July of 2011. Beach scarps were found to repeatedly form on this nourishment. Darnall studied the locations and developments of beach scarps at the Sand Engine. His data-driven study was based on elevation products obtained from an extensive monitoring campaign at this nourishment (chapter 4).

A script was developed to automate the detection of beach scarps based on the second derivative of the elevation (as presented in Ruiz de Alegria-Arzaburu et al. (2013)). Some fine-tuning to the script had to be made that are intertwined with the monitoring equipment used. Within the monitoring strategy, quad bikes are used to map the dry surface elevation, whereas jet-skis are used to map the (wet) bathymetry. This resulted in a more 'relaxed' beach scarp definition as compared to Ruiz de Alegria-Arzaburu et al. (2013);

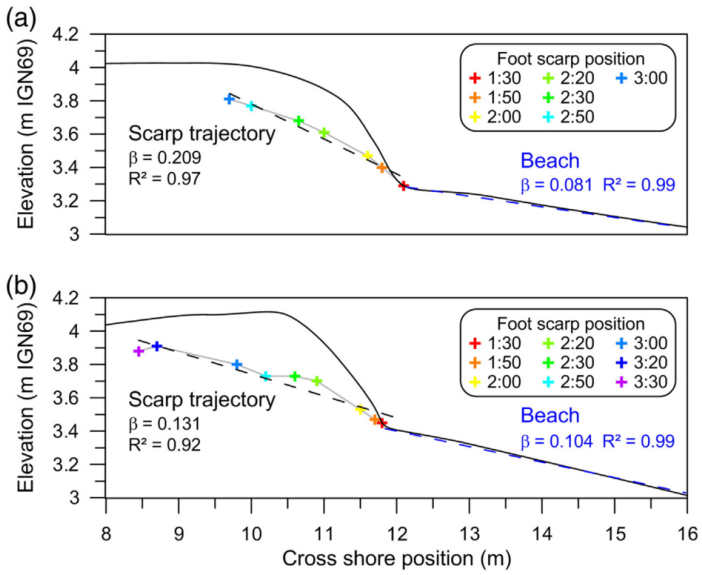

Figure A.11: Scarp toe retreat for an artificially constructed beach scarp at Luc-sur-Mer Beach, France. Retreat is given in time with respect to the initial profile for the cross sections at the east (a) and west side (b) of the study area. Source Bonte and Levoy (2015)

.

A feature with a slope steeper than 0.15 and a minimum height of 0.30 m.

This study showed that high energy events are capable of both creating and removing beach scarps. This seems to indicate that certain hydrodynamic and geometric/technical conditions are susceptible to the formation of scarps whereas others tend to result in more diffuse shorefaces. The majority of beach scarp destructions occurred during winter, coinciding with the most energetic periods along the Dutch coast. An alongshore variability was found to occur in beach scarp existence and height. This might indicate the importance of the incoming wave angle, leading to a formation of scarps at certain locations of the Sand Engine.

The impact regime framework developed by Sallenger Jr (2000) was modified to test whether a similar classification was applicable for the life-cycle assessment of beach scarps. The following regimes were defined; swash ($R_{HI} < S_{LO}$), collision ($S_{HI} > R_{HI} > S_{LO}$), overtopping ($R_{HI} > S_{HI} > R_{LO}$) and inundation ($R_{LO} \geq S_{HI}$) (Figure A.12).

From placing the detected beach scarps into this framework it was found that within the swash regime, beach scarps were not affected. Within the collision regime beach scarps were found to either grow in height or decrease. Both the overtopping and inundation regimes were found to cause destruction of beach scarps.

It was concluded from this study that storm surge levels and tidal variations are of great importance for beach scarp development. As beach scarp development is still a poorly understood subject to this date, this study lastly calls for additional studies in the initiation mechanisms leading to beach scarp development. Several suggestions are given in the study for future studies; process-based modelling of beach scarps (e.g. XBeach), laboratory tests with berm profiles (similar to Payo et al. (2008)) and a field measurement campaign with advanced high resolution monitoring systems.

Lastly, some of the documented beach scarps at the Sand Engine show that the sediment is quite rich in shell fragments. This was also reported for other nourished beaches around the

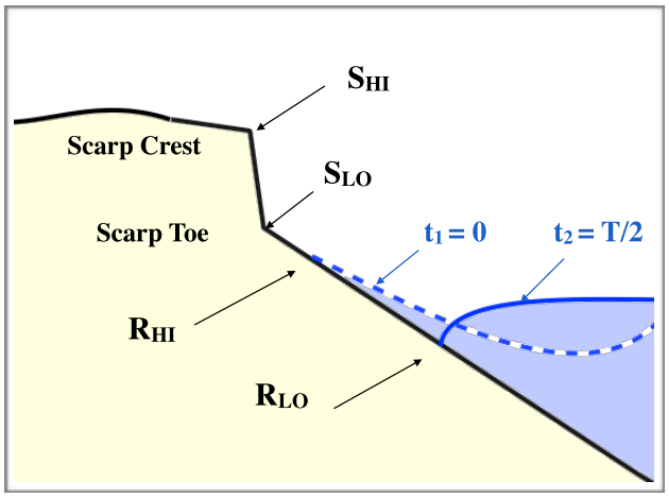

Figure A.12: The impact regimes as defined indicating the locations of the scarp crest (S_{HI}), scarp toe (S_{LO}), the runup (R_{HI}) and the rundown (R_{LO}). Source: Darnall (2016).

world including the Cádiz Province (Anfuso et al., 2001), California (Seymour et al., 2005) and Narrabeen Beach (Short and Wright, 1981).

B

Sand Engine field visits

In order to better understand the formation of beach scarps at the Sand Engine, two field visits have been conducted in June 2017. During these field visits the main objective was to get a feeling for the different environmental conditions affecting the Sand Engine. In a perfect world; the consecutive formation, migration and destruction of beach scarps would be witnessed during these field visits. These field visits were set-up rather basic; photos were taken using a smart phone, which was capable of geo-referencing the images using GPS. The first visit was on 03/06/2017, during which the conditions were rather calm. The second visit was on 07/06/2017, during which more energetic (erosive) conditions were present. Detailed descriptions of the field visits are given in the upcoming sections.

B.1. Observations and conditions - 03/06/2017

During the first visit, no scarps were visible along the perimeter of the Sand Engine. The conditions were rather calm during this visit ($H_{s,0} \sim 0.5$ m). Steep slopes (approximately 1:3) could be observed in the higher part of the beach profile, between 2 and 3 m NAP (Figure B.1). The sediment in this zone had a seemingly high shell content and the steep parts were not continuous along the Sand Engine perimeter; a rhythmic pattern could be observed, with alternating steep sections (10-15 m in length) and gently sloping sections (5-10 m in length).

Figure B.1: Field observation of steep beach slopes at the Sand Engine (52°03′18.7″N, 4°11′08.1″E). Male beach visitor (1.90 m) for scale. Photo facing south, taken 03/06/2017 15:26.

Figure B.2: Field observation of a vertical beach feature at the Sand Engine (52°03′19.5″N, 4°11′07.7″E). Water bottle (0.20 m) for scale. Photos facing north (left), east (centre) and south (right) taken 07/06/2017.

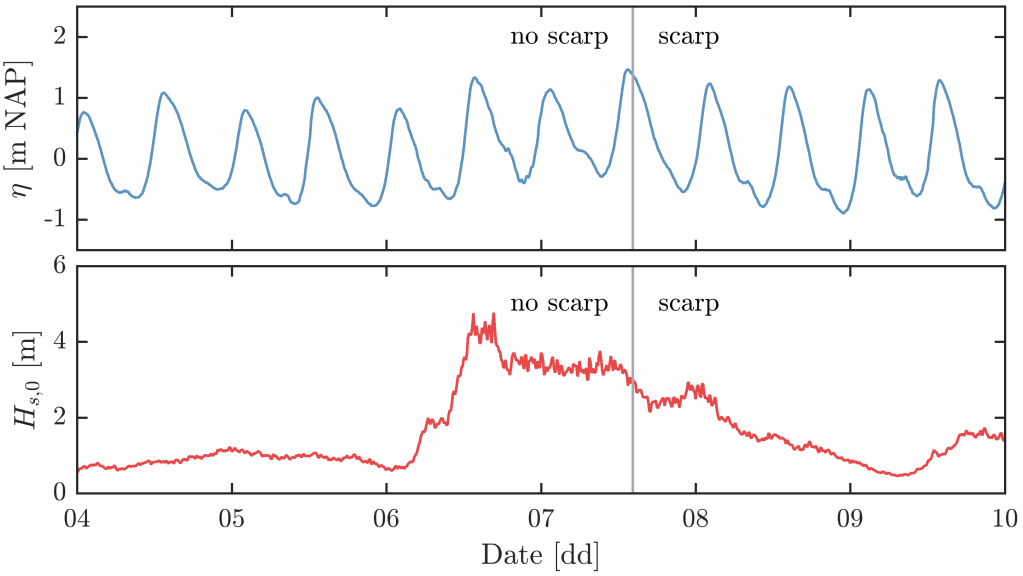

Figure B.3: Water level elevation η at Scheveningen and significant wave height $H_{s,0}$ at the Europlatform during the second visit (07/06/2017). Scarp formation was observed around 14:15 (vertical line).

B.2. Observations and conditions - 07/06/2017

The second Sand Engine visit was conducted at 07/06/2017, during rather energetic conditions. Offshore wave conditions and the water levels were significantly higher than during the first field trip (Figure B.3). Upon arrival at the Sand Engine around 11:00, a steep sloping feature was observed well above the swash zone (Figure B.2). With a length of 2.5 meters, this feature was rather small but interesting nonetheless. Due to the fact that the tide was rising, and this feature was located well above the swash zone, it was likely formed during the prior lowering of the tide. This feature was capable of withstanding several overtopping events and was eventually destroyed due to inundation.

Around 14:15, a steep slope formed at the limits of the swash excursion (Figure 3.1). This was during the lowering of the tide (Figure B.3). A beach scarp formed at this section after beam-type failure of the slope was initiated by swash uprush (Figure 3.1). The initial scarp had a height of about 0.10 m, which increased up to 0.60 m by 15:44. During the migration of the beach scarp the undercutting and slumping process as described Sherman and Nordstrom (1985) was clearly observed. Reflection of the incoming swash, which caused swash-swash interactions, was furthermore observed. Occasionally, the beach scarp was overtopped. This lead to a more diffuse profile, which was undercut by the swash action, leading to persistence of the scarp. During the end of the field visit, three sections could be identified along the Sand Engine perimeter at which scarps were formed during the visit. These sections had varying a scarp height (0.15 - 0.60 m) and lengths (10 - 30 m).

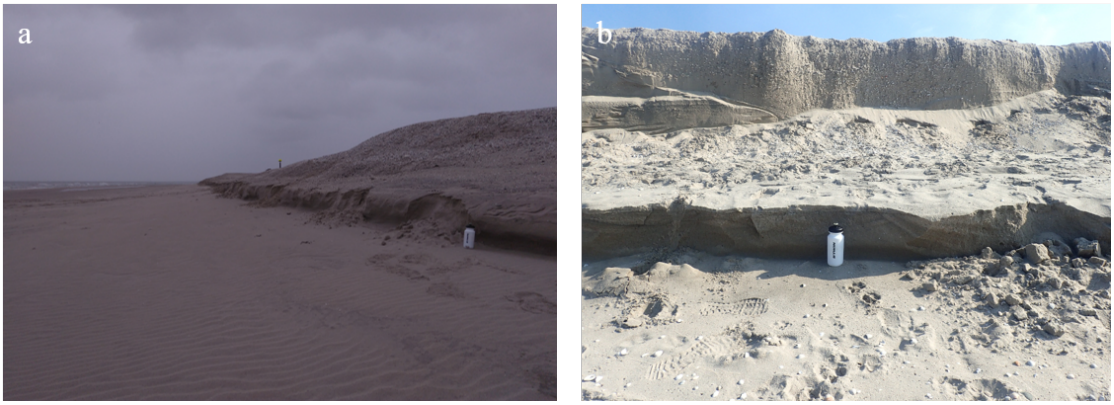

Figure B.4: a) Natural beach scarp formed at the Sand Engine after experiment A, length of approximately 250 meters with heights of up to 0.70 m. Taken on 29/07/2017 facing north. b) Observed 'two-beach scarp system' during field experiment B. Photo taken 26-10-2017 with a water bottle (0.20 m) for scale.

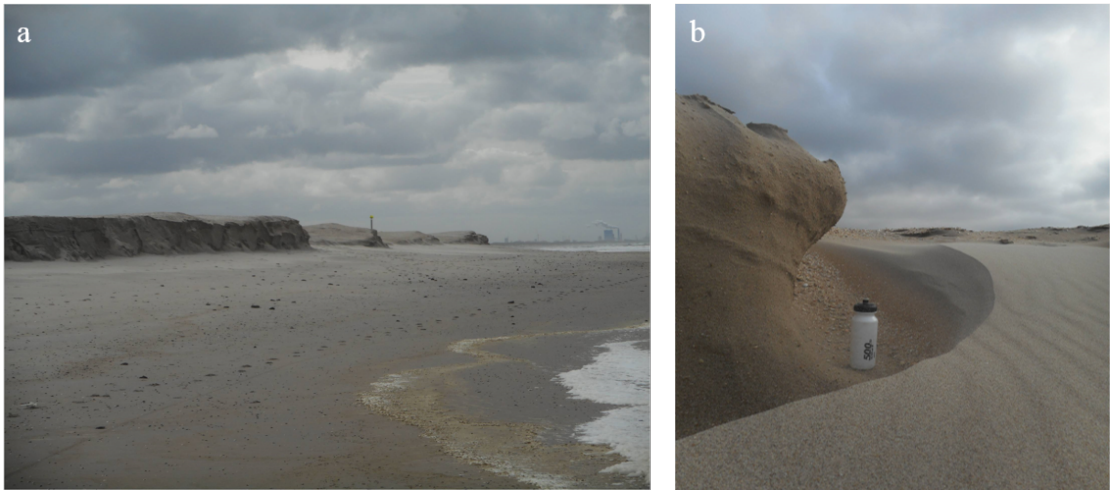

Figure B.5: a) Alongshore variability of beach scarp height at the Sand Engine (04/10/2017). b) Aeolian deposition of sand in front of a beach scarp at the Sand Engine (04/11/2017). Water bottle (0.20 m) for scale.

B.3. Argus imagery at the Sand Engine

(a) Camera 4 - 02/06/2013

(b) Camera 4 - 03/01/2017

(c) Camera 5 - 03/01/2017

(d) Camera 6 - 02/01/2017

Figure B.6: Argus images for three cameras (4, 5, 6) under the best lighting conditions and various moments in time (dd/mm/yyyy). The topographic surveys report beach scarps for these transects.

C

Beach scarp creation experiments

C.1. Materials

As mentioned in chapter 6, mounts were constructed for the field experiments performed in this study. For both experiments, a front loader was used to construct the designed mounts during low water. Monitoring the morphological development of these mounts over time was done using various types of equipment. During the first field experiment, topographical measurements were performed using a Leica Viva GS14 GNSS. For the second field experiment a RIEGL VZ-2000 terrestrial laser scanner was used to map the entire experiment field during low tide in combination with the Leica GPS during high tide wave attack. Furthermore, instantaneous changes to the mounts under wave attack were recorded using cameras fixed to a mast elevated at 3 meters.

In addition to these topographical measurements, a group of students conducted various other studies related to beach scarp characteristics as part of the course *Fieldwork Hydraulic Engineering* (CIE5318). These measurements consisted of; monitoring using drone imagery, sediment analysis (sieving & high resolution camera), stilling well measurements to record tidal variations and CTD divers for wave data.

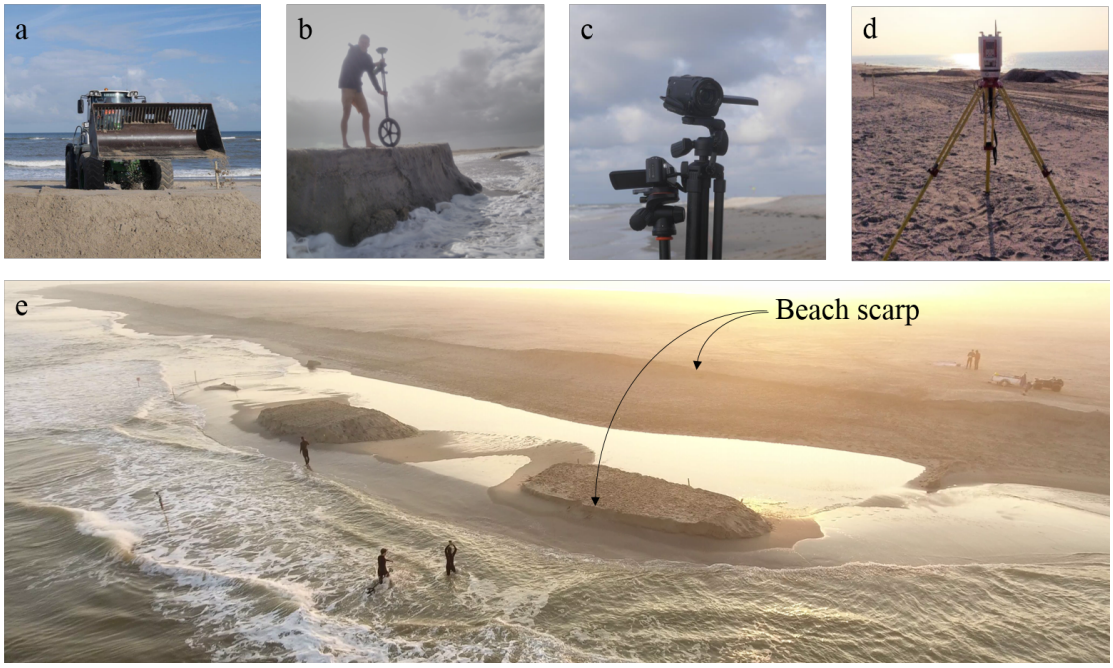

Figure C.1: Materials used to construct and monitor the constructed mounts. a) Front loader. b) Leica Viva GS14 GNSS. c) Sony cameras. d) RIEGL VZ-2000. e) DJI Phantom 4 drone snapshot.

C.2. Experiment A: Nourishment slope

To calculate the slope development over time, two sections of the cross-shore beach profile were selected to represent the 'upper' and 'lower' slope. For this, the seaward intersection point of the profiles was required (Figure C.2). Based on three profiles (before construction, during the experiment and after complete removal), the intersection point P was found.

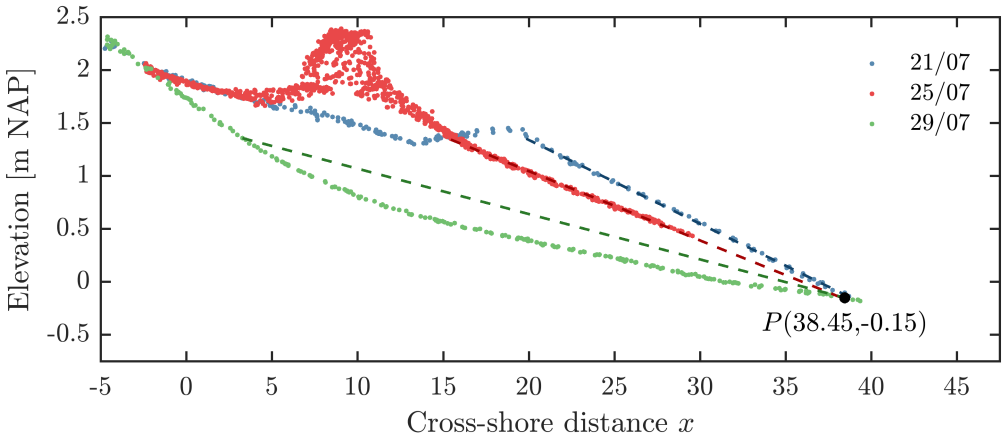

Figure C.2: Cross-shore profiles and the corresponding point P. Measurement points used for this figure between y = 4 and y = 14 m (mount A2). Profile 25/07 has been extrapolated from HWL to P (z = -0.0654*x + 2.36, RMSE = 0.016 m and R^2 = 0.996)

C.3. Experiment B: Platform elevation

During the course of this experiment, beach scarps were present at the Sand Engine with local height of up to 2 m (Figure C.3). It was found that these scarps followed an alongshore variation in height (and therefore also in existence). In addition, a very high shell content was found on several sections of these scarps. Apart from these observations, this part of the appendix presents the complete sedimentation and erosions dataset obtained from the LiDAR measurements (Figure C.4). Based on these LiDAR measurements during low tide, the migration of the sand bar is presented in Figure C.6 for mount B2 and Figure C.7 for mount B3.

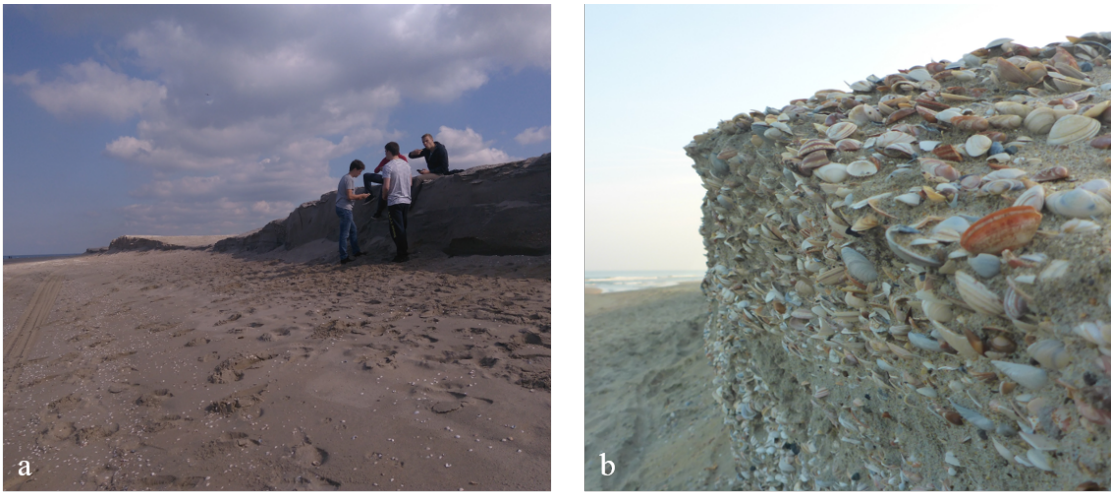

Figure C.3: a) Beach scarp at the Sand Engine present during experiment B with local heights of up to 2 m and a length of approximately 300 meter. b) Close up of shells on the beach scarp face. Photos taken on 23/09/2017 facing north.

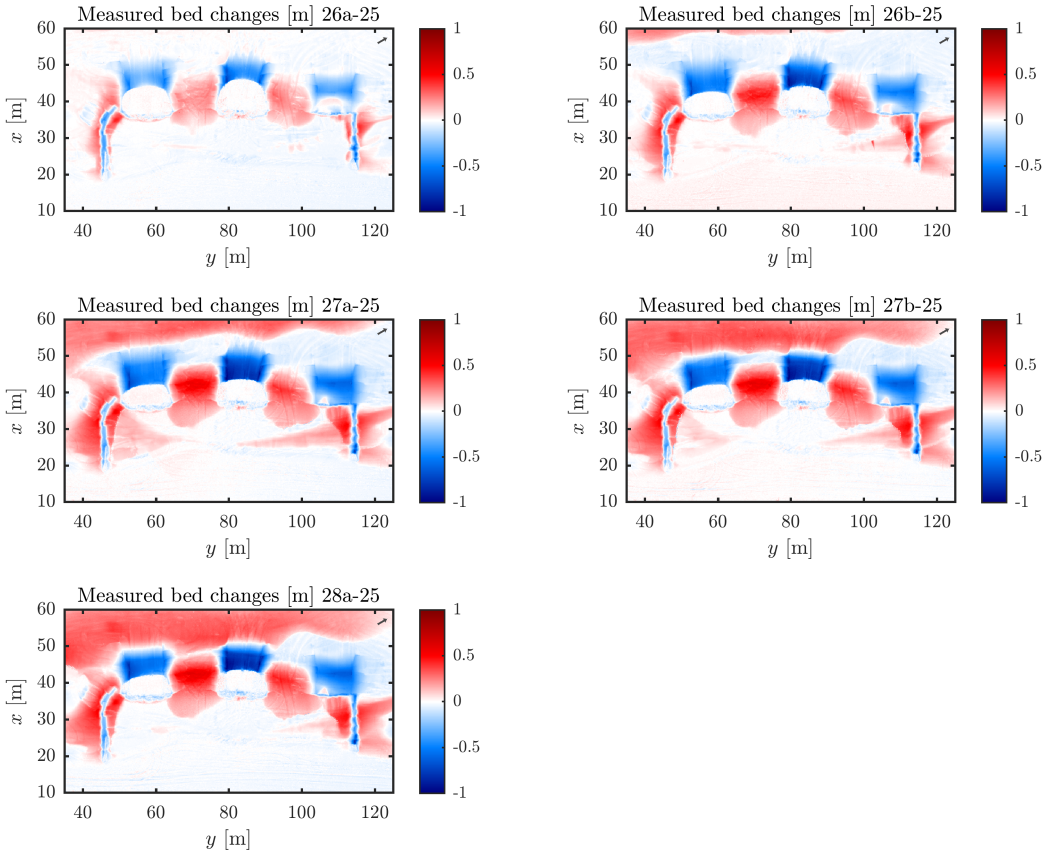

Figure C.4: Measured bed changes between for consecutive low tides. North arrow is given in the top right corner.

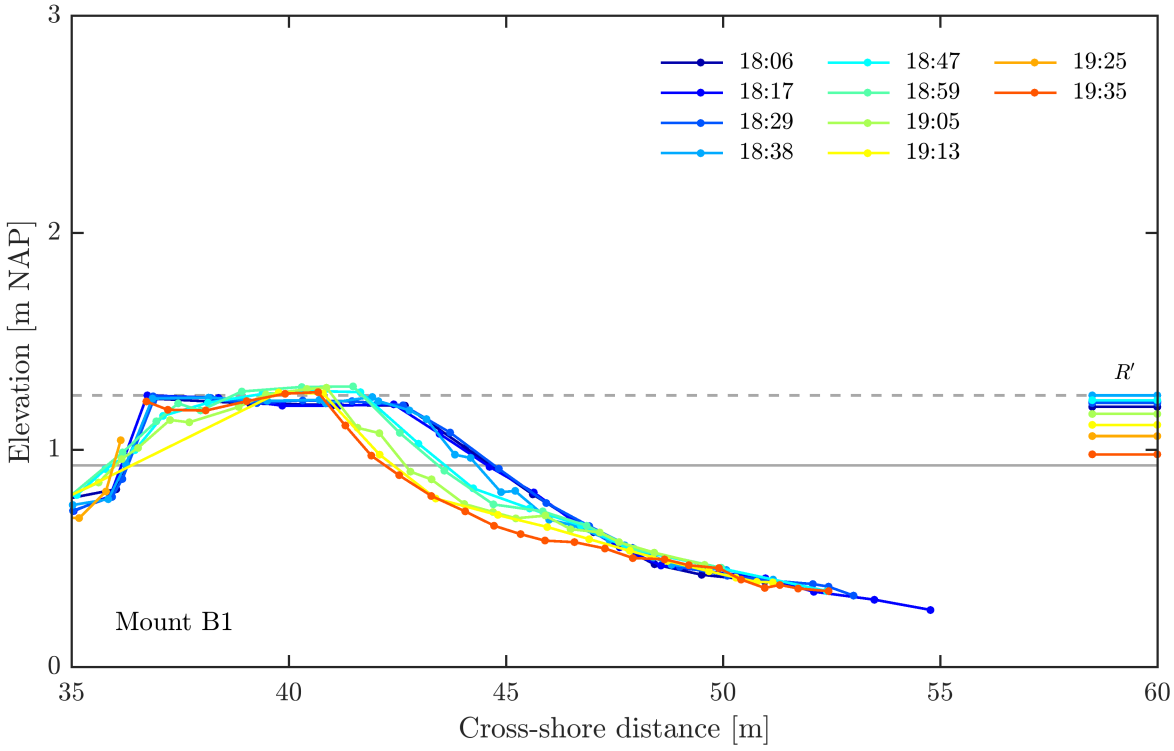

Figure C.5: Profile development of mount B1 at $y = 106$ m during high water wave attack on 25-09-2017. R' lines on the right indicate the runup elevation for all profiles, maximum water elevation η_{max} and maximum R' during the high water on the 25th are given in solid and dashed horizontal lines respectively.

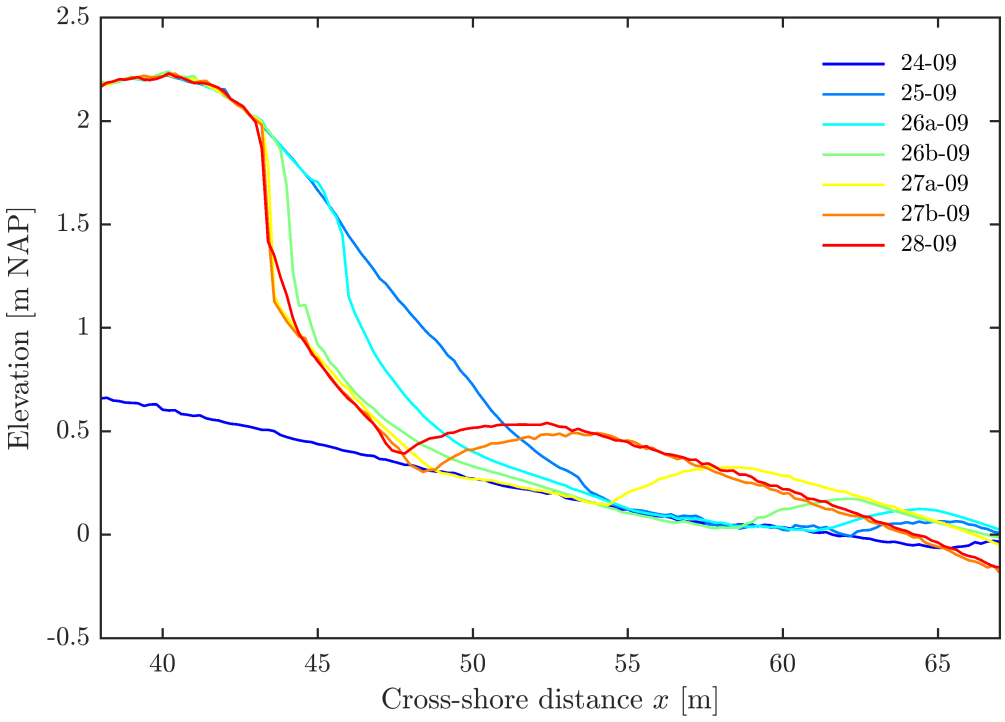

Figure C.6: Sand bar migration in front of mount B2 obtained from LiDAR measurements done during low tide. Note the scarped profiles above 1 m NAP (from 25-09 onwards).

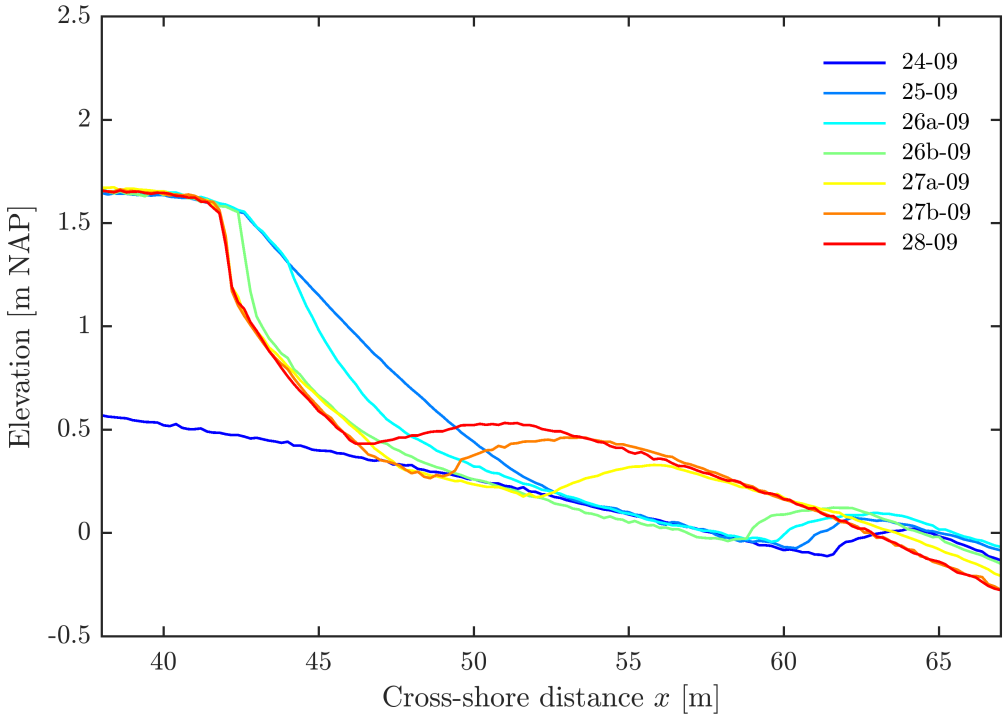

Figure C.7: Sand bar migration in front of mount B2 obtained from LiDAR measurements done during low tide. Note the scarped profiles above 1 m NAP (from 26b-09).

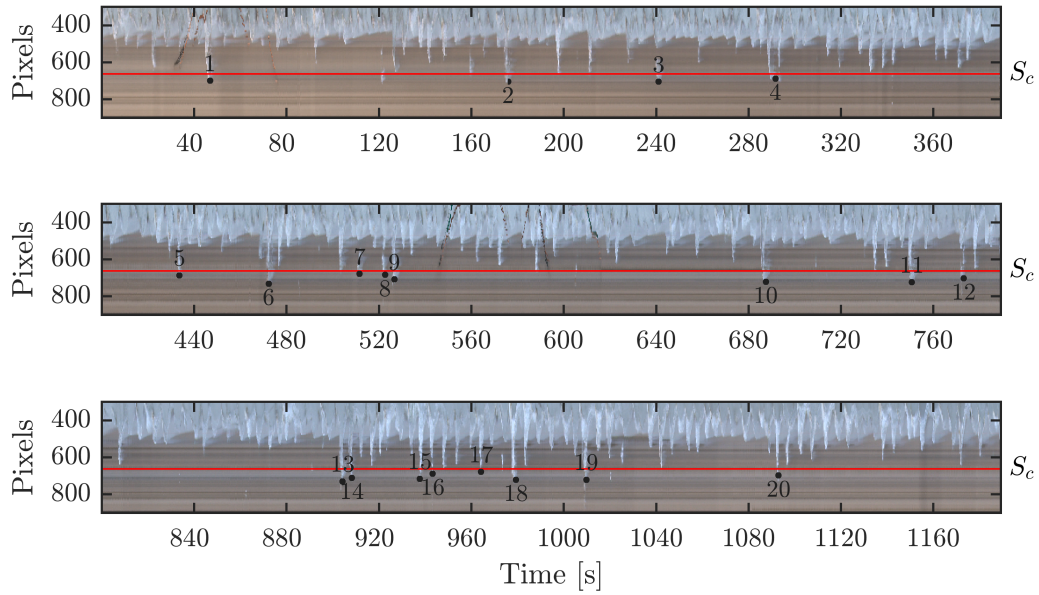

Figure C.8: Timestack of the cross-shore location of the swash edge (in pixels) at mount B3 on 25/09/2017. The coloured horizontal line indicates the final location of the scarp crest.

D

Statistical analysis

The formulae presented in this Appendix are used throughout this study to analyse and interpret the collected datasets. The structure of this appendix is largely based on Weiss and Weiss (1989). The following general notation is used; n = sample size, $\bar{x}$ = sample mean, and N = population size.

D.1. Descriptive measures

Population mean,

$$\mu = \frac{\Sigma x}{N} \tag{D.1}$$

Sample standard deviation,

$$s = \sqrt{\frac{\Sigma(x-\bar{x})^2}{n-1}} \tag{D.2}$$

D.2. Descriptive methods

S_{xx}, S_{xy}, and S_{yy},

$$S_{xx} = \Sigma(x-\bar{x})^2 \tag{D.3}$$

$$S_{xy} = \Sigma(x-\bar{x})(y-\bar{y}) \tag{D.4}$$

$$S_{yy} = \Sigma(y-\bar{y})^2 \tag{D.5}$$

Linear regression $\hat{y} = b_0 + b_1 x$,

$$b1 = \frac{S_{xy}}{S_{xx}} \tag{D.6}$$

$$b0 = \frac{1}{n}(\Sigma y - b_1 \Sigma x) = \bar{y} - b_1 \bar{x} \tag{D.7}$$

Total sum of squares,

$$SST = \Sigma(y-\bar{y})^2 = S_{yy} \tag{D.8}$$

Regression sum of squares,

$$SSR = \Sigma(\hat{y}-\bar{y})^2 = \frac{S_{xy}^2}{S_{xx}} \tag{D.9}$$

Error sum of squares,

$$SSE = \Sigma(y-\hat{y})^2 = S_{yy} - \frac{S_{xy}^2}{S_{xx}} \tag{D.10}$$

Coefficient of determination,

$$R^2 = \frac{SSR}{SST} \tag{D.11}$$

Mean squared error,

$$MSE = \frac{\Sigma(y-\bar{y})^2}{n} = \frac{S_{yy}}{n} \tag{D.12}$$

Root mean squared error,

$$RMSE = \sqrt{\frac{\Sigma(y-\bar{y})^2}{n}} = \sqrt{\frac{S_{yy}}{n}} \tag{D.13}$$

Bibliography

Addad, J. and Martins-Neto, M. A. Deforestation and Coastal Erosion: A Case from East Brazil. *Journal of Coastal Research*, 16(2):423–431, 2012. ISSN 0749-0208. URL http://journals.fcla.edu/jcr/article/view/80837.

Alves, M. and El-Robrini, M. Morphodynamics of a Macrotidal beach: Ajuruteua, Braganca north Brazil. *Journal of Coastal Research*, (39):949–951, 2006. ISSN 0749-0208.

Anfuso, G., Benavente, J., and Gracia, F. J. Morphodynamic responses of nourished beaches in SW Spain. *Journal of Coastal Conservation*, 7(1):71–80, 2001. ISSN 1400-0350. doi:10.1007/BF02742469.

Antia, E. E. Beach cusps and beach dynamics: A quantitative field appraisal. *Coastal Engineering*, 13(3):263–272, 1989. ISSN 03783839. doi:10.1016/0378-3839(89)90052-5.

Bauer, B. O. and Allen, J. R. Beach steps: an evolutionary perspective. *Marine Geology*, 123 (3-4):143–166, 1995. ISSN 00253227. doi:10.1016/0025-3227(95)00011-M.

Bergsma, J. *The down-wind change of aeolian sand transport over a beach.* Msc thesis, Utrecht University, 2016.

Bishop, A. W. The use of pore-pressure coefficients in practice. *Geotechnique*, 4(4):148–152, 1954. doi:10.1680/geot.1954.4.4.148.

Bodegom, M. *Beach nourishment: An evaluation of equilibirum design methods.* Msc thesis, Delft University of Technology, 2004.

Bonte, Y. and Levoy, F. Field experiments of beach scarp erosion during oblique wave, stormy conditions (Normandy, France). *Geomorphology*, 236:132–147, 2015. ISSN 0169555X. doi:10.1016/j.geomorph.2015.02.014.

Bosboom, J. and Stive, M. J. F. Coastal Dynamics 1, 2013.

Botero, C., Cervantes, O., and Finkl, C. *Beach Management Tools - Concepts , Methodologies and Case Studies.* Springer Science & Business Media, 2018. ISBN 9783319583037. doi:10.1007/978-3-319-58304-4.

Bowen, A. J., Inman, D. L., and Simmons, V. P. Wave 'set-down' and set-up. *Journal of Geophysical Research*, 73(8):2569–2577, 1968. doi:10.1029/jb073i008p02569.

Brandenburg, P. *Scale dependency of dune erosion models.* Msc thesis, University of Twente, 2010.

Calliari, L. J., Klein, A. H. F., and Barros, F. C. R. Beach differentiation along the Rio Grande do Sul coastline (Southern Brazil). *Revista Chilena de Historia Natural*, 69:485–493, 1996.

Carter, R. W. G. and Stone, G. W. Mechanisms associated with the erosion of sand dune cliffs, Magilligan, Northern Ireland. *Earth Surface Processes and Landforms*, 14(1):1–10, 1989. ISSN 10969837. doi:10.1002/esp.3290140102.

Carter, R. W. G., Hesp, P. A., and Nordstrom, K. F. Erosional landforms in coastal dunes. In *Coastal Dunes: Form and Process*, chapter Erosional, pages 217–250. John Wiley & Sons, 1990. ISBN 9780471918424.

Dapporto, S., Rinaldi, M., Casagli, N., and Vannocci, P. Mechanisms of Riverbank Failure Along the Arno River, Central Italy. 1323:1303–1323, 2003. doi:10.1002/esp.550.

Darnall, J. *Post-Nourishment Beach Scarp Existence at the Sand Engine*. Master thesis, Technical University of Delft, 2016. URL http://resolver.tudelft.nl/uuid:a05009a9-96c1-45b6-b2c7-3e71263ea8b9.

Das, B. M. and Sobhan, K. *Principles of geotechnical engineering*. Cengage Learning, 2013.

Davidson-Arnott, R. G. D. and Law, M. N. Seasonal patterns and controls on sediment supply to coastal foredunes, Long Point, Lake Erie. *Coastal dunes: form and process*, pages 177–200, 1990.

de Fockert, A. and Luijendijk, A. P. Wave look-up table. Technical report, Deltares, Delft, 2010.

de Schipper, M. A., de Vries, S., Ruessink, G., de Zeeuw, R. C., Rutten, J., van Gelder-Maas, C., and Stive, M. J. F. Initial spreading of a mega feeder nourishment: Observations of the Sand Engine pilot project. *Coastal Engineering*, 111:23–38, 2016. ISSN 03783839. doi:10.1016/j.coastaleng.2015.10.011.

de Schipper, M. A., Darnall, J., de Vries, S., and Reniers, A. J. H. M. Beach Scarp Evolution and Prediction. *Coastal Dynamics*, (251), 2017. URL http://resolver.tudelft.nl/uuid:bf8df3c5-06b7-4542-bd72-e5f7e72dc075.

de Vriend, H., Capobianco, M., Chesher, T., de Swart, H., Latteux, B., and Stive, M. Approaches to long-term modelling of coastal morphology: a review. *Coastal Engineering*, 21:45, 1993. doi:10.1016/0378-3839(93)90051-9.

de Zeeuw, R., de Schipper, M. A., Roelvink, J., de Vries, S., and Stive, M. J. F. Impact of Nourishments on Nearshore Currents and Swimmer Safety on the Dutch Coast. *Coastal Engineering Proceedings*, 1:1, 2012. ISSN 2156-1028. doi:10.9753/icce.v33.currents.57.

Dean, R. G. and Dalrymple, R. A. *Coastal Processes with Engineering Applications*. Cambridge University Press, Cambridge, 2001. ISBN 0511037910. doi:https://doi.org/10.1017/cbo9780511754500.

Dubois, R. N. Seasonal changes in beach topography and beach volume in Delaware. *Marine Geology*, 81(1-4):79–96, 1988. ISSN 00253227. doi:10.1016/0025-3227(88)90019-9.

Engineers, U. S. A. C. O. Coastal engineering manual. *Engineer Manual*, 1110:2–1100, 2002.

Erikson, L., Larson, M., and Hanson, H. Prediction of swash motion and run-up including the effects of swash interaction. *Coastal Engineering*, 52(3):285–302, 2005. ISSN 03783839. doi:10.1016/j.coastaleng.2004.12.001.

Erikson, L. H., Larson, M., and Hanson, H. Laboratory investigation of beach scarp and dune recession due to notching and subsequent failure. *Marine Geology*, 245(1-4):1–19, 2007. ISSN 00253227. doi:10.1016/j.margeo.2007.04.006.

Fernandez, G. B., Bulhoes, E., and da Rocha, T. B. Impacts of Severe Storm Occurred in April 2010 along Rio de Janeiro Coast, Brazil. *Journal of Coastal Research*, (SI 64):1850–1854, 2011. ISSN 07490208.

Fredlund, D. G. and Rahardjo, H. *Soil mechanics for unsaturated soils*. John Wiley & Sons, 1993. doi:10.1002/9780470172759.

Fredlund, D. G., Xing, A., Fredlund, M. D., and Barbour, S. L. The relationship of the unsaturated soil shear to the soil-water characteristic curve. *Canadian Geotechnical Journal*, 33(3): 440–448, 1994. doi:10.1139/t94-061.

Gabriel, R.-M., Edgar, M.-B., and Rodolfo, S.-C. Physical Characterizations of Sands and Their Influence in Fall Velocity. *American Journal of Environmental Sciences*, 4(March):238–244, 2008. doi:10.3844/ajessp.2008.238.244.

Gammons, J. Beach erosion at Ft. Pierce Inlet, 2011. URL http://stormvisuals.com/blog/tag/beach-erosion.

Hanks, T. C., Bucknam, R. C., Lajoie, K. R., and Wallace, R. E. Modification of wave-cut and faulting-controlled landforms. *Journal of Geophysical Research: Solid Earth*, 89(B7): 5771–5790, 1984. doi:jb089ib07p05771.

Hedges, T. S. and Mase, H. Modified Hunt's equation incorporating wave setup. *Journal of waterway, port, coastal, and ocean engineering*, 130(3):109–113, 2004. doi:10.1061/(asce)0733-950x(2004)130:3(109).

Herren, R. M. Habitat Conservation Plan for the Protection of Sea Turtles on the Eroding Beaches of Indian River County , Florida 2010 Annual Report. Technical report, U.S. Fish and Wildlife Service, Florida, 2010.

Hisgen, R. G. W. and Laane, R. W. P. M. *Geheim van het getij*. Sdu Uitgevers, 2004. ISBN 9789012106375.

Hoonhout, B. and den Heijer, C. Reliability of Dune Erosion Assessment along Curved Coastlines. *Coastal Engineering Proceedings*, 1(32):37, jan 2011. doi:10.9753/icce.v32.sediment.37. URL `https://doi.org/10.9753{%}2Ficce.v32.sediment.37`.

Hoonhout, B. and van Thiel de Vries, J. S. M. Modelling dune erosion, overwash and inundation of barrier islands. In *ICCE 2012: Proceedings of the 33rd International Conference on Coastal Engineering, Santander, Spain, 1-6 July 2012*, page 13, Santander, 2012. Coastal Engineering Research Council. doi:10.9753/icce.v33.sediment.30.

Hunt, I. A. Design of sea-walls and breakwaters. *Transactions of the American Society of Civil Engineers*, 126(4):542–570, 1959.

Jackson, N. L., Nordstrom, K. F., Saini, S., and Smith, D. R. Effects of nourishment on the form and function of an estuarine beach. *Ecological Engineering*, 36(12):1709–1718, 2010. ISSN 09258574. doi:10.1016/j.ecoleng.2010.07.016.

Johnson, D. W. *Shore processes and shoreline development*. Informa (UK) Limited, 1919. doi:00221342008984479.

Kana, T. W. Beach erosion during minor storm. *Journal of the Waterway Port Coastal and Ocean Division*, 1977.

Kobayashi, N., Payo, A., and Schmied, L. Cross-shore suspended sand and bed load transport on beaches. *Journal of Geophysical Research*, 113(January):1–17, 2008. doi:10.1029/2007JC004203.

Kobayashi, N., Buck, M., Payo, A., and Johnson, B. D. Berm and Dune Erosion during a Storm. *Journal of Waterway, Port, Coastal, and Ocean Engineering*, 135(1):1–10, 2009. ISSN 0733-950X. doi:10.1061/(ASCE)0733-950X(2009)135:1(1).

Kriebel, D. L. and Dean, R. G. Numerical simulation of time-dependent beach and dune erosion. *Coastal Engineering*, 9(3):221–245, 1985. ISSN 03783839. doi:10.1016/0378-3839(85)90009-2.

Leatherman, S., Zhang, K., and Douglas, B. Sea Level Rise Shown to Drive Coastal Erosion. *EOS*, 81(6):55–57, 2000. doi:10.1029/00eo00034.

Longhitano, S. G. Short-Term Assessment of Retreating vs . Advancing Microtidal Beaches Based on the Backshore / Foreshore Length Ratio : Examples from the Basilicata Coasts. *Open Journal of Marine Science*, (5):123–145, 2015. doi:10.4236/ojms.2015.51011.

Lu, N. and Likos, W. J. *Unsaturated soil mechanics*. Wiley, 2004. doi:10.2136/vzj2009.0115br.

Masselink, G., Ruju, A., Conley, D., Turner, I., Ruessink, G., Matias, A., Thompson, C., Castelle, B., Puleo, J., Citerone, V., and Wolters, G. Large-scale Barrier Dynamics Experiment II (BARDEX II): Experimental design, instrumentation, test program, and data set. *Coastal Engineering*, 113:3–18, 2014. ISSN 03783839. doi:10.1016/j.coastaleng.2015.07.009.

Mcfarland, S., Whitcombe, L., and Collins, M. Recent Shingle Beach Renourishment Schemes in the UK: Some Preliminary Observations. *Ocean & Coastal Management*, 25(1994):143–149, 1994. doi:10.1016/0964-5691(94)90044-2.

Morse, M. S., Lu, N., Asce, F., Wayllace, A., Asce, M., Godt, J. W., and Take, W. A. Experimental Test of Theory for the Stability of Partially Saturated Vertical Cut Slopes. 140(9): 1–10, 2014. doi:10.1061/(ASCE)GT.1943-5606.0001119.

Neshaei, M. A. L. and Ghanbarpour, F. The effect of sea level rise on beach morphology of caspian sea coast. *Frontiers of Structural and Civil Engineering*, 2017. ISSN 2095-2430. doi:10.1007/s11709-017-0398-6.

Nicholls, R. J. and Webber, N. Characteristics of shingle beaches with reference to Christchurch Bay, S. England. *Coastal Engineering 1988*, pages 1922–1936, 1989. doi:9780872626874.143.

Nishi, R. and Kraus, N. C. Mechanism and calculation of sand dune erosion by storms. In *Coastal Engineering 1996*, pages 3034–3047. 1996. doi:10.1061/9780784402429.235.

Nishi, R., Sato, M., and Wang, H. Field Observation and Numerical Simulation of Beach and Dune Scarps. In *Coastal Engineering 1994*, pages 2434–2448, 1995. doi:10.1061/9780784400890.177.

Pakpour, M., Habibi, M., Møller, P., and Bonn, D. How to construct the perfect sandcastle. *Nature*, 2:549, 2012. ISSN 2045-2322. doi:10.1038/srep00549.

Palmsten, M. L. and Holman, R. A. Infiltration and instability in dune erosion. *Journal of Geophysical Research: Oceans*, 116(10):1–18, 2011. ISSN 21699291. doi:10.1029/2011JC007083.

Palmsten, M. L. and Splinter, K. D. Observations and simulations of wave runup during a laboratory dune erosion experiment. *Coastal Engineering*, 115:58–66, 2016. ISSN 0378-3839. doi:10.1016/j.coastaleng.2016.01.007.

Payo, A., Kobayashi, N., and Yamada, F. Scarping predictability of sandy beaches in a multidirectional wave basin. *Ciencias Marinas*, 34(1):45–54, 2008. doi:10.7773/cm.v34i1.1265.

Pelletier, J. D., DeLong, S. B., Al-Suwaidi, A. H., Cline, M., Lewis, Y., Psillas, J. L., and Yanites, B. Evolution of the Bonneville shoreline scarp in west-central Utah: Comparison of scarp-analysis methods and implications for the diffusions model of hillslope evolution. *Geomorphology*, 74(1-4):257–270, 2006. ISSN 0169555X. doi:10.1016/j.geomorph.2005.08.008.

Puleo, J. A. *Hydrodynamics and Sediment Transport in the Inner Surf and Swash Zones*. Phd thesis, University of Florida, 2004.

Reeve, D. E., Karunarathna, H., Pan, S., Horrillo-caraballo, J. M., Rózynski, G., and Ranasinghe, R. Geomorphology Data-driven and hybrid coastal morphological prediction methods for mesoscale forecasting. 256:49–67, 2016. doi:10.1016/j.geomorph.2015.10.016.

Rinaldi, M., Casagli, N., Rinaldi, M., and Casagli, N. Stability of streambanks formed in partially saturated soils and effects of negative pore water pressures : The Sieve ... Stability of streambanks formed in partially saturated soils and effects of negative pore water pressures : the Sieve River ž Italy /. (May 2014), 1999. doi:10.1016/S0169-555X(98)00069-5.

Roberts, T. M., Wang, P., and Kraus, N. C. Limits of Wave Runup and Corresponding Beach-Profile Change from Large-Scale Laboratory Data. *Journal of Coastal Research*, 261(2):184–198, 2010. ISSN 0749-0208. doi:10.2112/08-1097.1.

Ruiz de Alegria-Arzaburu, A., Mariño-Tapia, I., Silva, R., and Pedrozo-Acuña, A. Post-nourishment beach scarp morphodynamics. *Journal of Coastal Research*, (SI 65):576–581, 2013. ISSN 07490208. doi:10.2112/SI65-098.1.

Sallenger Jr, A. H. Storm impact scale for barrier islands. *Journal of Coastal Research*, pages 890–895, 2000.

Schubert, J. E., Gallien, T. W., Majd, M. S., and Sanders, B. F. Terrestrial Laser Scanning of Anthropogenic Beach Berm Erosion and Overtopping. *Journal of Coastal Research*, 299(1): 47–60, 2015. ISSN 0749-0208. doi:10.2112/JCOASTRES-D-14-00037.1.

Seymour, R., Guza, R. T., O'Reilly, W., and Elgar, S. Rapid erosion of a small southern California beach fill. *Coastal Engineering*, 52(2):151–158, 2005. ISSN 03783839. doi:10.1016/j.coastaleng.2004.10.003.

Sherman, D. and Nordstrom, K. F. Beach scarps. *Zeitschrift Fur Geomorphologie*, 1(29.2): 139–152, 1985.

Short, A. D. and Hesp, P. A. Wave, beach and dune interations in Southeastern Australia. *Marine Geology*, 48(1982):259–284, 1982. doi:10.1016/0025-3227(82)90100-1.

Short, A. D. and Wright, L. D. Beach systems of the Sydney region. *Australian Geographer*, 15 (1):8–16, 1981. ISSN 0004-9182. doi:10.1080/00049188108702791.

Sorensen, R. M. *Basic coastal engineering*, volume 10. Springer Science & Business Media, 2005. doi:10.1007/978-1-4757-2665-7.

Stockdon, H. F., Holman, R. A., Howd, P. A., and Sallenger, A. H. Empirical parameterization of setup , swash , and runup. 53:573–588, 2006. doi:10.1016/j.coastaleng.2005.12.005.

Stronkhorst, J., Bruens, A., van Vliet, L., and Schasfoort, F. Effect van zandsuppleties op de kust en het wad (Dutch). Technical report, Deltares, Delft, 2016. URL `goo.gl/GhN5gG{%}0A`.

Taylor, D. W. *Fundamentals of soil mechanics*. Chapman And Hall, Limited.; New York, 1948. doi:10.1097/00010694-194808000-00008.

Turner, I. L., Sydney, U., Short, A., and Davidson, M. A. Evaluation of Opportunistic Shoreline Monitoring Capability Utilizing Existing 'Surfcam' Infrastructure. *Journal of Coastal Research*, (March), 2015. doi:10.2112/JCOASTRES-D-14-00090.

Uluapa, S. Punta Cancún: Graffiti de arena, 2011. URL `https://aclarando.wordpress.com/category/playa-gaviota-azul/`.

van Gaalen, J. F., Kruse, S. E., Coco, G., Collins, L., and Doering, T. Geomorphology Observations of beach cusp evolution at Melbourne Beach, Florida, USA. *Geomorphology*, 129(1-2): 131–140, 2011. ISSN 0169-555X. doi:10.1016/j.geomorph.2011.01.019.

van Gent, M. R. A., de Vries, J. S. M. v. T., Coeveld, E. M., de Vroeg, J. H., and van de Graaff, J. Large-scale dune erosion tests to study the influence of wave periods. *Coastal Engineering*, 55(12):1041–1051, 2008. ISSN 0378-3839. doi:10.1016/j.coastaleng.2008.04.003.

van Genuchten, M. T. A closed-form equation for predicting the hydraulic conductivity of unsaturated soils. *Soil science society of America journal*, 44(5):892–898, 1980. doi:10.2136/sssaj1980.03615995004400050002x.

van Rijn, L. C. Prediction of dune erosion due to storms. *Coastal Engineering*, 56:441–457, 2009. doi:10.1016/j.coastaleng.2008.10.006.

van Rijn, L. C., Walstra, D. J. R., and van Ormondt, M. A Machine Learning Approach To Modeling Sediment Transport. *Journal of Hydraulic Engineering*, 133(4):776–793, 2007. doi:10.1061/(ASCE)0733-9429(2007)133.

van Rijn, L. C., Tonnon, P. K., and Walstra, D. J. R. Numerical modelling of erosion and accretion of plane sloping beaches at different scales. *Coastal Engineering*, 58(7):637–655, 2011. ISSN 03783839. doi:10.1016/j.coastaleng.2011.01.009.

van Thiel de Vries, J. S. M., van Dongeren, A., Roelvink, J. A., and Schilperoort, T. Validation of dune impact models using European field data. Technical report, Deltares, Delft, 2011.

Vellinga, P. *Beach and Dune Erosion during Storm Surges*. Phd thesis, Delft University of Technology, 1986. URL http://resolver.tudelft.nl/uuid:eb7a4d20-86d2-469a-932a-dec0518274bb.

Vousdoukas, M., Almeida, L., and Ferreira, Ó. Modelling storm-induced beach morphological change in a meso-tidal, reflective beach using XBeach. *Journal of Coastal Research*, (SPEC. ISSUE 64):1916–1920, 2011. ISSN 07490208.

Vousdoukas, M. I. Erosion/accretion patterns and multiple beach cusp systems on a meso-tidal, steeply-sloping beach. *Geomorphology*, 141-142:34–46, 2012. ISSN 0169555X. doi:10.1016/j.geomorph.2011.12.003.

Wallace, R. E. Profiles and ages of young fault scarps, north-central Nevada. *Geological Society of America Bulletin*, 88(9):1267–1281, 1977. doi:10.1130/0016-7606(1977)88<1267:paaoyf>2.0.co;2.

Weerd, A. J. V. D., Wijnberg, K. M., Weerd, A. J. V. D., and Wijnberg, K. M. Aeolian Sediment Flux Derived from a Natural Sand Trap Aeolian Sediment Flux Derived from a Natural Sand Trap. *Journal of Coastal Research*, 75:338–342, 2016. doi:10.2112/SI75-068.1.

Weiss, N. A. and Weiss, C. A. *Elementary Statistics*. Addison-Wesley Reading, MA, 1989. doi:10.2307/2347395.

Wengrove, M. E., Henriquez, M., de Schipper, M., Holman, R., and Stive, M. Monitoring morphology of the Sand Engine leeside using Argus' cBathy. *Coastal Dynamics*, pages 1893–1904, 2013.

Winegardner, D. L. *An introduction to soils for environmental professionals*. CRC Press, 1995. doi:10.5860/choice.33-6320.

Wodzinowski, T. The Role of the Day by Day Beach Monitoring in Shore Transformation. *Polish Geological Insitute Special Papers*, 11:77–82, 2004.

Wright, L. D. and Short, A. D. Morphodynamic variability of surf zones and beaches: A synthesis. *Marine Geology*, 56(1-4):93–118, 1984. ISSN 00253227. doi:10.1016/0025-3227(84)90008-2.

Zapata, C. E., Houston, W. N., Houston, S. L., and Walsh, K. D. Soil-water characteristic curve variability. In *Advances in unsaturated geotechnics*, pages 84–124. 2000. doi:10.1061/40510(287)7.

Zarkogiannis, S. D., Kontakiotis, G., Vousdoukas, M. I., Velegrakis, A. F., and Collins, M. B. Scarping of arti fi cially-nourished mixed sand and gravel beaches : Sedimentological characteristics of Hayling Island beach , Southern England. *Coastal Engineering*, 133(2016):1–12, 2018. doi:10.1016/0964-5691(94)90044-2.